To Marcela, my wife, for
her love and moral support.

To my mother and to the
memory of my father.

THE ROLE OF PARTICLE ACCELERATION IN SOLAR FLARES

A Thesis

submitted by

ROMAN PEREZ ENRIQUEZ

for the degree of

Doctor of Philosophy

in the

University of London

February 1987

ABSTRACT

The Solar Flare Phenomenon is explained in terms of a model (first proposed by Elliot in 1964) for which energetic particles, accelerated while trapped in the intense Bipolar Magnetic Field Regions above Sunspots, are responsible for all the dramatic observations that we recognize as a Solar Flare. It is proposed that the particles are first heated and then accelerated by absorbing part of the wave energy which is continuously travelling upward from the convection zone. Since the Magnetic Field Region is closed, the particles are trapped and the energy density of the particles tends to increase. There is a limit, however, to the amount of energy that the particles can acquire to maintain stable trapping. When this limit, imposed by the magnetic field pressure is exceeded, plasma instabilities lead first to dumping of the surplus energy by the release of some of the particles to the Chromosphere through the loss cone of the magnetic field. The Chromosphere at the feet of the magnetic trap is then heated substantially until it may become unstable and produces an invasion of "cool" plasma

into the magnetic trap. As a result, a further increase of energy density inside the region takes place leading to a chaotic dumping of the whole particle population from the region. The interaction of the energetic particles with the chromospheric material produces X-rays and white light, accompanied by radio emission (synchrotron emission by the electrons spiralling in the magnetic field lines). The occasional gamma-ray emission is assumed to be produced by relativistic ions accelerated by shock waves produced by the chromospheric heating at the feet of the magnetic region. Finally, while the instability arises in the flare region, an anomalous particle composition establishes itself and is observed in Interplanetary Space after the Flare. Thus a reexamination of the role of energetic particles in the Flare is carried out in the light of the recent observations by the SMM and Hinotori Satellites during the last Solar Maximum which point to the continuous and violent evolution of the solar atmosphere.

CONTENTS

		Page
ABSTRACT		2
ACKNOWLEDGEMENTS		7
1.	INTRODUCTION	8
	1.1. Particle trapping in Magnetic Field Loops above Active Regions.	16
	1.2. Heating and Acceleration of Trapped Particles.	18
	1.3. Solar Wind or Solar Flare Particles?	20
	1.4. The Observations	22
2.	SOLAR FLARE OBSERVATIONS IN RELATION TO PARTICLE ACCELERATION	25
	2.1. The Coronal Magnetic Field	27
	2.2. The Electromagnetic Emission	31
	2.2.1. X-ray emission	36
	2.2.2. Radio burst emission	41
	2.2.3. Gamma-ray emission	47
	2.3. Particles and Mass Ejecta	51
	2.3.1 Electrons	52
	2.3.2. Protons	56
	2.3.3. Other Nuclei	60

3. THE ROLE OF ENERGETIC PARTICLES IN THE SOLAR FLARE 76

3.1. Coronal Heating and Magnetic Structure. 81

3.2. Possible Acceleration Mechanisms in Flares. 84

3.2.1. The first phase of acceleration. 88

3.2.2. The second phase of acceleration. 89

3.2.3. Acceleration by shocks. 93

3.3. The Acceleration Mechanism in the Context of the Energetic Particle Model. 96

3.3.1. The energy balance in the Active Region (AR). 98

3.3.2. The role of scattering in the acceleration. 101

3.3.2.1. Coulomb scattering. 107

3.3.2.2. Magnetic scattering. 111

3.3.2.3. Scattering by hydromagnetic turbulence. 115

3.3.3. The acceleration of the protons. 119

3.3.4. The acceleration of the electrons. 121

3.3.4.1. Langmuir turbulence dissipation (Buneman Instability) 122

3.4. The Flare. 128

3.4.1. The Preflare Situation. 130

3.4.2. Instability by chromospheric heating 133

3.4.3. Instability by emergence of new magnetic flux. 136

3.5. The Overabundance Problem. 138

3.5.1. The nuclear reactions model. 139

3.5.2. The plasma models. 143

3.5.3. The overabundance problem and the particle model. 148

4. DISCUSSION AND CONCLUSIONS 152

4.1. Predictions of the Model. 157

4.1.1. The building-up stage. 158

4.1.2. Development of the instability and the Flare 161

4.1.3. Magnetic expansion without a Flare. 166

4.2. Observational evidence available for testing the Model. 167

4.2.1. Thermal energy vs magnetic flux 168

4.2.2. Energetic particle, soft and hard X-ray emissions from non-flaring regions. 172

4.2.3. Flare instability and related phenomena. 177

4.2.4. Evolution of Solar Flare electrons. 187

4.3. Future measurements for testing the Model. 191

4.3.1. Ion cyclotron waves in space. 192

4.3.2. X-ray and isotope-rich flares. 194

REFERENCES 199

ACKNOWLEDGEMENTS

I would like to express my sincere recognition to Dr. R. Hynds for most careful criticisms and suggestions to this thesis which were invaluable in making the manuscript consistent and readable. I also would like to thank Dr. X. Moussas for interesting discussions and to Prof. H. Elliot for his suggesting the problem of study and continual guidence as my first supervisor. I specially thank Marcela, my wife, for her perpetual encouragement and moral support. Without her always at my side this thesis could have never been written.

I am idebted to the Universidad Nacional Autonoma de México and the British Council for their financial support during my stay at Imperial College. I am grateful to Mrs. M. Vázquez for the typing of the manuscript and to J.A. Vivar for his help with the drawings.

CHAPTER 1

INTRODUCTION

The role that particle acceleration plays in the development of solar flares and related phenomena has been underestimated if not completely neglected. The reason is that although it is widely recognized that energetic particles are present in the flare environment, they are generally considered to be only the result of the flare. The majority of the models proposed so far rely on the rapid conversion of magnetic energy into flare energy (see for example the books by Svestka, 1976; Sturrock et al, 1980; Priest, 1982). However, in spite of the fact that the phenomenon has been studied for many years, it is still far from being well understood. We believe that this is perhaps due to the severe conditions that current models impose on the solar atmosphere to produce a flare. This statement seems to be supported by the observational evidence from flares that is now available; mainly the results from Skylab, ISEE-3, the Solar Maximum and Hinotori Satellite missions as well as the radio studies with the Very Large Array (VLA) telescope on the ground.

We know, for example, that a strong magnetic field in the flare region is a necessary condition for a flare to occur. Great controversy still

persists, however, concerning the state of the magnetic field after flares. It used to be believed that flares developed when the rate of change of sunspot area is greatest (Giovanelly, 1939). However, Newton (1948) and Ellison et al (1961) showed that large flares tend to take place when no great changes in the magnetic field occur. The most recent observations from the SMM satellite indicate that while some flares are triggered by the emergence of new magnetic flux (Hoyng et al, 1981; Woodgate et al 1981; de Jager et al, 1983), there are others which take place with no apparent trigger from simpler arch structures (see Tandberg-Hansen et al, 1984). In any case, the so-called two ribbon flares seem to produce the energetic particles, or at least those flares which show the presence of energetic particles in space.

Coronal magnetic loops were discovered by Skylab (see Svestka et al, 1977) and were thought as relatively cool regions. This is no longer the case and observations of hot loops at temperature of up to 10^7 K are now most common. Electron density and temperature for the August 1973 event were deduced from X-ray observations by Smith et al (1977). They coincide with Rust et al (1980) that there was addition of mass and energy for a period of hours as shown in Fig. 1 1. On the other hand, Petrasso et al (1975) recognised that coronal loops sometimes brighten gradually only to fade away later with no flare being present. There

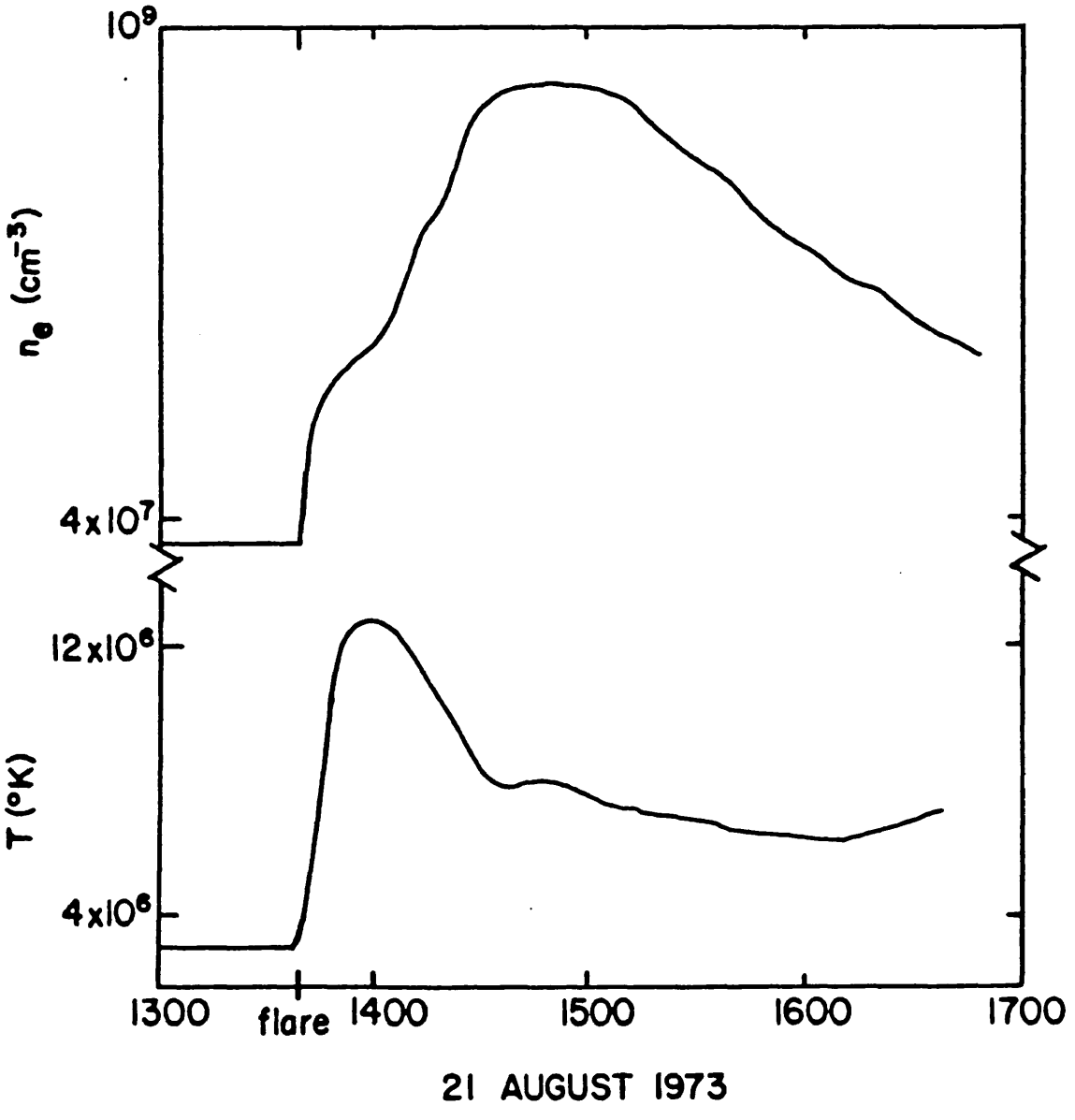


Fig. 1.1. X-ray deduced electron temperature and density VS. time for the eruptive prominence event of 21 August 1973 (Dryer et al,1978).

is ample corroboration of this result from the Hard X-ray Imaging Spectrometer (HXIS) on board the SMM Satelitte observations (Svestka et al, 1982 a, b; de Jager et al 1983; Schadee et al, 1983). These authors have found that the X-ray emission is not restricted to the time of the flare. Sometimes no flare takes place at all. In large flares, radio burst observations are a common feature with type III bursts present even for the smallest events. More rarely, gamma-rays are present when the particle acceleration is so intense that nuclear reactions can actually take place in the solar atmosphere (Chupp et al, 1973; Chupp, 1983; Bai et al, 1983). There is finally the presence of the particles themselves in interplanetary space.

The magnetic loops seem to be in a continuous state of evolution and energetic particles may be present at all times and not only when a flare takes place. We propose therefore to reexamine the old idea of Elliot (1964) and Schatzman (1967) that particles trapped in the magnetic field loops above active regions can provide the energy necessary to trigger the flare. All that is required is that the magnetic field be of the correct geometry (such as a magnetic loop or a loop arcade as is actually observed) to be capable of storing particles for some time(Elliot, 1969, 1973). The energy necessary for the particles to fulfill

their role in the flare trigger mechanism comes from the wave energy flowing continuously from the solar convective zone up into the chromosphere and corona.

The particle trapping is limited by the magnetic field of the region itself (Kennel and Petschek, 1966). According to these authors there is a critical energy $Ec = B^2/8\pi n$ where B is the average magnetic field of the trap and, n, is the number density of the contained particles, such that particles above this limit become unstably trapped. This means that the surplus energy in the trap escapes to counteract the energy gain through acceleration when this situation is reached. A balance between the incoming and escaping energy eventually takes place. Elliot (1969, 1973, 1979) proposed that this steady state situation can on occasions, be broken. That is,the situation in which the impinging of the particles into the chromosphere is sufficient to heat the atmosphere below in such a way that "cool" plasma rises into the trapping region. In such case the system becomes unstable as the critical energy decreases and many particles suddenly become "unstably trapped". As a result there will be a catastrophic release of most of the particles in the distribution into the chromosphere. This catastrophic dumping of the particles into the atmosphere and interplanetary space would constitute,according to the model, a solar flare. It is interesting to note that only

recently X-ray emission from magnetic loops has been explained in terms of the catastrophic release of matter from the top of the loop down the legs of the arch (Levine and Withbroe 1977, Berman, 1982).

While, most of the electromagnetic emission from flares is recognized as being connected with the presence of energetic particles (Svestka, 1976; Ramaty et al, 1980), the idea still persists that particles, although important as they might be, are a by-product of other processes which really constitute the flare. There is however, little doubt in almost any model, that the majority of the electromagnetic emissions produced in the flare are a consequence of the acceleration of particles. Table 1 - 1 shows the relation between the observed electromagnetic emission and the acceleration of the particles. The questions which then arise are where and when does the acceleration take place and why. In this context then, the purpose of this thesis is to show that energetic particles continuously accelerated in the magnetic field loops above active regions are an important factor in explaining many of the observed features of the flare. In order to do that, we need to show first that the particles can become trapped in a magnetic field loop for the sufficient time necessary to be accelerated. Furthermore, that the acceleration process is efficient enough to increase

TABLE 1 - 1

OBSERVATIONAL EVIDENCE FOR ACCELERATION OF PARTICLES IN SOLAR FLARES

1. RADIO EMISSION produced by fast electrons interacting with the solar plasma and magnetic fields (Wild et al, 1963).

2. X-RAY EMISSION from the bremsstrahung of energetic electrons (10-100 KeV) (Paterson and Winckler 1959, Kane 1971).

3. GAMMA-RAY LINE AND CONTINUUM due to nuclear interactions of energetic ions and the bremsstrahung of relativistic electrons (Chupp et al 1973, Ramaty et al 1975).

4. DIRECT SPACECRAFT AND GROUND-BASED OBSERVATIONS OF ENERGETIC ELECTRONS AND IONS which escape from the Sun (McCracken and Rao 1970, Lin 1974, Simmet 1974, McDonald et al 1974).

5. OTHER EMISSIONS such as WHITE-LIGHT CONTINUUM AND IMPULSIVE EUV BURSTS not directly attributable to energetic particles, but appear to be good indicators of particle acceleration (e.g. Svestka 1976).

the particle energy density of the region to a value comparable with the magnetic pressure.

Finally, that an instability can arise in the chromosphere to produce radical changes in the physical conditions of the region. The development of such a situation is of course restricted to such factors like magnetic field geometry and changes which might take place to it in the course of the flare build-up. The stability of the coronal magnetic field has been studied theoretically by Hood (1983). He found those conditions which permit the active region magnetic field to stand perturbations and remain stable. Meerson and Rogachevskii (1983) have studied the storage of high energy protons in the solar corona in terms of ion cyclotron wave instability. More recently Simnett and Ryan (1985) have proposed that micro γ-ray flares can be explained in terms of the pre-flare acceleration of protons over $\sim 10^3$ s by a series of mhd shocks in the low corona.

1.1. Particle trapping in Magnetic Field Loops above Active Regions.

It is clear that the magnetic field stability does not constitute by any means a sufficient condition for an efficient trapping of particles. The reason is that there is an equal probability for particle trapping and escape in a closed magnetic field geometry if no other process is involved. It can be easily proved, however (shown in Chapter 3) that if heating or acceleration take place then the probability for particle escape from the trap tends to decrease. The consequence of this is that there is an increase of the particle energy density in the trap. But even if this is so the physical conditions in the region must somehow guarantee that the pitch angle distribution of the particles be maintained nearly isotropic. Otherwise, as a result of acceleration the pitch angle of the particles diminishes and a rapid escape through the loss cone of the field cannot be avoided. We shall see in Chapter 3 that the conditions necessary for a reasonable building-up of an energetic particle population in the trapping field can be fullfilled without difficulty (see also Meerson and Rogachevskii, 1983). If we accept that a steady, intense magnetic field, with trapping capabilities can persist for long periods as has been observed during the Skylab mission (McGuire et al 1977), it becomes very difficult to

imagine a static behavior of the plasma under the arch. Instead, a dynamic behavior of the plasma in which material is sometimes dumped down the legs of the loop as reported by Levine and Withbroe (1977)or electromagnetic emission from the loop itself (Howard and Svestka, 1977; Petrasso et al, 1977, Svestka et al 1982 a, b; de Jager et al, 1983; Schadee et al, 1983) should be expected.

1.2. Heating and Acceleration of Trapped Particles.

There is considerable advantage in treating the plasma in the trapping region as a dynamic environment. If a good coupling between acceleration and scattering takes place then there is no need to require an extremely efficient and rapid process for the acceleration of the particles. A slow, inefficient process is sufficient to increase significantly the energy density in the trap. In such conditions, the particles can be accelerated until no further trapping can persist as it would be the case when the energy of the particles became above the Kennel and Petschek's energy limit. Those particles above the limit are of most importance because they become sufficiently anisotropic to start escaping through the loss cone of the field at the feet of the loop. This, however, is not a straightforward procedure because if a sufficient number of particles start streaming towards the loss cone, they excite resonant waves in the plasma. For this reason the particles with energies above E_c are called resonant particles.

The interaction of particles and the generated waves give rise to two important results. First the escape of some particles is prevented with the immediate consequence that the energy density in the

trap can increase further; and second, there is a heating of the region produced by the resonant interaction of waves and particles.

We shall try to show that this dynamic behavior of the solar atmosphere is crucial to the development of instabilities in the plasma so that they can actually trigger a solar flare. This can better be appreciated if we consider the coronal magnetic field in general.

1.3. Solar Wind or Solar Flare Particles?

We know that in the solar atmosphere energy is continuously flowing upwards from the convection zone towards the chromosphere and the corona where part of this energy is dissipated with consequent heating. In those regions where the magnetic field presents an open geometry the heating of the coronal plasma probably leads to its expansion in the form of solar wind. However, when the magnetic field has the form of a loop or of a loop arcade; in other words, when the field is closed, the plasma is confined to move in the magnetic field as β (the ratio of magnetic to kinetic pressure)is greater than one and part of the energy which goes with the heating remains stored within the region in the form of energetic particles. The observations that have become available in the last few years thanks to the SMM give overwhelming evidence of the dynamic behavior of active regions. The situation is then such that it is no longer possible to ignore that most features in the active atmosphere are intimately related to situation where energetic particles take an active role. The hot loops, for instance, are perhaps the best place to search for suprathermal particles stored in a magnetic field. Alternatively,

we shall prove that due to wave growth in the loss cone, some of the waves produced could reach open magnetic field tubes and can therefore escape into interplanetary space with the solar wind. Inside such tubes the waves can survive for a long time and could be observed as high frequency plasma waves.

1.4. The Observations.

It is clear that any model of the solar flare must be capable of explaining the extensive amount of observations which are now available from active regions before, during, and after flares and even when no flares are present. Here we try to explain most observations in terms of a model for which energetic particles play the most important role. We concentrate particularly in showing that the isotopic overabundances sometimes observed in the particle flux from flares can better be explained if, as our model suggests, the relative composition is formed slowly during the evolution of the active region; this whether there is a flare or not. It seems very improbable that the conditions for the preferential heating take place in the region in exact coincidence with the flare. Instead a plasma heating mechanism taking place as long as there are particles streaming in the trapping region seems more likely. Furthermore, in the case of iron only, if the heating of this isotope takes place early in the building-up of the flare, it seems possible to understand the apparent contradiction between theory and observations.. That is, the charge state of the iron in ^{3}He-Fe rich flares is usually + 11, 12 (Gloeckler et al 1976; Sciambi et al, 1977) and only occasionally (MaSung et al 1981) it is + 17 as propose by the preferential heating

model of Fisk (1978).

We study the flare then from an unconventional point of view, but one which takes fully into account the physics behind this interesting phenomenon. We start in the next Chapter with an overall discussion of the observations which are related to the particle acceleration. We point out those observations which support our view as well as those which cannot be explained directly with our model. The third Chapter is concerned with the model itself. We propose there to revise our current ideas concerning the acceleration of particles and prove first, that the magnetic field loops above active regions can store particles for a time long enough for heating and acceleration to take place; second, that acceleration can develop fully in the region so that the particle energy density can become eventually close to the magnetic pressure; and third, that in some circumstances the conditions that make a flare possible can be fulfilled. It is interesting to notice here that there are many cases in which either the solar flare conditions lie much beyond the capabilities of a particular region and plasma or there are changes in the geometry or intensity of the field, such as those due to the emergence of new magnetic flux. These situations are not outside the scope of the model but they are well explained as natural events during the life of the active region.

We end up therefore with a discussion of the predictions which the model is capable of making and conclude that the presence of energetic particles in the solar active regions and their dynamic role in the solar flare phenomenon should no longer be underestimated.

CHAPTER 2

SOLAR FLARE OBSERVATIONS IN RELATION TO PARTICLE ACCELERATION

Putting aside for the moment the problem of when does the acceleration process start working on the particles we shall be concerned in this Chapter with those observations which are going to be useful in determining the type of acceleration which flare particles undergo. Let us remark again the intimate connexion that exists between the electromagnetic emission and the particle acceleration. In the case of the magnetic field the situation is somewhat different since no information of the microstructure of the field is at present available and the controversy still persist as to whether the field as a whole takes an active or a passive role in the particle acceleration. Another problem arises when we want to compare the particle fluxes at 1AU with the electromagnetic emission. In general, to do that it is necessary to correct for the propagation effects in the energy spectrum in order to obtain the corresponding energy spectrum at the source. However, should the particle acceleration be such that particles are accelerated before the flare then the event characteristics are not only given by acceleration and propagation but also by the way in which the particles are released

into the chromosphere and interplanetary space. Let us start by summarising the observations which are connected with the acceleration process.

2.1. The Magnetic Field.

The magnetic field of an active region is the result of the magnetic interaction of a sunspot group. Each one of the spots composing the group contributes together with the current system which might be flowing above the chromosphere to the total magnetic flux, and for that reason the magnetic field can be extremely complicated.

Since Severny's observations of the sunspot magnetic field intensity distribution in 1964, it is known that a potential dipole field is not a good approximation. Instead, an azimuthal component must exist. Nevertheless, as Kadomtzev (1966) has suggested the set of vertical magnetic tubes of the sunspot umbra should acquire the general azimuthal component from the helical instability of the plasma with the field, so that for the general structure of the sunspot field it can be regarded as force free (Mogilevsky and Shelting, 1966; Mogilevsky et al, 1968).

That the magnetic field is expected to be force free was pointed out before by Schlüter (1950) on the basis that the gas pressure in the corona is insufficient to balance the Lorentz forces. Therefore, the condition $\underline{J} \times \underline{B} = 0$ holds. If currents exist they must flow parallel to the field and it can be assumed that the currents are proportional to the field, thus

$\nabla \times \underline{B} = \alpha \underline{B}$, where α is a constant along the field line but may vary among different field lines because

$$\underline{B} \cdot \nabla \alpha = 0 \qquad (2.1)$$

Solar flares and related phenomena take place in magnetic field loops above active regions. The field configuration in the loops can in some cases be extremely complicated but in general it is bipolar with two feet in the chromosphere forming a kind of tunnel between the opposite polarities which has been identified with the neutral line (Fig. 2.1). The changes in the geometry of the region during a flare are now known (Rust, 1976) to be no different from the continuous changes which are normal to the evolution of an active region. However, some flares seem to be associated with the emergence of new magnetic flux (Zirin, 1974; Rust, 1976; Neiding, 1978; Hoyng et al, 1981; Woodgate et al, 1981; Syrovatsky, 1982; de Jager et al, 1983). The presence of the loops in the active region became evident only after the Skylab observations in EUV and X-rays (Foukal, 1975; Vorpahl, 1976; Widing and Cheng, 1974; McGuire et al, 1977; Svestka et al, 1977) and more amply corrobborated by the SMM and Hinotori satellites. The observations indicate that the loops are in reality systems of loops above active regions in the form of arcades with temperatures of about 2.5×10^6k. The evidence for the association of the loops arcades with the magnetic field comes from

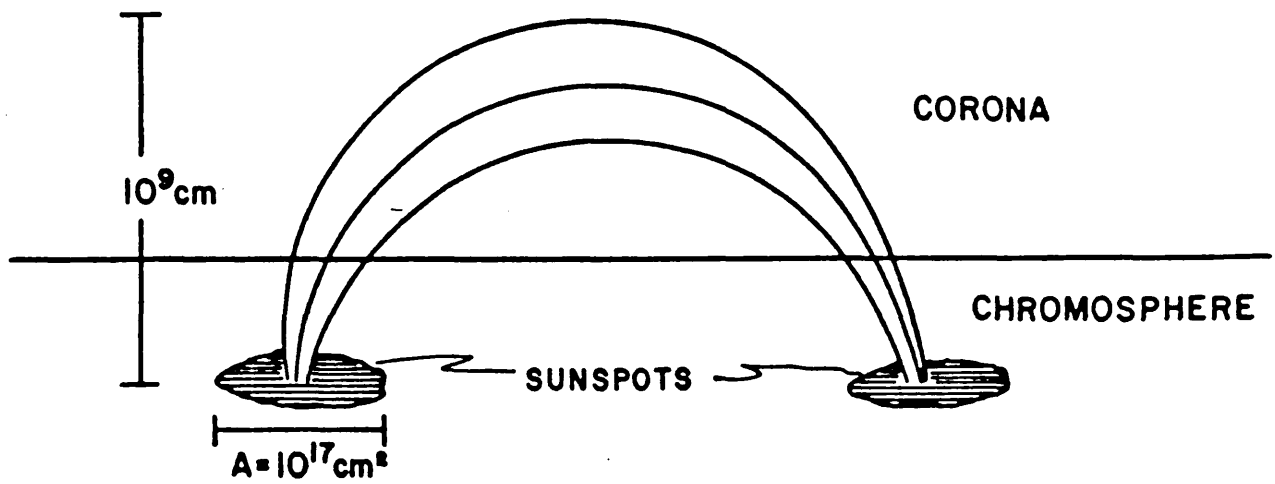


Fig. 2.1. Magnetic Field Geometry of Coronal Loop.

the filament observations in Hα (Tanaka and Nakagawa, 1973), where the filaments represent, according to Brown and Smith (1980), masses of cool gas stored in the corona by the magnetic field. In this way, the relation between a flare and the disappearence of a filament can be interpreted in terms of the release of energy, part of which is stored in the corona. We shall return to this problem in the next Chapter where we deal with our own interpretation. For the time being let us say that since measurements of the actual microstructure of the magnetic field are lacking, little can be said at present in relation to the fate of the plasma trapped in the magnetic field.

2.2. Electromagnetic Emission

Typically the flare is described in terms of the Hα emission. Two phases are then evident. A flash phase (lasting from 5 minutes to an hour) in which the intensity and area of the emission increases, and the main phase (lasting from an hour to a day) in which the system goes back slowly to its initial conditions. However, observations of flares in EUV and X-rays (summarized schematically in Fig. 2.2) have made possible to distinguish another phase in the flare evolution. Several minutes prior to the Hα there can exist a preflare phase in which soft X-rays increase in intensity (Thomas and Teske,1971; Petrasso et al,1975; Vorpahl et al,1975; Kahler,1979; Simnett and Strong, 1984). This is due to enhanced thermal emission coming from the coronal loop. During this phase the coronal loop structure brightens in soft X-rays and the filament is activated. The filament expands in synchrony with the increase in the emission. An impulsive phase is also sometimes observed (usually from large two-ribbon flares) when hard X-rays, microwaves (type III radio bursts) and EUV show a burst like emission. Hard X-rays images from HXIS on board the SMM satellite (Jordan, 1981) as well as XSM aboard Honotori satellite (Yoshimori et al, 1983) show that the emission comes first from the loop footpoints and later from the top

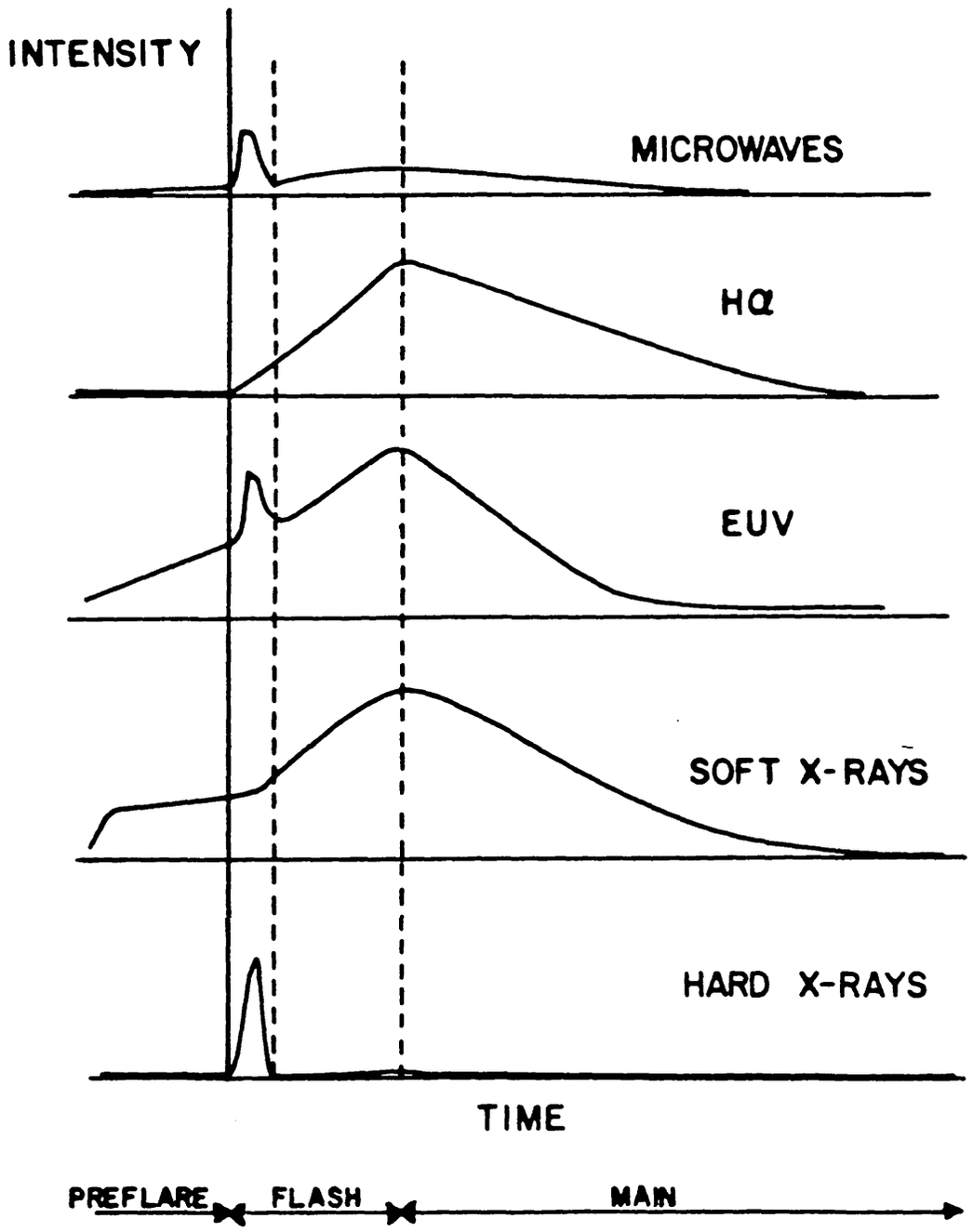


Fig. 2.2. Solar Flare Intensity in various wavelenoths as a function of time.

of the loop (Fig. 2.3, Schematic picture). Concerning the speed with which the intensity rises it is observed that while small "thermal" flares are correlated with a slow rise, flares in which nonthermal particles are produced show a rapid rise (see Fig. 2.2).

The main phase or recovery time (lasting for several hours to a day) is characterized by a clear picture of two Hα ribbons connected to the foot-points of the loop (Svestka 1976, (Fig. 2.4). Two kinds of loops are then distinguished: hot rising loops ($n = 2 \times 10^{10}$ cm^{-3}; $T = 40 \times 10^{6}$ K), and smaller cooler loops below ($n = 15 \times 10^{10}$; $T = 20 \times 10^{6}$ K) (observed by Duijrman, 1983). The X-ray emission is long lasting because of the persistence of the loop with high temperature and density, the latter changing more rapidly than the temperature. The density of the hotter parts of the plasma during a prominence on 20 May 1980 was observed by Poland and Tandberg-Hansen (1983) with the Ultraviolet Spectral Polarymeter (UVSP) on board SMM to reach 3×10^{11} cm^{-3}.

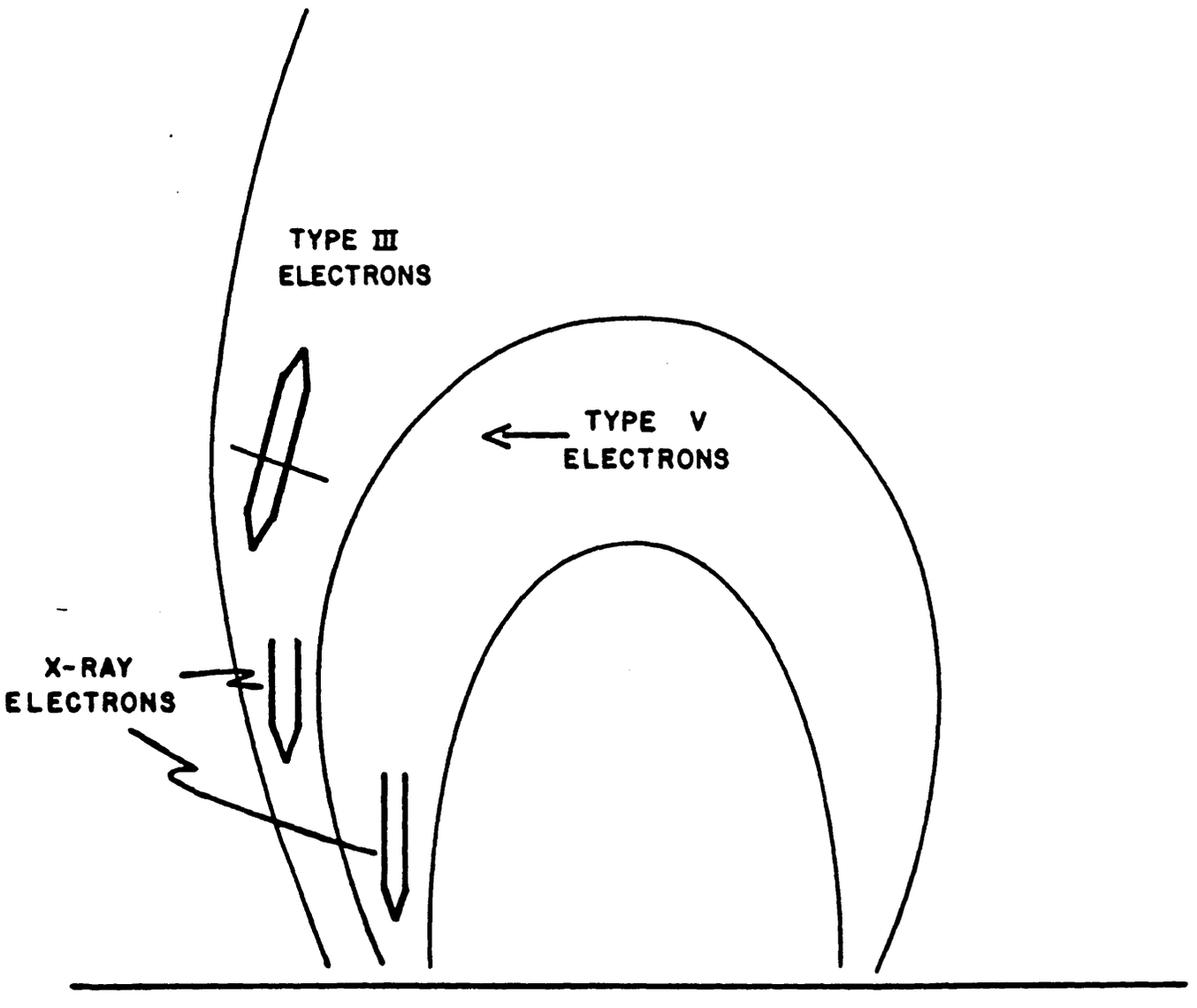


Fig. 2.3. Schematic representation of X-ray and Radio Emission from coronal Loops (from Petrosian and Leach,1983).

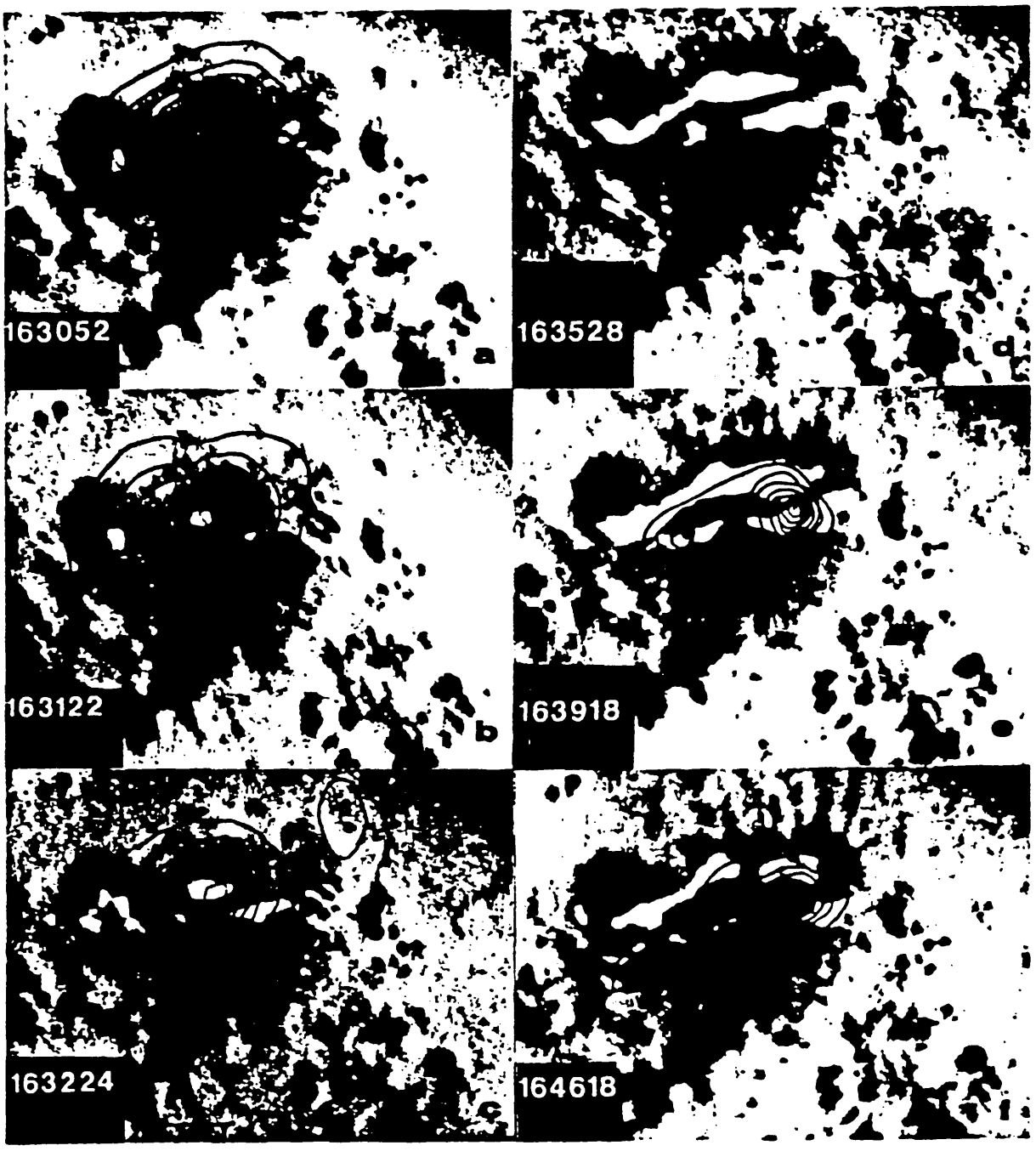


Figure 2.4. D3 emission in the June 6, 1982 flare with Hinotori hard X-ray contours overlaid. The first frames show many footpoint flashes, and the two-strand emission grows as the thermal flare builds up. Late in the flare bright loops between the ribbons are visible (from Zirin, 1985).

2.2.1. The X-ray emission

The study of the soft and hard X-ray emission in flares has become of primary importance because it apparently carries a substantial amount of the energy of the flare (Simnett and Strong 1984; Veck et al 1984; Antonucci et al 1985). Since the most widely recognized theory for the production of the X-rays is the bremsstrahling of energetic electrons as they pass through the solar atmosphere, it follows that energetic electrons must carry this energy. The correct interpretation of the X-ray emisión is then of vital importance in the study of the acceleration of the electron component.

There are two distinct X-ray emission in the flare. The soft X-rays which sometimes take place before the flare onset and the hard X-rays taking place mainly during the impulsive phase. A classification of the X-ray emission from flares is summarized in Table 2-1. The soft X-ray emission is believed to be the result of thermal emission enhanced by the heating of the coronal loop structure. The hard X-rays, on the contrary, are thought to represent a genuine non thermal footprint of the flare. A summary of the hard X-ray burst characteristics observed with Hinotori satellite (Ohki et al, 1983) is given in Table 2-2.

It seems that the hard X-ray burst and the Hα brightening are caused by electrons impinging in a thick target. The heating produced in the chromosphere is

Table 2 - 1. CLASIFICATION OF FLARE X-RAY SOURCES

Type	Dynamics	Spectral Characteristics
Hard	Impulsive	Spikes Burst "Second Step"
Hard	Gradual	Hard Spectrum Soft Spectrum Hot Thermal
Soft	Flare Loops Post-Flare Loops Sveska's Giant-Arches	Thermal

Table 2 - 2. SUMMARY OF HARD X-RAY BURSTS OBSERVED WITH HINOTORI SATELLITE (OHKI ET AL, 1983).

	GRADUAL BURST	IMPULSIVE BURST
Image	A. Large Loop B. Double Source (not low)	A. Single Source (small or extended) B. Double or More Sources
Height	High ($\gtrsim 10^4$ Km)	Low (At Least Main Source)
Spectrum	Power Law Prevails	Exponential (Early Phase) Power Law (Late Phase)
Energy Dependent Peak Delay	Some Delays	No Delays

thus manifest by a simultaneous EUV burst and the optical (Hα) emission (see Simnett and Strong 1984; Simnett 1985, for an alternative explanation).

In order to explain the presence of hard X-rays in the impulsive phase it is required that at least 10^{36} to 10^{38} electrons with effective temperature of 5×10^{8} K are produced (probably by bulk energization) in the flare environment (see Brown and Smith 1980). The study of flares and active regions in X-rays has been extended immensely following the launch of the SMM and Hinotori satellites. The X-ray imaging has facilitated substantially the analysis. So,for example, a whole coverage of the evolution of active regions up to the flare onset and even beyond it was made possible with these instruments. In connection with this,for instance, it has been revealed that hard X-ray emission is not restricted to the time of the flare. Sometimes it take place before the flare as a flare precursor, and even sometimes there is no flare at all (Svestka et al, 1982 a, b; de Jager et al, 1983; Schadee et al, 1983). In their report on the limb flare of 30 April 1980, de Jager et al (1983) indicate the presence of a flare precursor approximately 30 minutes prior to the onset. Likewise, Schadee et al (1983) have probably found evidence for a flare precursor taking place as long as 90 minutes before the event of 21 May 1980.

The limb flare of 30 April 1980 has been studied also by other authors (Woodgate et al 1981, Gabriel et al, 1981). Although Woodgate et al agree with de

Jager et al in that the flare was possibly triggered by the emergence of new magnetic flux they suggested that the interaction between brightened loops was perhaps more likely. Gabriel et al (1981), on the other hand, observed the event with a different instrument, a Polychromator, and indicate the possible presence of turbulence for several minutes, coincident with the hard X-ray burst. They also suggest the continuous heating of the plasma since the estimated cooling time is less than the duration of the hot source.

Concerning the flare triggering mechanism Hoyng et al (1981) found evidence from the 21 May 1980 event which they analysed with the HXIS on SMM, Hα emission and magnetic development, that the flare was produced by the emergence of new magnetic flux. In contrast, for the large two-ribbon flare in 1 Nov 1980 observed by Tandberg-Hansen et al (1984), they conclude that the flare took place with no apparent trigger. The magnetic field configuration was a simple closed arch although containing non potential substructure.

2.2.2. Radio Emission

Until relatively recently (Wild, 1950) the observation of radio bursts was confined to the microwave band. A summary of the microwave type IV bursts is given in table 2-3. The study of hectametric and kilometric wavelengths were only possible with the advent of satellites. Metre wave radio bursts have been clasified by Wild et al (1963) into five types according to their dynamic spectra (Fig. 2.5) The radio burst characteristics are described in table 2-4. We can distinguish there the type III bursts which are of short duration with a rapid drift from high to low frequency. They are believed to be produced by streaming electrons in the energy range 10 to 100 Kev, which excite Langmuir waves through the two-stream instability. Also type III bursts are thought to be radiation near both the fundamental and the second harmonic in the plasma frequency $\omega = (4\pi n\, e^2/m)^{\frac{1}{2}}$, where n is the number electron density and m the electron mass, which is the characteristic oscillation frequency of the electrons. According to Melrose (1980) the situation can be summarised by saying that the fundamental emission comes from the conversion of the Langmuir waves into transverse electromagnetic waves due to the interaction with thermal particles, whereas the second harmonic is a consequence of the interaction of two Langmuir waves to produce a transverse electromagnetic

Table 2 - 3

MICROWAVE TYPE IV EMISSION FROM FLARS

MICROWAVE BURST TYPE	TIME SCALE (MIN)	TEMPERATURE (K)	CORREL-ATION	PRODUCTION MECHANISM	Ne (CM^{-3})	B (GAUSS)	# PART. > 100 KeV	TOTAL ENERGY REQUIRED	SPECTRAL EXPONENT
Impulsive	1-5	up to 10^9	X-rays	gyrosynchr	?	?		$1-2X10^{29}$ ergs	
Gradual	tens	10^6	none		$\lesssim 10^{10}$	$\lesssim$ 350	$\lesssim 10^{34}$		3-5 not unique
Type IV	5-30	up to 10^9	none		$\lesssim 10^{10}$	$\lesssim$ 350	$\lesssim 10^{34}$		3 - 5
Moving IV (highly polari-sed)			Large proton flares	Synchro-ton		10		200KeV/ part.	

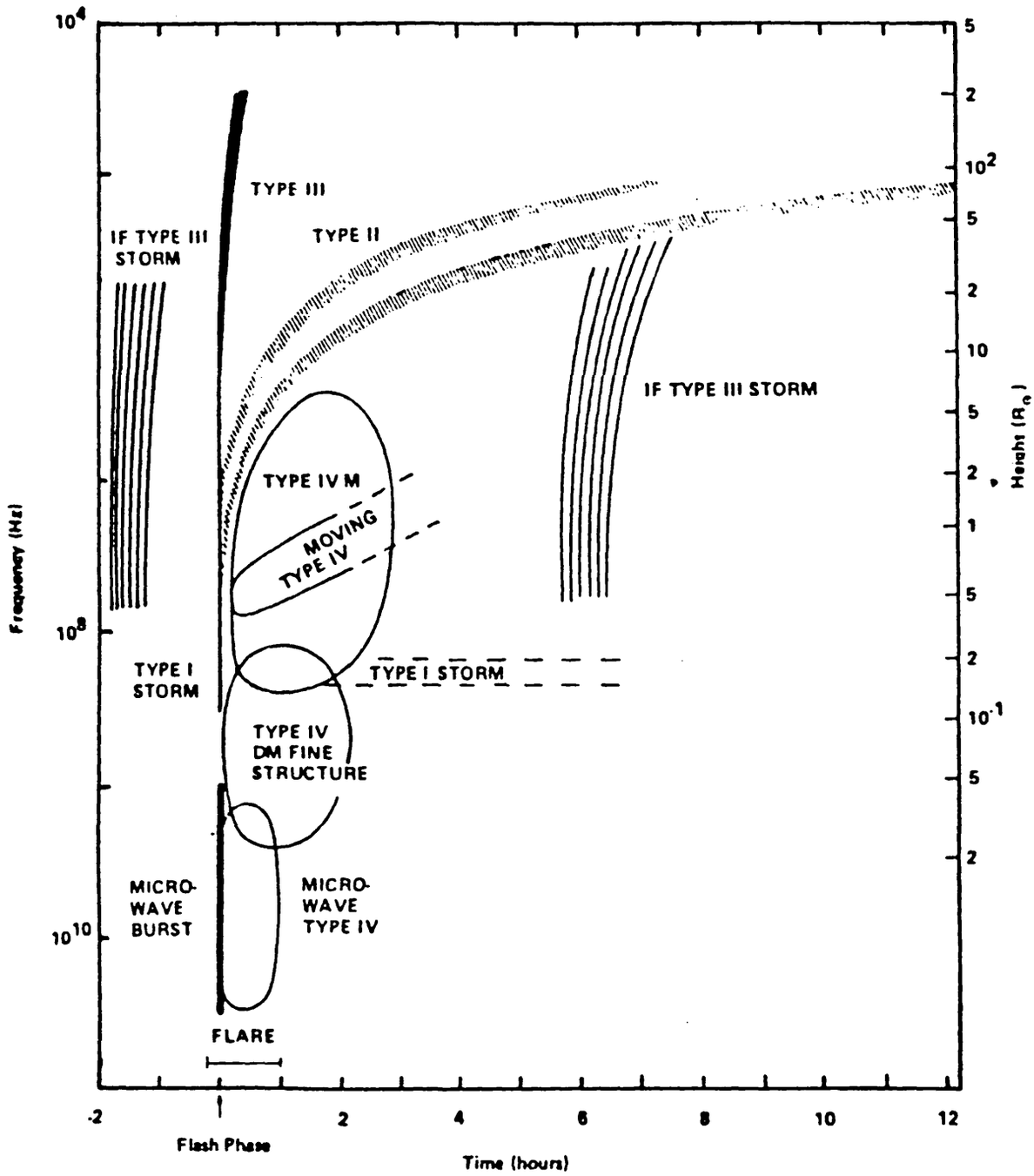


Fig.2.5. Solar Flare Radio Spectrum (after Rosenberg,1976).

TABLE 2 - 4

RADIO BURST CLASSIFICATION (Melrose, 1980)

TYPE OF BURST	PROBABLE EXCITING AGENCY	PROBABLE EMISSION PROCESS	POLARIZATION	DURATION
I	Trapped fast electrons?	Fundamental Plasma	Strong o-mode	burst: 0.1 to 10_s storm: hrs to day
II	Shock wave	Plasma	f - weak o-mode 2f - none	5-30 min
III	Electron stream	Plasma	f - moderate o-mode 2f - weak o-mode	10_s
IV (Early) (Flare cant)	Trapped fast electrons?	Second harmonic plasma	Weak or absent	∿ 10 min
IV (Late)	" " "	Fundamental plasma	Strong o-mode	> 1 hr. ∿
IV (Moving)	Ejected plasmoid	Gyro	Weak to strong X-mode	20 min - 2 hr

wave. The problem with this interpretation is that Langmuir waves have not been observed from the flare environment (Melrose, 1980). However, according to Goldman (1983) the most recent experiments seem to confirm that streaming electrons do in fact excite Langmuir waves, which produce type III bursts as they become electromagnetic waves through their collision with the electrons. Furthermore, Gergely et al (1984), studying the coronal transient on 9 April 1980, located the source of the type III burst along a nearby streamer (much in the way it was shown in Fig. 2-3). The type II burst from this event appeared to be moving parallel to the solar surface to the sides of the loops instead of the outward direction and showed a very low drift rate.

Type II bursts consist of slow drifting bands near the fundamental and second harmonic of the plasma frequency. This type of burst implies a radial velocity of 800 to 2000 Km/s and for this reason it has been identified with an mhd wave ascending through the corona (Wild et al 1963). Thus flares which produce type II bursts also produce shock waves.

Type IV bursts are perhaps the only ones connected exclusively with flares. The impulsive emission comes probably from the upper part of the arch as described by Tandberg-Hansen et al (1984) for the large two-ribbon flare of 1 Nov. 1980 where the 22 GHz impulsive emission

was produced by high energy (∿ 100 keV) electrons. Both type IV and II radio bursts have been found by Bai et al, 1983 to be produced in gamma-ray line flares. However, the microwave burst emission is delayed for about 5 seconds with respect to the hard X-ray emission (Bai et al, 1983; Farnik et al, 1983).

The radio noise type I emission is probably not connected with flares. Its origin is still not known. Type V bursts are a continnum emission probably connected to type III emission but restricted to the streaming of the electrons in the loop (see Fig. 2 - 3).

2.2.3. Gamma-ray Emission.

The most clear cut clue that protons and heavy ions are accelerated to high energies in solar flares comes from the gamma-ray lines sometimes observed. In fact, as much as 10 or more gamma-ray line flares have been observed with the SMM satellite (Rieger, 1982). Furthermore this satellite has also shown that the acceleration process is very fast, i.e., a few seconds in some cases (Forrest et al,1981; Chupp et al, 1982; Bai et al, 1983). The first gamma-ray line observations from flares come from the 4 August 1972 event (Chupp et al, 1973). The extension of the study followed with Hudson et al (1980) Prince et al (1982) Yoshimori et al (1983) Chupp (1983) and Bai et al (1983). Meanwhile Ramaty et al (1975, 1979, 1983) have correctly predicted that the neutron absorption line at 2.223 MeV would be the strongest line. The gamma-ray spectrum for the intense 3 June 1982 event near 2.223 MeV is shown in Fig. 2.6. The time profile of the 27 April 1981 event is shown in Fig. 2.7 (from Chupp, (1983). This event was chosen because it is one event in which the burst feature consists of several peaks (see the Chapter on Discussion and Conclusions).

Bai et al (1983) argue that for most gamma-ray line events there is a delay of a few seconds in the

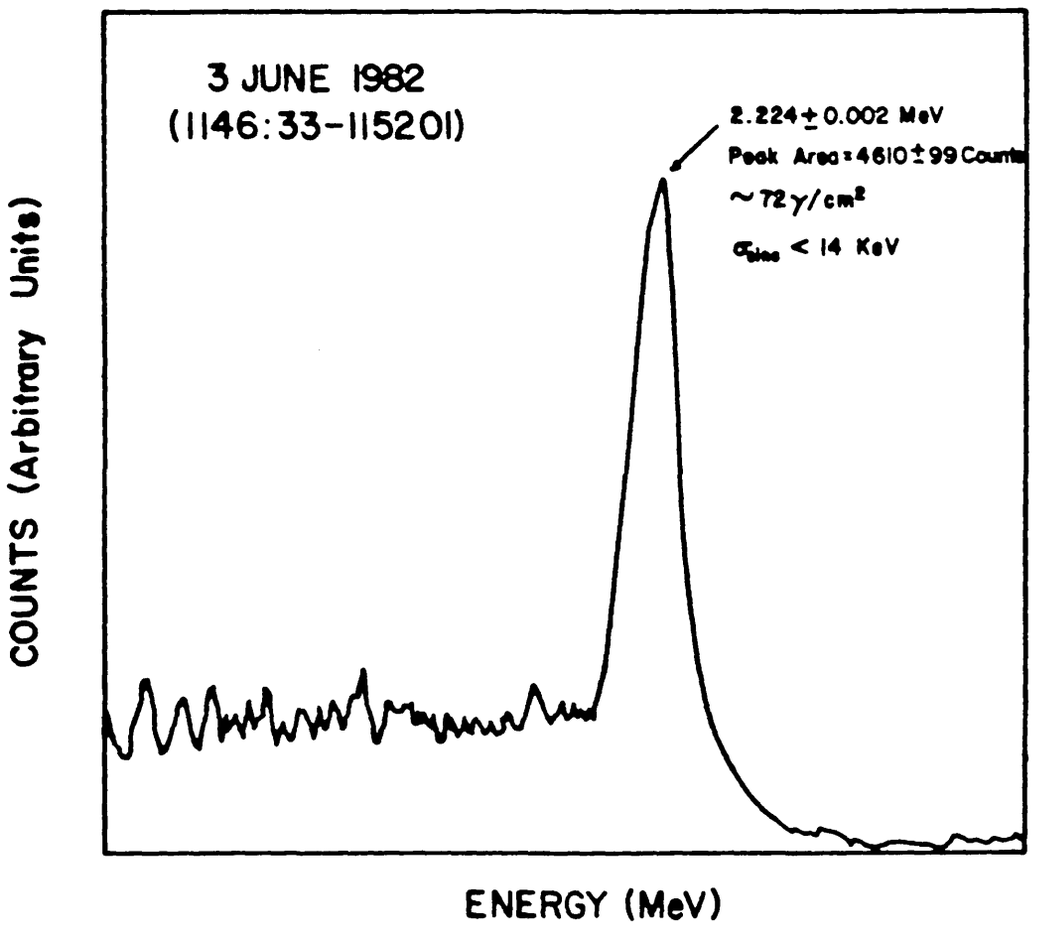


Fig. 2.6. Gamma-ray line spectrum near 2.223 MeV for the 3 June 1982 event with SMM Gamma Ray Spectrometer (from Chupp,1983).

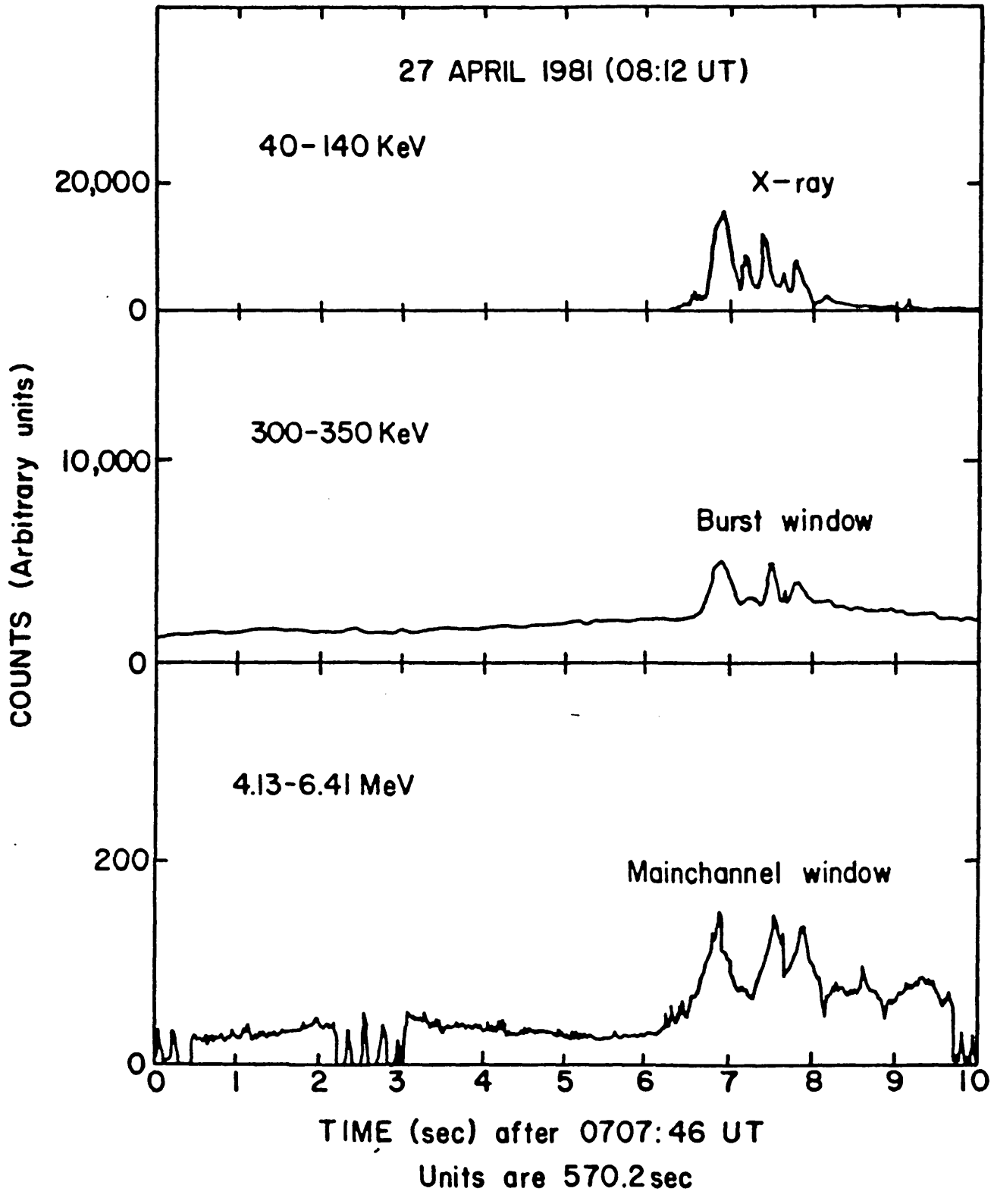


Fig. 2.7. Time profile of 27 April 1981 gamma-ray line event for various energy channels.

time profile of the high energy ($\gtrsim$ 300 keV) hard X-rays with respect to those of lower energy hard X-rays. They conclude that shock acceleration of trapped protons is possible. On the other hand, Chupp (1983) indicates that ion and electron acceleration take place simultaneously in the impulsive phase as well as their interaction with matter. He points out that any apparent delay between electron and ion acceleration is unreal since the ions, in order to produce the gamma rays, must have been already accelerated.

Apart from gamma-ray lines which give information on the acceleration of the ions, gamma-ray continumn provides information on the acceleration of electrons to MeV energies.

2.3. Particles and Mass Ejecta.

The real confirmation that particles are accelerated in the solar flare comes, of course, from their direct observation in interplanetary space and sometimes even at Earth. There are mainly two ways in which the particles manifest themselves in space. One is as individual particles accelerated by first or second stage flare mechanisms and a second one in which plasma moves outwards with speeds of from several hundred up to a thousand Km per sec. This mass ejecta exerts a pressure on the ambient material and produces a shock wave propagating through interplanetary space,reaching the Earth's magnetosphere after 48 hrs to 60 hrs,and generating geomagnetic disturbances.

The energetic particles, produced at the Sun are accelerated in one or two acceleration stages and some reach very high energies. One has to distinguish then between different populations produced in the flare by these two mechanisms. Four distinct populations are evident: energetic electrons ($E \lesssim 200$ keV), relativistic electrons, energetic protons and ions and relativistic protons and ions.

2.3.1. Electrons

According to the event characteristics, there are events in which only non relativistic electrons are produced (Lin, 1974a). These are called "pure electron events", or PE events. The main characteristic of PE events is that they come from small flares. That is, flares in which the energy is probably of thermal origin. It has been observed that the energy spectrum from these events undergoes a rapid steepening above $\sim$ 100 KeV. This is clearly shown in Fig. 2.8 (from Lin, 1974a). The differential energy spectrum at injection illustrated has been constructed from Fisk and Axford's (1969) model for diffusive propagation in the interplanetary medium.

The spectral shape is a power law in the range 5 to 100 KeV with spectral exponent usually ranging between 3 and 4.5 for diffusive events. Events for which no substantial scattering in the interplanetary medium is present are more difficult to model due to the uncertainties in the parameters. For diffusive PE events the number of particles released to the interplanetary medium can be deduced from the propagation model. The result is that approximately 10^{33} electrons above 20 KeV are released into space for a typical event.

The density of the acceleration region was calculated by Lin (1974 b) by assuming that energy losses are

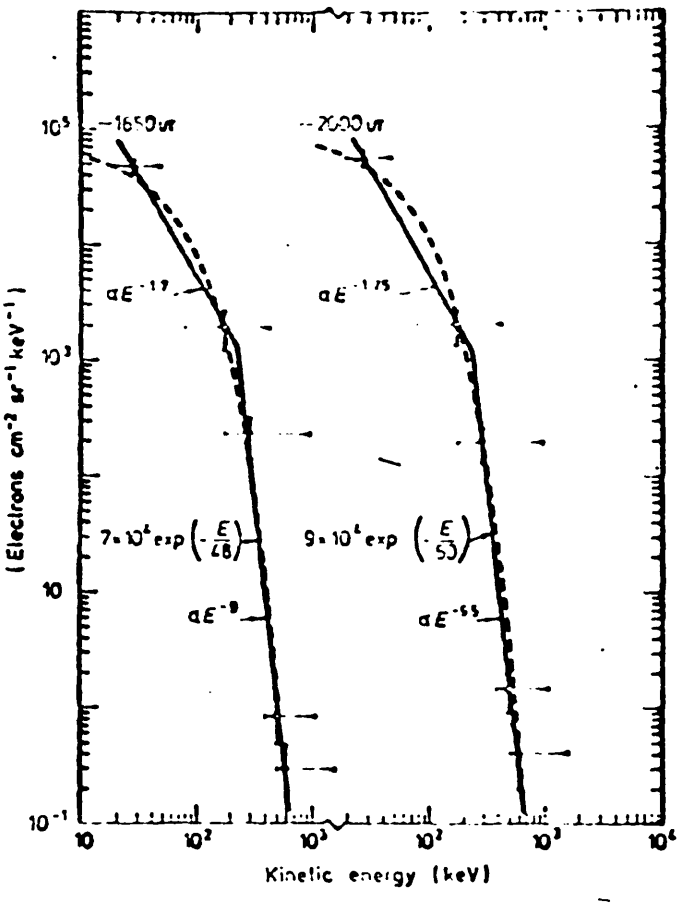


Fig. 2.8 - Energy spectrum of pure electron event on 30 July 1967 (After Lin 1974a).

collision dominated and then using the Trubnikov's (1965) expression for the energy loss in ionized hydrogen. The result was of less than 10^{10} cm^{-3} at the acceleration region.

Particle events in which protons are also present are called mixed events. They are characterised by the presence of both electron populations, non-relativistic and relativistic. The differential energy spectrum for the electron component in these events is constructed in the same way as for PE diffusive events. For the longer lasting mixed events the differential energy spectrum runs smoothly from 5 KeV to relativistic energies as a power law (Fig. 2.9). The spectral index lies between 2 and 4.5 (Simmet, 1974) and the number of electrons in the acceleration region for typical event is calculated to be 10^{36} electrons above 20 KeV. For the 28 May 1967 event compiled by Lin (1974 a), Brown and Smith (1980) calculated the number of electrons above 200 KeV to be $\sim 10^{34}$.

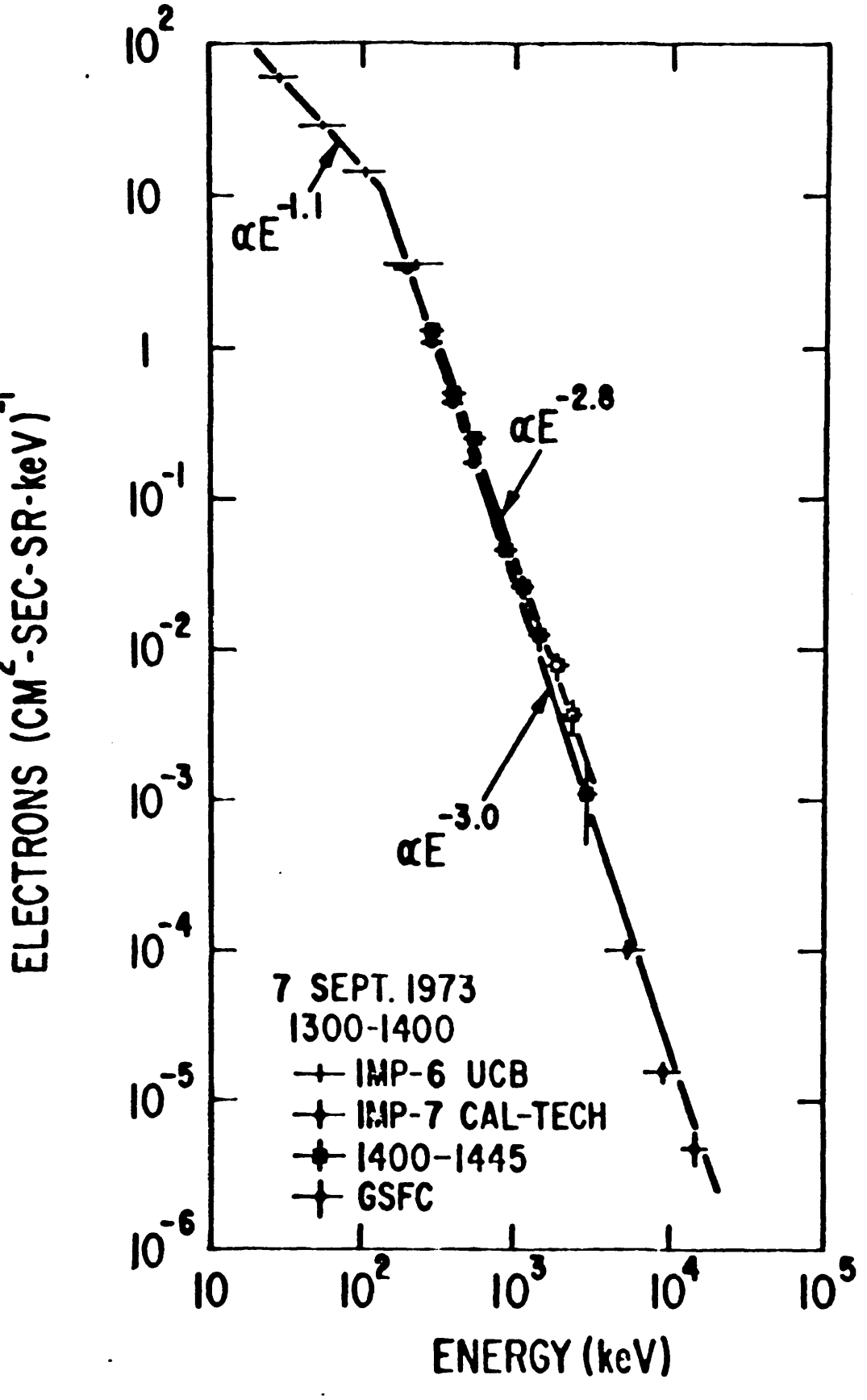


FIG III.2.9 - Electron energy spectrum from 7 September 1973 flare.

2.3.2. Protons.

Proton events are not as common as nonrelativistic electron events (see Brown and Smith, 1980). As we have seen above the protons accompany stronger long lasting relativistic electrons. This indicates, on the one hand, that the acceleration mechanism is different in that it is more efficient but, on the other, that the building-up process might be completely different. This stems from the fact that the behavior of high energy protons in space is usually of diffusive nature. Therefore, for these events, their source energy spectra are relatively easily deduced (Brown and Smith, 1980). In contrast with the electron spectra, those of the protons corresponds better to an exponential in rigidity, R. Fig. 2.10, from Freir and Webber (1963) illustrates different proton energy spectra for different events. Biswas and Radhakrishnan (1973) calculated the number of particles in the interplanetary medium for the 28 September 1961 event as $\sim 2 \times 10^{33}$ protons with total energy of 4×10^{27} ergs. Since they assumed that only 0.01% of the protons escaped to space they calculated that $\sim 1.5 \times 10^{37}$ protons with an energy of 3×10^{30} ergs were at the acceleration site for this particular event, if their assumption is correct.

Even more rare are the relativistic proton events or "solar cosmic ray" events. They can be

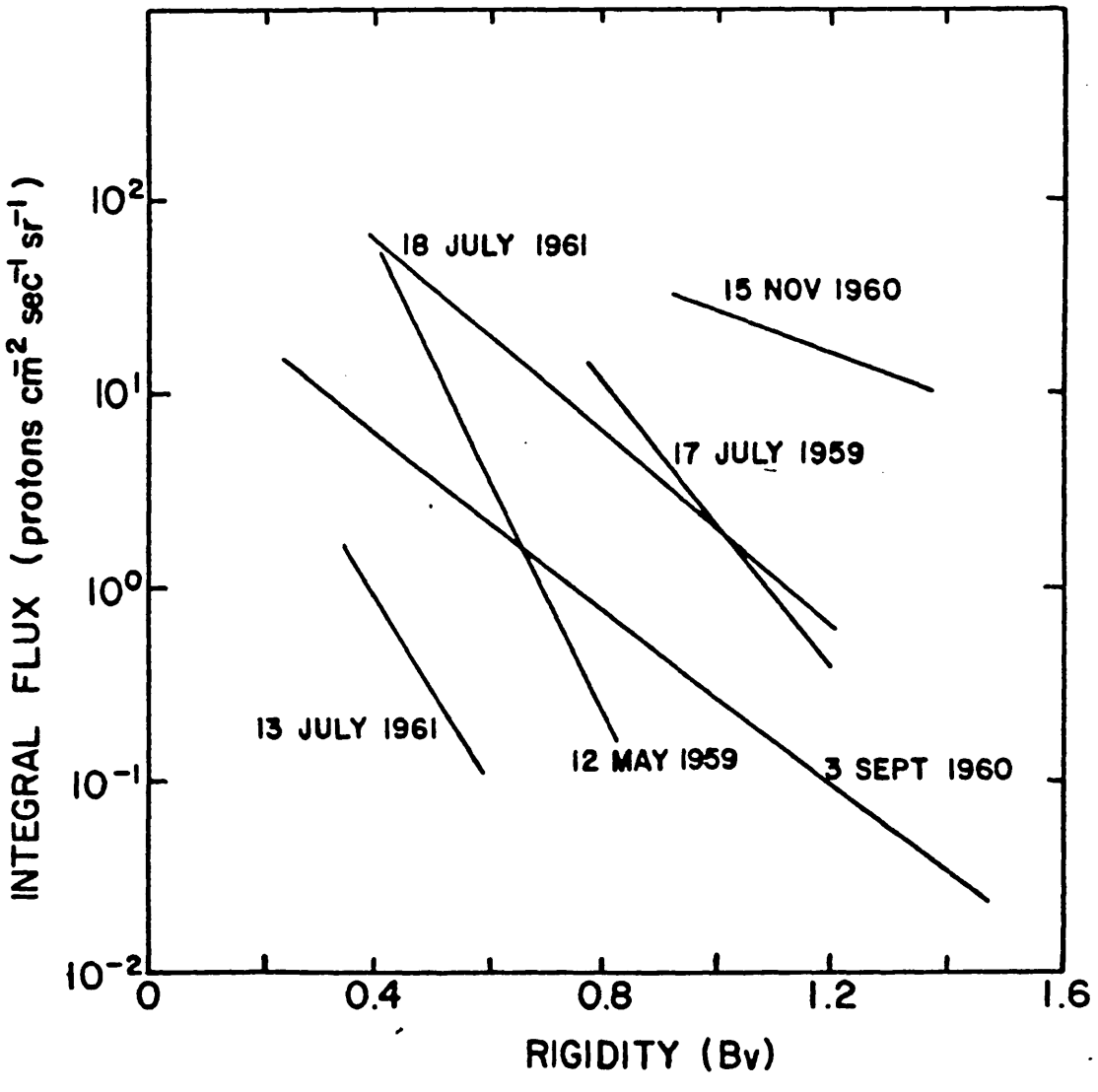


Fig 2.10. Exponential Rigidity spectra of Solar Cosmic Ray events (after Freir and Webber, 1963).

observed at the Earth with neutron monitors and for this reason are also called "Ground Level Events". In this sort of events (like that of 4 August 1972 event) as much as 10^{32} ergs are released to space and are usually accompanied by a blast wave moving at about 1000 Km/s which arrives to the Earth's magnetosphere more than 40 hours after the particles producing a Sudden Comencement as it interacts with the geomagnetic field, and is followed by geomagnetic storms. As the shock passes across the Earth's environment a Forbush decrease is observed by neutron monitors.

The ratio of electrons-to-protons released into interplanetary space can be obtained from Fig. 2-11, where the electron spectrum has been calculated from the hard X-ray and the γ-ray continua emissions, and the proton spectrum from γ-ray lines (Ramaty et al, 1980).

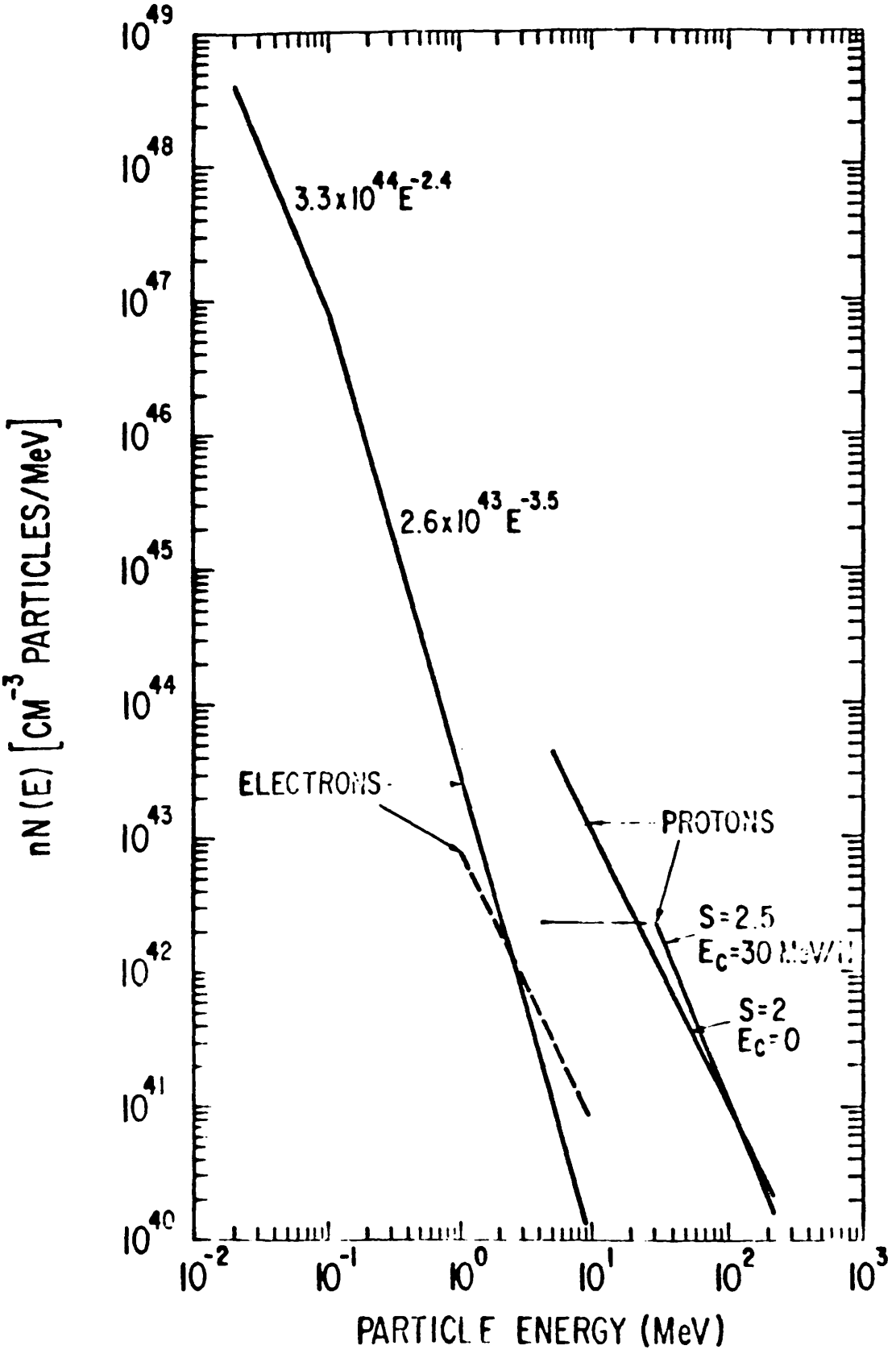


FIG. 2 - 11. Electron and proton energy spectra for release into interplanetary medium as calculated from X-ray and γ-ray continua and γ-ray line emission, respectively (from Ramaty et al, 1980)

2.3.3. Other Nuclei

Energetic nuclei usually accompany energetic protons. Although the relative composition of nuclei in proton events is close to the normal composition of the solar atmosphere, on many occasions some isotopic species show overabundance in the particle flux relative to normal photospheric abundances. The most widely known are the so-called "^{3}He-rich" and "Fe-rich" events. In general, also other species show abnormal abundances in some flares. Ma Sung et al (1981) studied the charge state of heavy ions in ^{3}He-Fe-rich 14-15 May 1974 event with IMP 8 and compare it to the "normal" flare event of 4-5 Nov 1973. They found that for the ^{3}He-Fe-rich event Ne, Mg, Si, O and S are also overabundant while C is underabundant.

Furthermore, they found for this event that apart of Fe $^{+11,12}$ there is also Fe $^{+16,17,18}$. They interpreted this result in terms of temperature variations in the corona between $\sim 4 \times 10^5$ and 5×10^6K. More recently, however, Klecker et al (1984) have determined the iron charge distribution for five ^{3}He-Fe-rich events in 1978 and 1979 using ISEE-3 data. The mean charge state of iron, $\bar{Q}$, for the events in 1978 and 1979, was 19 ± 2 instead of 13 to 15 as in events with normal composition.

The first observation concerning the composition of ^3He and ^4He isotopes was made by Schaeffer and Zähringer in 1962. From then on the isotopes of H and ^4He, first, and heavier nuclei, later, have been observed for a number of solar events and for a wide range of energies by a number of authors. Table 2.5 gives the relative abundances of D, T, and ^3He measured with respect to H and ^4He and of CN and Fe measured with respect to O. From the results, some characteristics have been determined (see Fisk 1978 b; Kocharov and Kocharov 1978).

The first and most important characteristic of ^3He-rich events is that the $^3He/^4He$ ratio measured over the energy range from 1 to 20 Mev/nucleon is high although showing great variability: from about 10^{-2} to more than 1. There are of course flares where the $^3He/^4He$ ratio is small. These events can be explained in terms of nuclear reactions between energetic particles and the ambient material but as it has already been mentioned this model is incapable of explaining the big ratios.

The second most striking characteristic is the presence of only small amounts of D and T in the observations. This constitutes by far the strongest evidence against the nuclear models because if nuclear

TABLE 2.5 RELATIVE COMPOSITION OF D, T, ^3He, ^4He, CNO, AND Fe IN SOLAR FLARES

EVENT	(1) D/H (2) D/He RATIO	ENERGY (MeV/nucl)	(1) T/H (2) T/He RATIO	ENERGY (MeV/nucl)	(1) $^3He/H$ (2) $^3He/^4He$ RATIO	ENERGY (MeV/nucl)	$^4He/H$ RATIO	$^4He/H$ ENERGY	CNO/O RATIO	CNO/O ENERGY	Fe/O RATIO	Fe/O ENERGY
SOLAR[a]												
ABUNDANCE	(1)1.6×10^{-5}	8.6-11.7	---		(1)1.7×10^{-4}	2.2-2.6	0.11±.04	6.7-15.0	1.66±.39	6.7-15.0	4.0×10^{-5}	6.7-15.
12.11.60	(1)3×10^{-3}	25.-50.[b]	(1)$<10^{-3}$	20.-45.[b]	(2)0.2	70.[c]						
18.07.61	(1)$<2\times10^{-3}$	50. [d]	(1)$<6\times10^{-4}$	50. [d]								
AVERAGE OVER 7					(2)$2.1\pm.4\times10^{-2}$	10-100[e]	9.33×10^{-3}	10-100[e]				
2.9.66							79.±13.	15.[f]$_a$	=1.65	>15.[f]$_a$	0.031±.007	>15.[f]$_a$
19.4.68					(2).13±.04	4.6-19.[g]	$4.2\pm.3\times10^{-2}$	4.-19.[g]				
23.4.68					(7).08	4.6-19.[g]	$3.1\pm2\times10^{-2}$	4.-19.[g]				
17 IMP V FLARES AVERAGE	(1)$\sim8\times10^{-5}$	8.4-12.5[h]	(1)$\lesssim4\times10^{-5}$	7.7-12.1[h]	(2)2.2×10^{-3}	11.2-43.[h]						
OVER 7 FLARES(1969)	(1)$<3\times10^{-4}$	4.-5. [i]	(1)$<10^{-4}$	4.-5. [i]	(2)0.1±.02	4.-5 [i]						
12.4.69							91.±13.	15.[f]$_a$	=1.65	>15.[f]$_a$	0.047	>15.[f]$_a$
5.5.69	(2)2.12×10^{-2}	4.-19. [j]	(2)2.1×10^{-2}	4.-19. [j]	(2)0.53±.07	4.6-19. [j]						
28.5.69	(2)5.5×10^{-13}	" [j]	(2)2.7×10^{-3}	" [j]	(2)1.52±.1	4.2-18.2[jk]						
29.5.69(A)	(2)2.8×10^{-3}	" [j]	(2)5.7×10^{-3}	" [j]	(2)0.71±.09	4.6-19. [j]						
29.5.69(B)	(2)5.6×10^{-3}	" [j]	(2)3.9×10^{-3}	" [j]	(2)0.35±.03	" [j]						
4.10.69	(2)$\gtrsim2.5\times10^{-2}$	" [j]	(2) 10^{-2}	" [j]	(2)0.45±.06	" [j]						
2.11.69					(2)$7.7\pm2\times10^{-2}$	11.2-43.[h]						
30.7.70	(2)5×10^{-3}	" [j]	(2)2.3×10^{-2}	" [j]	(2)0.45±.06	4.6-19. [j]						
	(2)2.2×10^{-5}	10.5-22.[i]										

TABLE 2.5 (Cont.)

EVENT	(1) D/H (2) D/H_e RATIO	ENERGY (MeV/nucl)	(1) T/H (2) T/H_e RATIO	ENERGY (MeV/nucl)	(1) $^3H_e/H$ (2) $^3H_e/^4H_e$ RATIO	ENERGY (MeV/nucl)	$^4H_e/H$ RATIO	ENERGY (MeV/nucl)	CNO/O RATIO	ENERGY (MeV/nucl)	Fe/O RATIO	ENERGY (MeV/nuc.
25.1.71					(2) $2.\pm1.\times10^{-2}$	11.2-43.[b]	0.1	1.5 [a]		-	0.12	1.5 [a]
							0.09	2.5 [a]			0.12	2.5 [a]
							0.06	3.5 [a]			0.13	3.5 [a]
							46.$\pm$10.	>15. [f]	=1.65	>15. [f]	0.059$\pm$0.14	>15. [f]
							70.	>15. [f]			0.67$\pm$.013	>15. [n]
SUM OF 7. ^{3}He POOR FLARES					(2) 1.5×10^{-2}	11.2-43.[b]						
SUM OF 5 ^{3}He RICH FLARES					(2) 3×10^{-2}	11.2-43.[b]						
6.4.71							68.$\pm$14.	15. [o]	1.49$\pm$.13	15. [o]	0.17$\pm$.08	15. [o]
2.9.71							36.$\pm$7.	" [f]	=1.65	" [f]	0.55$\pm$0.18	" [f]
							42.$\pm$2.5	" [o]	1.61$\pm$.04	" [o]	.028$\pm$.005	" [o]
							32.	" [n]			.03$\pm$.01	" [n]
							66.$\pm$12.	" [o]	=1.65	" [n]		
4.8.72							68.$\pm$2.	" [q]	1.63	" [q]	$^{16}_{Z}$ 0.07$\pm$.03	" [q]
							100.	" [r]			0.1$\pm$.025	" [r]
30.10 to 2.11.72	(1) 1.4×10^{-5}	3.1-30.6[a]	(2) $<9\times10^{-6}$	2.4-23.[a]								
EVENT(1972)											~ 6.5×10^{-3}	5.-14. [t]
											~ 3.7×10^{-2}	" [t]
											~ 2.5×10^{-2}	" [t]
											~ 7×10^{-2}	" [t]
											~ 4×10^{-1}	5.14. [t]
											~ 2.5×10^{-2}	" [t]
17.4.72											1.4×10^{-7}	10. [a,u]
											1.5×10^{-5}	3. [a,u]
											8.3×10^{-5}	1. [a,u]
											8.3×10^{-4}	0.3 [a,u]

TABLE 2.5 (Cont.)

EVENT	(1) D/H (2) D/H_e RATIO	ENERGY (MeV/nucl)	(1) T/H (2) T/H_e RATIO	ENERGY (MeV/nucl)	(1) ^3He/H (2) $^3He/^4He$ RATIO	ENERGY (MeV/nucl)	^4He/H RATIO	ENERGY (MeV/nucl)	CNO/O RATIO	ENERGY (MeV/nucl)	Fe/O RATIO	ENERGY (MeV/nuc
AVERAGE IN 1973	(1) $7.^{+10.}_{-6.}\times10^{-6}$	1.6-8.6[v]	(1) 3.4×10^{-6}	1.2-6.8[v]								
14.2.73					(1) $.05\pm.02$	2.9-15.[v]						
					(2) $0.2\pm.07$	" [v]						
26.6.73					(1) $.09\pm.04$	" [v]						
					(2) $\sim2.$	" [v]						
5.9.73					(1) $\sim1.$	" [v]						
					(2) $\sim6.$	" [v]						
20-23.2.74	(2) 0.02	0.6-1.6[w]	(2) 10^{-3}	0.6-1.6[w]	(2) 0.08	0.6-1.6[w]	0.1	0.6-1.6[w]				
20-21.2.74					(2) $0.38\pm.08$	2.2-2.6[x]	$0.14\pm.03$	4.8-6. [x]				
					(2) $1.\pm.2$	4.8-6. [x]						
					(2) $1.1\pm.2$	6.-13.8[x]						
					(2) >1.0	2.-2.7 [x]	$0.2^{+.24}_{-.09}$	" [x]				
18-19.4.74					(2) $<.06$	4.8-6. [x]						
					(2) $<.2$	6.-13.8[x]						
9-10.5.74					(2) $4.6^{+2.4}_{-1.6}$	2.2-2.6[x]	$0.2^{+.4}_{-.12}$	" [x]				
					(2) $7.4^{+10.}_{-3.4}$	4.8.6. [x]						
					(2) $2.1^{+1.8}_{-0.6}$	6.-13.8[x]						
7-13.5.74	(2) 0.04	0.6-1.6[w]	(2) 0.01	" [w]	(2) 1.06	0.6-1.6[w]	0.16	0.6-1.6[w]			3.67	0.6-1.6[w]
											$1.35\pm.24$	.7-4. [x]
14.5.74					(2) $0.21^{+.08}$	2.2-2.6[y]	$.05\pm.01$	4.8-6. [y]			$\sim1.$	2.1-2.6[x]
					(2) $0.06\pm.04$	4.8-6. [y]						
					(2) <0.1	6.-13.8[y]						
30.11 to 2.12.74	(2) 0.05	0.6-1.6[w]	(2) 0.02	" [w]	(2) 0.64	0.6-1.6[w]	0.14	0.6-1.6[w]			1.5	0.6-1.6[w]
					(2) $0.9\pm.4$	2.-2.7 [y]	$<.2$	4.8-6. [y]				
19-20.1.75					(2) $1.\pm.05$	2.-2.7 [y]	$0.9^{+.25}_{-.12}$	" [y]				
					(2) $0.25^{+.5}_{-.12}$	4.8-6. [y]						
					(2) $0.8^{+1.}_{-.4}$	6-13.8 [y]						
19.3.75					(2) $2.4\pm.5$	5.-10. [z]						
20.3.75					(2) $2.8\pm.8$	5.-10. [z]	$0.19\pm.08$	5.-10. [z]				

TABLE 2.5 (Cont.)

EVENT	(1) D/H (2) D/H_e RATIO	ENERGY (MeV/nucl)	(1) T/H (2) T/H_e RATIO	ENERGY (MeV/nucl)	(1) $^3H_e/H$ (2) $^3H_e/^4H_e$ RATIO	ENERGY (MeV/nucl)	$^4H_e/H$ RATIO	ENERGY (MeV/nucl)	CNO/O RATIO	ENERGY (MeV/nucl)	Fe/O RATIO	ENERGY (MeV/nuc
					(2) $0.55\pm.15$	5.-10. [z]	$0.19\pm.08$	5.-10. [z]				
22.3.75					(2) 1.66 ± 1.21	" [z]	$0.21\pm.14$	" [z]				
21-22.4.75					(2) $0.3\pm.2$	2.2-2.6 [y]	< .2	4.8-6. [y]				
29.10.76					(2) $0.7\pm.3$	2.2-2.6 [y]	$0.45\pm.16$	" [y]				
					(2) $0.48.\pm.25$	4.8-6. [y]						
					(2) $0.13^{+.15}_{-.05}$	6.-13.8 [y]						
31.12.76 to 1.1.77					(2) $0.35\pm.11$	2.2-2.6 [y]	< .33	" [y]				
					(2) $0.3\pm.2$	4.8-6. [y]						
					(2) $0.35\pm.15$	6.-13.8 [y]						
6.10.77					(2) $0.45\pm.25$	5.-10 [z]	$0.07\pm.02$	5.-10. [z]				
12-13.10.77					(2) $.13\pm.02$	2.2-2.6 [y]	$0.03\pm.002$	4.8-6. [y]				
					(2) $0.26\pm.02$	4.8-6. [y]						
					(2) $0.27\pm.02$	6.-13.8 [y]						
28.10.77					(2) $0.85\pm.23$	5.-10. [z]	$0.33\pm.07$	5.-10. [z]				
					(2) $0.64\pm.36$	" [z]	$0.13\pm.05$	" [z]				
6-8.12.77					(2) $1.0\pm.35$	2.-2.7 [y]	< .01	4.8-6. [y]				
					(2) 2.6	4.8-6. [y]						
					(2) .3	6.-13.8 [y]						
					(2) $0.48\pm.17$	5.-10. [z]	$.005\pm.001$	5.-10. [z]				
					(2) $0.39\pm.15$	" [z]	$.004\pm.001$	" [z]				
26-27.12.77					(2) $.92\pm.26$	2.2-2.6 [y]	$0.01^{+.01}_{-.004}$	4.8-6. [y]				
					(2) $1.1\pm.4$	4.8-6. [y]						
					(2) $0.7\pm.3$	6.13.8 [y]						
					(2) $0.4\pm.33$	5.-10. [z]	$0.19\pm.008$	5.-10. [z]				
					(2) $1.12\pm.37$	" [z]	$0.03\pm.01$	" [z]				
22.5.78					(2) $0.51\pm.07$	2.2-2.6 [y]	$0.3\pm.07$	4.8-6. [y]				
					(2) $0.42\pm.1$	4.8-6. [y]						
					(2) $0.4\pm.15$	6.-13.8 [y]						
19-20.9.78					(2) 1.0	2.-2.7 [y]						
23-24.10.78					(2) $1.1\pm.4$	2.2-2.6 [y]	<.1	" [y]				

TABLE 2.5 (Cont.)

EVENT	(1) D/H (2) D/He RATIO	ENERGY (MeV/nucl)	(1) T/H (2) T/He RATIO	ENERGY (MeV/nucl)	(1) $^3He/H$ (2) $^3He/^4He$ RATIO	ENERGY (MeV/nucl)	$^4He/H$ RATIO	CNO/O ENERGY (MeV/nucl)	CNO/O RATIO	Fe/O ENERGY (MeV/nucl)	Fe/O RATIO	ENERGY (MeV/nuc.
					(2) 2.	4.8-6. [y]						
3.11.78					(2) $0.7^{+.2}_{-.2}$	2.2-2.6[y]	<.33	" [y]				
					(2) $1.^{+1.}_{-.6}$	4.8-6. [y]						
					(2) $1.2^{+2.}_{-.8}$	6.-13.8[y]						
26-27.12.78					(2) $0.6^{+.2}_{-.2}$	2.2-2.6[y]	<.05	" [y]				

Notes and References to the TABLE

* Per) in Mev/amu

** Per H

. HELIOS 1

.. HELIOS 2

a) Cameron (1973), Meyer and Reeves (1977) and Meyer (1978)

b) Biswas et al (1962)

c) Shaeffer and Zahringer (1962)

d) Waddington and Freier (1964)

e) Hsieh and Simpson (1970)

f) Bertsch et al (1973)

g) Ramaty et al (1980)

h) Anglin et al (1973)

i) Garrard et al (1973)

j) Serlemitsos and Balasubramahnyan (1975)

k) Mc Donald et al (1975)

l) Anglin (1975)

m) Lanzarotti et al (1972)

n) Sullivan and Price (1973)

o) Teegarden et al (1973)

p) Biswas et al (1973)

q) Webber et al (1974)

r) Crawford et al (1975)

s) Rothwell et al (1973)

t) Mogro Campero and Simpson (1972)

u) Fleisher and Hart (1973)

v) Hurford et al (1975)

w) Bovestadt et al (1975)

x) Gloecker et al (1975)

xx) Gloecker et al (1976)

y) Mc Guire et al (1979)

z) Hempe et al (1979)

reactions were responsible of the enrichment, $^3He/D$ should also be present in the particle composition. Some suggestions have however been made to explain the absence of deuterium and tritium by their supression from the particle flux but, again, only events with small ^3He enrichment can be explained in this way.

The third characteristic of ^3He-rich events is that they are most likely associated with small flares or with no flare at all. Ramaty et al, (1980) plotted the $^3He/^4He$ ratio as a function of the maximum proton intensity (see Fig. 2.12).It is clear from there that small flares tend to have bigger $^3He/^4He$ ratios.

The fourth characteristic of these events is that, together with ^3He, there are enhancements in heavier elements, iron in particular. This is shown in the Fig. 2.13 taken from Anglin et al., 1977 where the ratio $fe/^4He$ is plotted as a function of the ratio $^3He/^4He$. This fact presents a further difficulty for the nuclear models which do not provide an explanation for such an enhancement. It must be noticed that some events in which heavier elements are present do not necessarily show an enrichment in ^3He. As noted from the figure for events with $^3He/^4He$ ratios of only 10%, the correlation between ^3He and iron enhancements is not very good.

Fig. 2-14 taken from Ramaty et al (1980) shows very clearly the fifth characteristics of ^3He-rich flares.

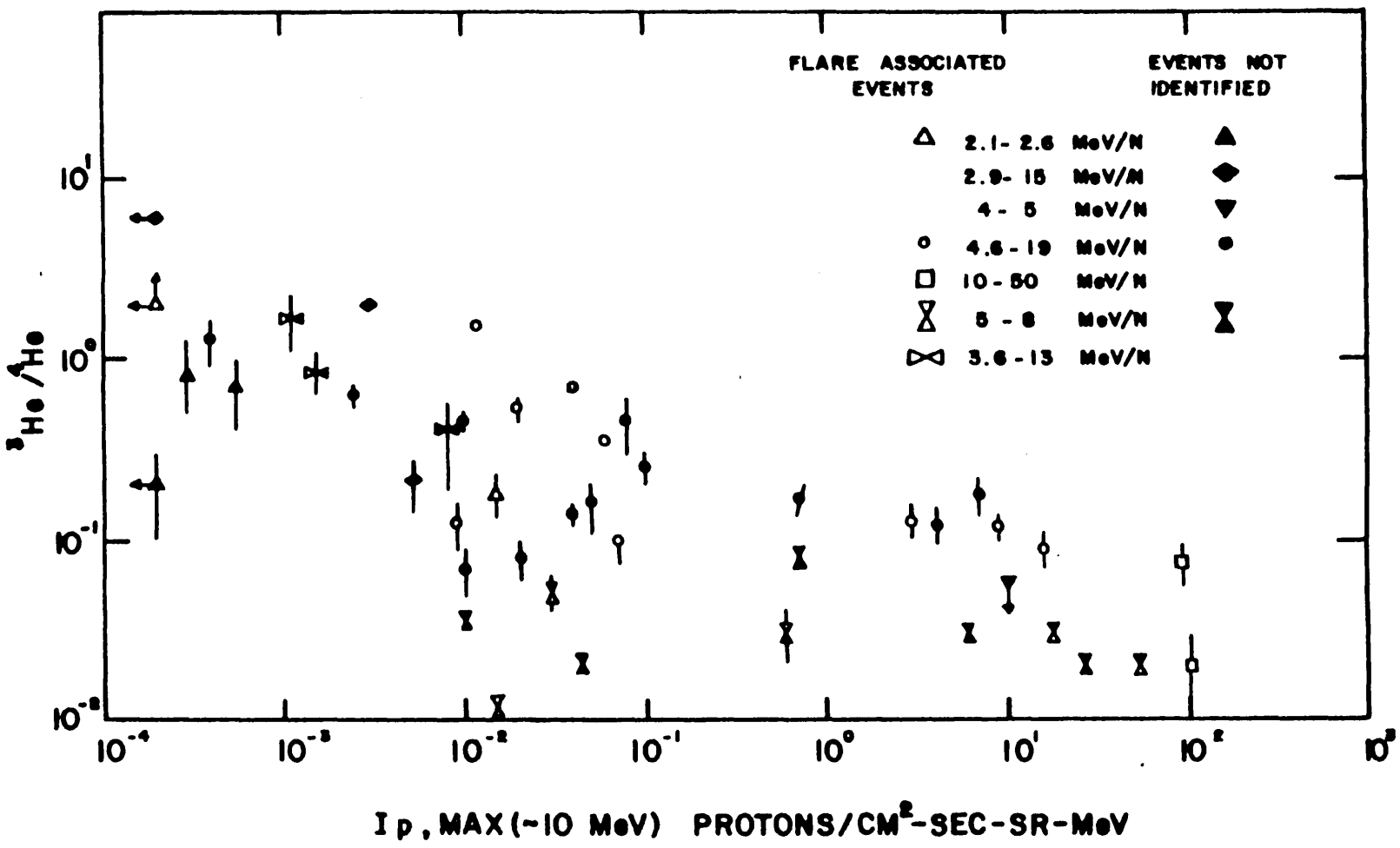


Fig. 2.12 - The ratio $^3He/^4He$ measured at varius energies as a function of maximum intensity of the event (Pamaty et al, 1980)

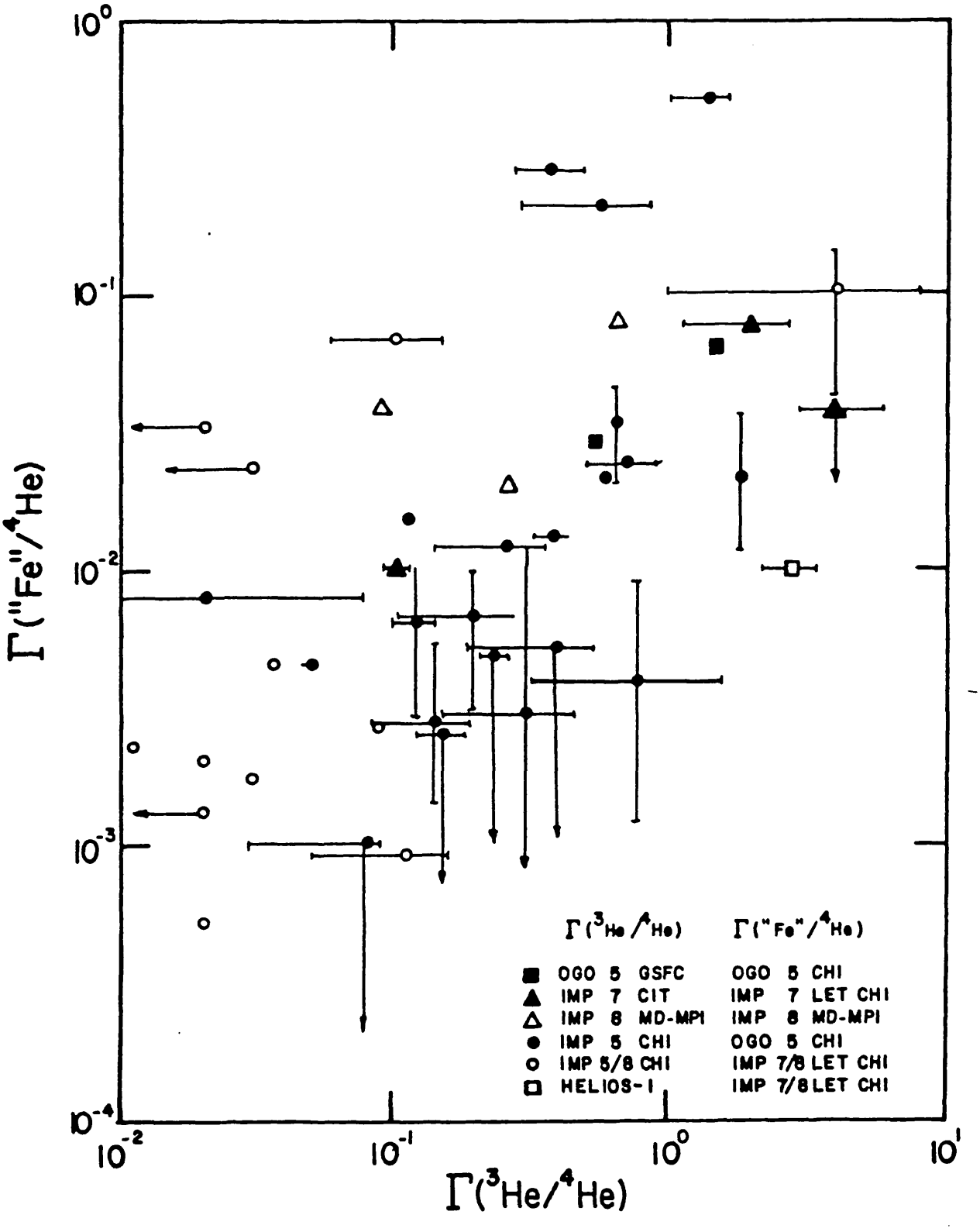


Fig. 2.13 - The ratio Fe/^{4}He as a function of ^{3}He/^{4}He (Anglin et al, 1977).

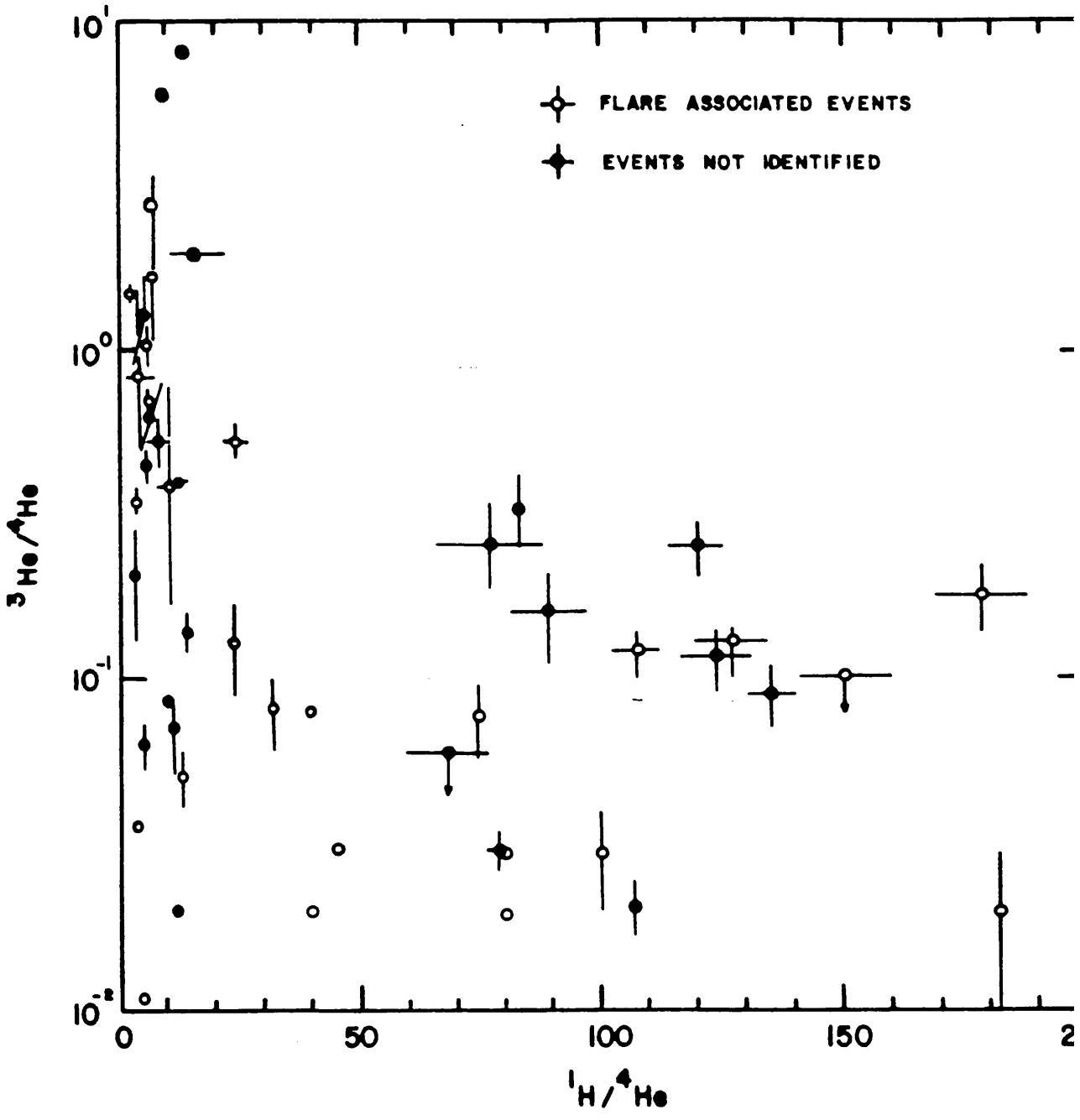


Fig. 2.14 - The ratio $^3He/^4He$ as a function of the ratio $H/^4He$ for all available energies (Ramaty et al, 1980).

TABLE 2.6 - ENERGY SPECTRA OF ^3He AND FOR SEVERAL ^3He-RICH SOLAR EVENTS.

EVENT DATE	POWER LAW EXPONENT $\gamma_{^4He}$	POWER LAW EXPONENT $\gamma_{^3He}$	RATIO $^3He/^4He$	ENERGY RANGE MeV/Nucleon	REFERENCE
Aug. 4 1972	2.65±0.03	1.35	$(1.7 \pm 0.6) \times 10^{-2}$	50 - 70	Webber et al (1975)
Jan.25, 1971	3.5 ± 0.3	2.1 ± 0.8	$(2 \pm 1) \times 10^{-2}$	10 - 50	Dietrich (1973)
Flare Sum	~3	1.8	$(2.1 \pm 0.4) \times 10^{-2}$	10 - 100	Hsieh and Simpson (1970)
Nov. 2, 1969	3.5 ± 0.2	1.9 ±0.6	$(7.7 \pm 2) \times 10^{-2}$	10 - 50	Dietrich (1973)
Oct. 14, 1969	~3	~3	0.33 ± 0.08	10.5 - 22.1	Anglin (1975)
May 29, 1969	3.24 ± 0.05	3.24 ± 0.05	0.35 ± 0.03	4.6- 19	Serlemitsos & Balasubrahmanyan (1975)
July 30, 1970	~3	~3	0.54 ± 0.09	10.5- 22.1	Anglin (1975)
May 29, 1969	3.55 ± 0.12	3.69 ± 0.12	0.71 ± 0.06	4.6- 19	Serlemitsos & Balasubrahmanyan (1975)
May 29, 1969	4.16 ± 4.04	4.04 ± 0.1	1.52 ± 0.1	4.6- 19	Serlemitsos & Balasubrahmanyan (1975)

In it, the ratio of ^3He to ^4He is plotted against the ratio of H to ^4He for several events some associated with flares and others not associated with them. The ^3He-rich event seem to be associated with high abundance of ^4He in the ambient plasma. Note that, as it was finally noticed by Kocharov and Kocharov (1978) the enrichment factors of ^3He and heavy elements may change in time during the same solar event.

The sixth characteristic of ^3He-rich event is that they are always accompanied by X-ray and radio burst emission (Kocharov and Kocharov, 1978). According to the same authors the events have a frequency of 3-4 times per year and they can occur at any time during the whole 11-year cycle of solar activity.

Nevertheless, not all the events behave according to these characteristics. In particular, there are some ^3He-rich events which do not present high abundance of ^4He. Furthermore, there is the fact that for events with large $^3He/^4He$ ratios the respective spectra of the two isotopes are parallel, while for events with small $^3He/^4He$ ratios the ^3He spectra is flatter than ^4He spectra (see table 2.6). This has led Fisk (1978 b) and Ramaty et al, (1980) to believe that there are two kinds of ^3He-rich events: dramatic events where the $^3He/^4He$ ratio is $\sim$ 1 and less dramatic events where $^3He/^4He$ ratio is about 0.1 These

classification is illustrated in table 2-7.

In the 2nd. Skylab Workshop on solar flares Ramaty et al (1980) proposed that even though nuclear reaction are incapable of explaining the dramatic events, they could explain the less dramatic events. On the other hand there is of course the proposition by Fisk (1978 b) that the less dramatic events are nothing more than dilute forms of the more dramatic events.

The important points which have arisen from the results presented in this Chapter can be summarised as follows:

1. Solar flares and related phenomena are always associated with regions exhibiting a strong, bipolar magnetic field structure (the loops) with non potential microstructure (Tandberg-Hansen et al, 1984).
2. The nonthermal emission associated with active regions is not restricted to the flare. Flare precursors are common and there are events with no flare association.
3. X-ray events can be classified in Impulsive one burst in hard X-rays) and gradual (more than one burst in hard X-rays) the latter involving more energy dissipation.

TALE 2 - 7. ^{3}He-RICH SOLAR EVENTS (FISK, 1978)

DRAMATIC EVENTS	LESS DRAMATIC EVENTS
$^{3}He/^{4}He \sim 1$	$^{3}He/^{4}He \sim 0.1$
$D/^{3}He$ < few %	$D/^{3}He$ < 10%
VERY SMALL EVENTS	SOMEWHAT LARGER EVENTS
IRON ENHANCEMENTS	IRON ENHANCEMENTS NOT AS OBVIOUS
$H/^{4}He$ < 30	$H/^{4}He$ > 50

4. There is evidence of electrons streaming in the flare region to produce type III radio burst from the foot points of the loop and type V radio burst from the top of the loop (see Petrosian and Leach, 1983).
5. Gamma-ray-line flares are well correlated with the presence of high energy protons (observed directly in space and indirectly through type IV bursts) as well as with shock waves (type II bursts).
6. The most common type of events are the PE events, followed by the mixed events which include relativistic electrons and energetic ions, and only rarely there are GLE events which include also relativistic ions.
7. There are flares for which the particle composition is anomalous with respect to that of the photosphere. Mainly ^{3}He, $Fe^{+11,12}$ and to a lesser extent Ne, Mg, Si, O S and $Fe^{16,17,18}$ are overabundant, while C is sometimes underabundant.

CHAPTER 3

THE ROLE OF ENERGETIC PARTICLES IN THE SOLAR FLARE.

The difficulties in explaining the Solar Flare process by assuming the conventional view that only the conversion of magnetic energy into solar flare energy can be responsible for this complex phenomenon, has led us to reexamine the problem on the basis of a model developed over the last 20 years, mainly by Elliot (1964,1969,1973). The model proposes that particles can be continuously accelerated in the trapping magnetic field of a bipolar active region. The basic requirement is to show that an efficient stochastic mechanism of acceleration can counteract the particle loss through the loss cone of the magnetic field and at the same time increase the particle energy density in the trap up to the limit imposed by the magnetic field pressure. The instability which will lead to the catastrophic release of the particles into the solar atmosphere, and to a lesser extent to space, can be triggered either by the emergence of new flux to the loop or by the heating of the chromosphere. In the latter case, an invasion of "cool" plasma into the trapping region can suddenly decrease the Kennel and Petschek's limit

for stable trapping.

The behavior of the particles in the magnetic field loop above active regions can better be understood by looking at the flow diagram in Fig. 3.1. In the upper part of the diagram we have put the coronal plasma particles, the main source of trapped particles in the magnetic field loop. These two particle populations are connected through the mechanisms of scattering: the Coulomb scattering comes from the same plasma particles, the magnetic scattering from irregularities in the magnetic field, and the hydromagnetic turbulence from plasma instabilities. The interaction of the trapped particles with mhd waves which are continuously being produced in the convective zone may give rise to a Fermi mechanism (type I or II) of acceleration with an eventual anisotropic flux of particles at the loss cone of the magnetic field. The particles which escape downwards produce nuclear reactions as they interact with the chromospheric material. The secondary products (deuterium, tritium and helium-3) are either lost to the denser atmosphere below or go outwards with the result that some become trapped in the magnetic field. However, the anisotropic flux at the loss cone is unstable and so tends to excite plasma turbulence, which produces energy dissipation and contributes to the heating of the plasma at the foot-

PARTICLE BEHAVIOR IN ACTIVE REGIONS.

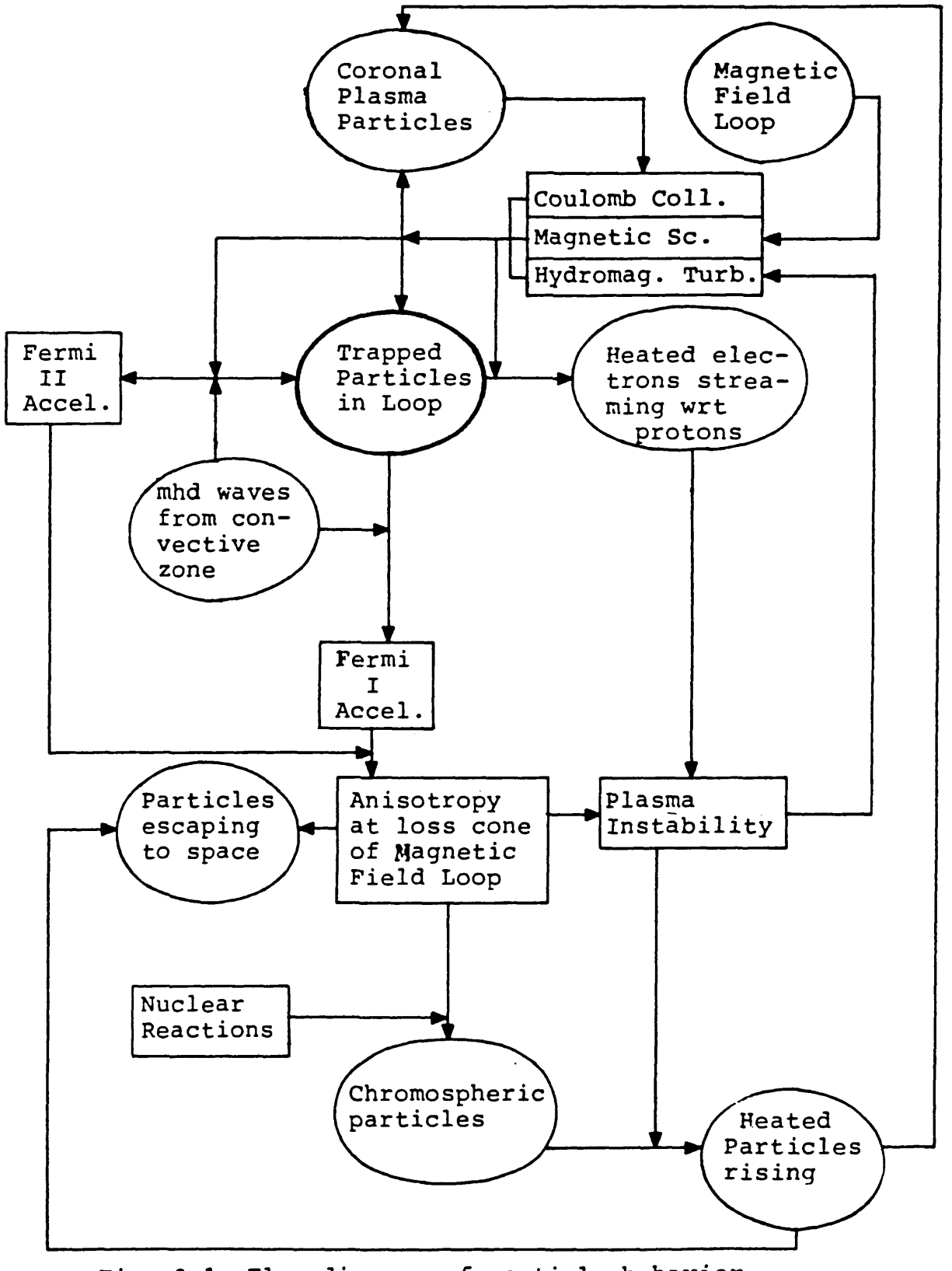


Fig. 3.1. Flow diagram of particle behavior in the Active Region.

points of the magnetic field loop. As the chromospheric heating becomes more intense, some material tends to rise thus increasing the density in the loop, increasing the rate of particle precipitation down the legs of the loop, and producing more heating at the footpoints. Accordingly, this instability could lead to a flare. It becomes clear then that the source of particles and energy into the trapping region is highly dependent of the scattering process in operation, the former by taking particles from the ambient plasma and the latter by making the acceleration more efficient.

As the mhd waves which are produced in the convection zone travel upwards, meet with the particles in the trap and, if the energy of the particles is above the threshold, accelerate them by a Fermi type of mechanism. Otherwise, the process is one of bulk energization. Although the direct mechanism of acceleration is very ineffective for the energization of the trapped particles, it strongly contributes to the turbulence and therefore to the scattering. Notice then that the scattering due to hydromagnetic turbulence (ion cyclotron waves and magnetoacoustic waves for ions and Langmuir waves for electrons) becomes efficient once there is substancial streaming. Since this does not necessarily happens in the early

stages of the building up of the trapped energetic particle population, it means that both Coulomb collisions and magnetic scattering by irregularities in the magnetic field are very important for the acceleration. Although very little is known about the magnetic irregularities, we have studied here theoretically those cases in which this kind of scattering ought to be considered.

In order to study the flare process from the energy build up to its release into the atmosphere and outer space, we have examined the behavior of protons (ions) and electrons separately. It is precisely this difference in behavior of one type of particles with respect to the other which permits the development of the instabilities and leads to the observed features from active regions and flares. The study of the overabundances observed in the solar flare particle flux, in the context of the model, concludes this Chapter.

Recently, Simnett and Ryan (1985) have proposed a similar model in which the pre-flare acceleration of ions can explain the optically small γ-ray flares.

3.1. Coronal Heating and Magnetic Structure.

The heating of the Corona has been extensively studied for several years now. However, it was realized only during the last decade that the heating might be most important in the coronal loops above active regions. In fact, EUV and X-ray observations of the Sun by Skylab revealed that the Corona is not homogeneous but is structured by intense closed magnetic fields in the form of loops (Withbroe and Noyes,1977; Vaiana and Rosner,1978) which are hotter and denser than the surroundings (cf. Smith et al,1977; Rust,1978). Furthermore, most of the coronal emission comes from them (Sakurai and Granik,1984). The heating of regions in which a strong magnetic field is present was studied by Billings and Saito (1964). In 1970, Vaiana, Krieger and Speybroeck,were able, with the aid of X-ray observations of the Corona, to reveal the connection between the emitting regions and the presence of strong magnetic fields. Subsequent studies involving the X-ray imaging by rockets (van Speybroek et al,1970; Vaiana et al,1973) and Skylab (Mc Intosh et al,1976) have only emphasised the importance that the magnetic field of coronal loops have as a reservoir where a substantial amount of the coronal heating takes place (see reviews

by Heyvaerts and Schatzman,1980; Chiuderi,1981,1983; Kuperus et al,1981; Wentzel,1981; Priest,1982; Golub, 1983, and the recent works by Hollweg,1984; Sakurai and Granik,1984).

There seem to be two types of loops. "Cool" loops in which the temperature is 10^4 to 10^5 K, and "hot" X-ray loops with temperatures of approximately 2.5×10^6K. The stability of the hot loops has been studied by Martens and Kuperus (1983). They found that the X-ray brightenings that are sometimes observed from coronal loops are thermal in origin with no magnetic reconnection. Levine and Withbroe (1977), on the other hand, have observed that when new magnetic flux emerges into the loop, or the length of the loop decreases a flow or surge of plasma occurs from the top of the loop down to its footpoints. So, Martens and Kuperus argue that the temporal behavior of the loops can be understood as catastrophic changes in the thermal properties of the system. From this, there seems to be strong grounds to believe in the idea that the coronal plasma can become trapped in the loop structure and be heated afterwards by some kind of magnetic shearing (see the recent papers by Ionson,1982; Hollweg,1984; Sakurai and Granik,1984). Furthermore, in the X-ray studies by the Einstein Observatory (reviewed by Vaiana,1983),

for stellar objects, two important results are evident. For late-type stars there is a high correlation between stellar rotational velocity (Pallavicini et al,1982), as well as CaII emission strength (Mewe and Zwann, 1980; Vaiana,1981; Pallavicini et al,1982) and the X-ray emission. These results strongly support the hypothesis that the plasma heating process leading to soft X-ray emission in late-type stars is a consequence of the magnetic field coupling with the surface turbulence. This, in turn, supports the solar observations (Rosner and Vaiana,1980) that the coronal heating is a magnetic field related process. There is one important thing which is lacking, however. No measurements of the fine structure of the coronal magnetic field exist at present. This implies that for some time yet we have to rely only on theoretical studies of the microstructure of the field and its role in the behavior of the plasma. We deal with this problem in section 3.2.2.2.

3.2. Possible Acceleration Mechanisms in Flares.

A great controversy still persists concerning one of the most fundamental problems intimately related to Solar Flares, i.e., what is the mechanism for the production of the high energies that particles have been observed to have acquired in the flare.

Perhaps the most generalized idea in this respect is that probably there is not a single process which, by itself, can explain the acceleration of those particles (see Wild et al,1963). Instead, the acceleration is believed to take place mainly in two stages: one which heats the particle population to just above a certain energy threshold after which a different process leads the particles to relativistic energies (see Svestka,1966; de Jager,1968). The principal reason for this suggestion comes from the number of different particle populations that the flare seems to produce (Ramaty et al,1980). In fact, it used to be believed that only the most intense flares were able to generate energetic particles, but with the advent of more sensitive detectors on board of satellites (like ISEE-3), detectors capable of measuring particles with energies as low as few kev, it has been shown that even very small flares can produce energetic particles.

From the number of possibilities offered for the acceleration of the particles one has to distinguish between basically two types of mechanisms. Those called deterministic, in which the acceleration is continual and direct, and those called indeterministic, whose principal characteristic consists of a process which is stochastic in character. The second type is believed to be more realistic and also more efficient. For the direct acceleration some extreme conditions must be fullfilled by both the field and the particles; mainly the magnetic field should be constrained to only certain directions of motion.

In this classification there is no possibility of distinguishing between those situations in which particles are free to move around and those in which there is a kind of confinment. If a magnetic field with containment properties is introduced the situation changes radically. In such case, there will be both direct and stochastic mechanisms of acceleration but the confinment time will depend on the physical characteristics of the region in consideration, in a manner similar to the free moving case but different in that the containment properties can vary.

In general one says that a population of particles

can be accelerated if the rate of acceleration is greater than the rate of energy loss. Nevertheless, for the case in which the particles are trapped in a magnetic field, this condition, although necessary, is not sufficient. The reason is that if the acceleration mechanism is all the time more efficient than deceleration or particle loss then the mechanism itself becomes very inefficient because, in absence of collisions, the acceleration makes the flux anisotropic and thus the magnetic field fails eventually to preserve the containment of the particles.

Basically only two theories of particle acceleration have been proposed: magnetic pumping or betatron acceleration first proposed by Swann (1933) and later modified by Schlüter (1957) and Berger et al (1958) and the Fermi mechanism I type of acceleration, in which particles are accelerated by approaching magnetic reflectors (Fermi,1949, 1954). A number of modified versions of this theory have been proposed. For instance, Thompson (1955) and Kaplan (1956) suggested that the acceleration was performed by hydromagnetic waves; and Thompson (1955), Davis (1956), Parker (1958), and Parker and Tidman (1958) found that a proper scattering mechanism should to be present to make acceleration more effective. Although extensive work has been advocated to these two theories, there is still, of course, no guarantee that the cor-

rect acceleration process which can explain satisfactorily the origin of cosmic rays both solar and galactic is now available. Nevertheless, it seems that at least and rather than search for a different model, what we have to look for is a better understanding of the physics underlying the situation in which energetic particles are originated and only then choose the best model. For example, in the case of the flare, an understanding of the process is more important than the acceleration mechanism itself because it is the knowledge of the flare phenomenon which will bring us closer to the solution of how the particles are accelerated. Although I believe this to be correct in the sense that the acceleration process is extremely model dependent, I restrict myself in this section to a description of the most important theories for the mechanisms of particle acceleration and leave for the next section the model which best correspond to the particle model of solar flares.

3.2.1. The first phase of acceleration.

Rather than being a proper acceleration, the so-called first stage of acceleration consists of a heating process which increases the energy of the whole particle velocity distribution. In this sense, it actually constitutes a thermal process which enhances the high energy tail of the distribution, so that those particles which are above the energy threshold for acceleration, are injected into the acceleration mechanism proper wherupon they can reach relativistic energies. The possible energization process can be of three types: bulk energization, in which the energy gain is collision dominated; Fermi I type of acceleration, in which the particles are accelerated freely; and acceleration by hydromagnetic turbulence (Fermi II type), in which a good coupling between acceleration and scattering provide the necessary efficiency.

It should be argued that, whatever the process invoked for the energization of the particles, a considerable fraction of the energy available goes into heat rather than acceleration (Brown and Smith,1980). In order to explain the relativistic energies observed, a second stage of acceleration by Fermi mechanisms presents then no difficulty if the wave energization works as an injection mechanism.

3.2.2. The second phase of acceleration.

With respect to the second stage of acceleration, the theoretical work has evolved in such a way that turbulence seems to provide both the necessary scattering for maintaining the particle flux nearly isotropic, and the proper acceleration of the flux. In this way, both energy loss and acceleration become a diffusive process as is described by Parker and Tidman (1958) and Tverskoi (1967), where the distribution of particles can be described by the Fokker-Planck equation

$$\frac{\partial N(E)}{\partial t} = \frac{1}{\tau_a} \{- \frac{\partial}{\partial E} (\frac{v}{c} EN(E)) + \tfrac{1}{4} \frac{\partial^2}{\partial E^2} [(\frac{v}{c})^3 E^2 N(E)]\}, \quad (3\text{-}1)$$

where $N(E)$ is the number of particles with energy E, τ_a is the acceleration time and v is the particle velocity. Kulsrud and Ferrara (1971) noted that the equation can be written in the form of an isotropic diffusion equation in momentum space as

$$\frac{\partial f(p)}{\partial t} = \frac{1}{p^2} \frac{\partial}{\partial p} (p^2 D(p) \frac{\partial f(p)}{\partial p}) \quad (3\text{-}2)$$

where $f(p)$ is the particle distribution function and $D(p)$ is the diffusion coefficient. These authors also

showed that if κ and ω are the wave number and wave frequency, respectively,

$$D(p) = p^2 \int \frac{d^3\kappa\, d\omega}{(2\P)^4} \gamma\ (\kappa,\omega)\ \frac{<\delta B\ (\kappa,\omega)\, \delta B^*\ (\kappa,\omega)>}{Bo^2} \qquad (3\text{-}3)$$

where $\gamma\ (\kappa\ ,\omega\ )$ is the rate of acceleration, B is the magnitude of the magnetic field and $\delta B(\kappa\ ,\omega\ )$ is the Fourier transform of the magnetic fluctuations associated with the turbulence. Notice that γ depends on ν, the rate of scattering, and that, as Melrose (1974) proposed, ν adjusts itself to satisfy Kulsrud and Ferrara's theory. Basically the proposition is that the turbulence causes the particles to become anisotropic, and these, in turn, generate the resonant waves which scatter them. The resulting rate of acceleration for $\frac{\omega}{\kappa} = v_A$ is

$$\gamma\ (\kappa,\omega) = \frac{\P}{2}\ \omega\ \frac{v_A}{v} \qquad (3\text{-}4)$$

which is independent of ν and essentially the same as the one occurring in the early theories of Fermi acceleration.

The plausibility of this mechanism in solar flares has been examined by (Ramaty et al,1980). Their results are summarized in Figure 3.2. The energy losses for

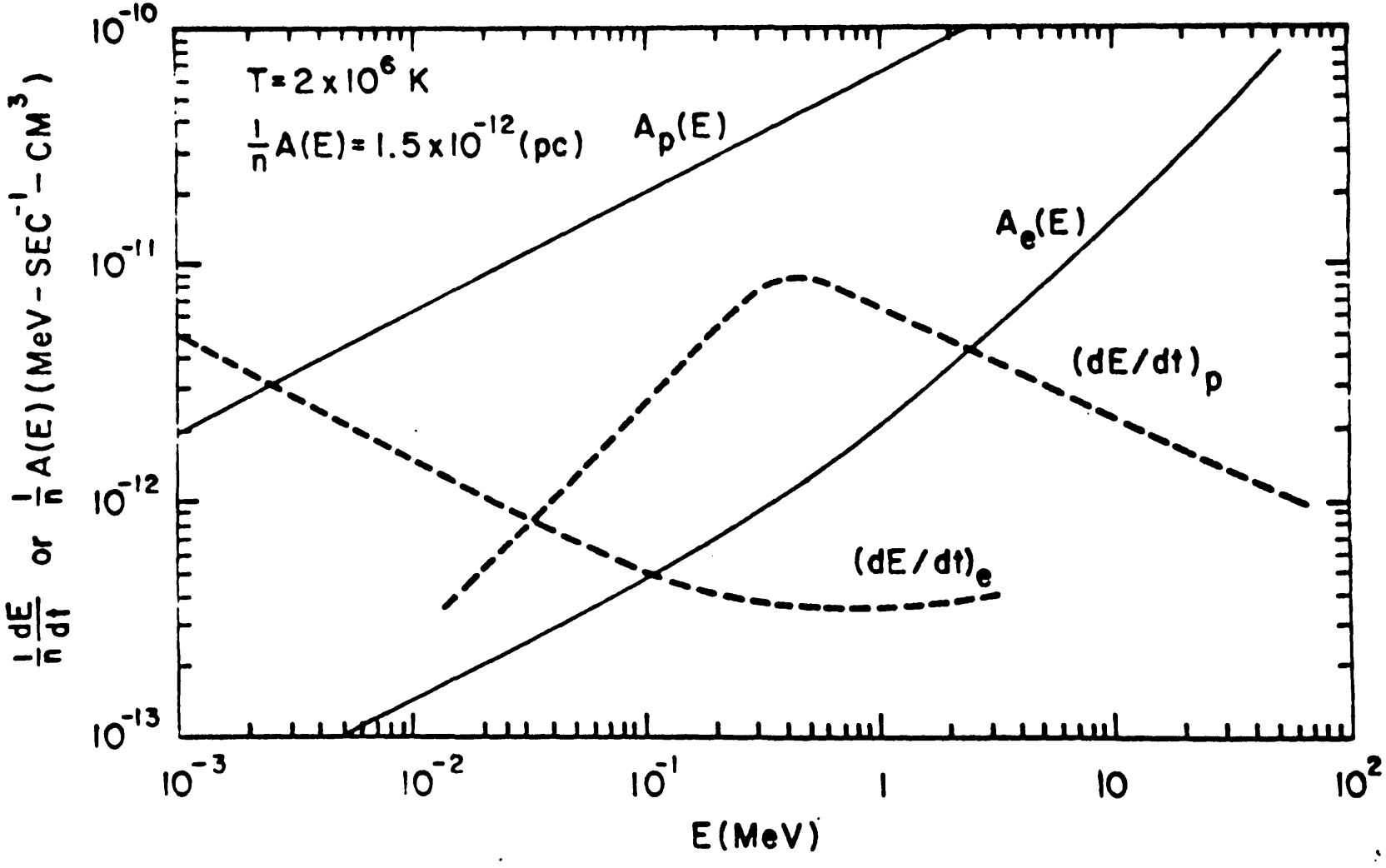


FIG. 3.2. Particle acceleration and energy loss for protons and electrons as a function of energy

protons and electrons are $(dE/dt)_{p,e}$ and the rate of energy gain are given by $A_{p,e}(E)$. It is found that electrons from the high energy tail of the first phase mechanism could be injected into the second phase acceleration at about 100 keV, energy at which $A_e(E)$ exceeds $(dE/dt)_e$. Concerning the protons, the only injection condition is $v >> v_A$ since $A_p(E) > (dE/dt)_p$ at all energies, and this can be satisfied by ambient protons in the high energy tail of the Maxwell-Boltzmann distribution.

3.2.3. Acceleration by shocks.

Apparently, the acceleration of particles to relativistic energies is only possible in shock waves in the same manner as it is supposed to happen in supernova remnants (Hartquist and Morfill, 1983).

The first attempts to deal with theoretical aspects of shock acceleration were made by Dorman and Freidman (1959), and Shabansky (1961) on the one hand, Parker (1963), Wentzel (1962, 1964) and Hudson (1965) on the other, all considering scatter free acceleration i.e. scattering is neglected and particles interacting with shocks approximately conserve their magnetic moments (Parker, 1958; Alexeyev and Kropotkin, 1970; Sarris and Van Allen, 1974; Pesses, 1981; Chirkov et al, 1981; and Toptygin, 1980). Thus

$$\frac{P_{\perp 1}^2}{B_1} = \frac{P_{\perp 2}^2}{B_2} \qquad (3\text{-}5)$$

where subscripts 1/2 refer to upstream/downstream conditions respectively and p is the particle momentum.

Cosmic ray spectra have been calculated by García Muñoz, Mason and Simpson, (1975 a, b) after extensive studies taking into account the effects of

solar modulation and assuming energy independent propagation. The best result is a power law $dJ/dT \alpha (T + 400\ MeV)^{-2.6}$ at energies below a few GeV. This kind of spectrum seems to be consistent with shock acceleration as reviewed by Axford (1981). The general results are:

a) the acceleration mechanism involves momentum rather than rigidity because the particle changes momentum at each crossing due to the relative motion of shocked and unshocked material; b) a power law spectrum is obtained with the higher energy particles traversing the shock many times; c) when more than one shock is present the spectrum is determined by the strongest shock; and d) the maximum energy which particles can gain depends on the trapping time near the shock front.

The propagation effect of these particles have been studied by Ormes and Protheros (1983). Although their results appear to be inconsistent with the most recent electron spectra observations of Nishimura et al. (1980), Prince (1979) and Mauger (1981), they argue that shock acceleration is nevertheless possible.

However, in the solar case the finite time which is necessary to form the shock is highly inconsistent with observations, Nevertheless, recent observational evidence by the SMM indicating a delay of 3 s between the time profile of hard X-rays above 253 keV and the

time profile of lower energy X-rays. This has made Bai et al (1983) to propose that second-step acceleration takes place at the flash phase and furthermore, that First-order Fermi acceleration induced by a shock wave is responsible for this second-step. The shocks are supposed to be produced by the sudden heating of the chromosphere by the energetic electrons responsible of the hard X-ray burst, they travel upwards and mett the particles in the loop accelerating them to MeV energies (see also Smith and Brecht, 1984).

3.3. The Acceleration Mechanism in the Context of the Energetic Particle Model.

It has already been pointed out in the preceding chapter that the sunspot field should be able to store particles and therefore the acceleration of these particles is possible in principle. The reason for this is that even if the acceleration is a very slow process there is no reason to doubt that the particle flux can acquire a substantial amount of energy provided, of course, that it can be injected into the acceleration mechanism.

In the context of the energetic particle model the picture in which the first stage of acceleration takes place is very simple because the particle population is already present and can be heated in the same way that the corona is heated by taking part of the wave energy originated in the convection zone (see the review on wave generation by Stein and Leibacher, 1981 and the papers by Ionson 1982, Hollweg, 1984 and Sakurai and Gramik, 1984). The mechanism is perhaps identical to the production of the solar wind with a difference; in our case a substantial amount of the energy remains trapped in the particles flux.

Once the energy threshold for a second stage of acceleration is reached, the particles can be accele-

rated further to higher energies. The relevant process is then the scattering because, in absence of collisions, the flux tends to anisotropy and we have a poor efficiency of acceleration. The scattering can be of two types: electric (coulomb collisions) or magnetic (wave-particle interactions).

As we shall see in section 3.3.2., the scattering is coupled to acceleration in a diffusive manner which will tend to make the acceleration more efficient. However, different scattering processes interact differently with the particle population and most likely act in different ranges of energy. Thus since scattering is most important in shaping the source spectrum, it is essential to know the range of action of the different scattering mechanisms.

3.3.1. The energy balance in the Active Region (AR).

The structure of the corona is largely determined by the magnetic field (see for instance Zirker, 1981 and Wentzel, 1981). In fact, in X-ray images of the solar corona (Vaiana et al.,1973) it is possible to identify the brilliant regions with regions of closed magnetic field. It is clear that in such regions the energy balance involves not only the source of energy and the radiation but it also implies the accumulation of energy in the plasma. As the plasma is heated, an acceleration mechanism can be implemented for those particles which have an energy beyond certain threshold. The problem of finding the energy threshold has been extensively studied (Ginzburg and Syrovatskii, 1957; Parker, 1963; Korchak and Syrovatskii, 1959). It can be obtained by simply equating the energy gain with the energy loss. Assuming Fermi acceleration and Coulomb loss then

$$E_i = \frac{4\pi e^4 z^2 n_e \Lambda \tau_a}{m_e v}, \qquad (3\text{-}6)$$

where τ_a is the characteristic time of the acceleration, m_e and n_e are the mass and number density of the electrons in the medium, v is the particle velocity, and $\Lambda = \ln (2 mv^2/h\omega_e)$, ω_e being the plasma frequency (Korchak and Syrovatskii,1958). It should be noticed that

this energy does not imply free acceleration but only that above this threshold the energy diffusion equation can be applied provided we know the rate of acceleration and diffusion.

If we start with a particle distribution which is Maxwellian in form, only the few particles in the tail of the distribution which are above E_i can be accelerated. Nevertheless, wave energy is continuously flowing upward from the convective zone and part of that energy can be deposited in the loop by bulk energization. So for particles below the threshold the acceleration process is in reality a heating process.

The energetics of a coronal loop with a volume of the order of 10^{27} cm^3, a number density of $3X10^9$ cm^{-3}, and a magnetic field of about 200 gauss, on average, can be written as follows

$$E_H = E_R + \nabla \cdot F_C + \nabla \cdot F_V \,, \qquad (3\text{-}7)$$

where E_H is the rate of mechanical energy density deposited in the loop, E_R is the radiative loss rate, F_C is the conductive flux and F_V is the energy flux resulting from mass loss.

If we assume that the rate of energy deposited in the AR is due to waves, then

$$E_H = \frac{F_{P'}}{v_W} \,, \qquad (3\text{-}8)$$

where F_W is the energy flux carried by the waves and v_W is their velocity.

If we now assume that the microturbulence is a measure of the wave amplitude (see Athay, 1981) then the energy flux is

$$F_W = \tfrac{1}{2} \rho \, V_a^2 \, V_p \, , \qquad (3\text{-}9)$$

where ρ is the density 2×10^{-8} gr cm^{-3}; V_a is the microturbulent velocity which is of the order of 10^5 cm s^{-1}; and V_p is the wave propagation speed, which in the case of sound waves is also of the order of 10^5 cm s^{-1}. Hence,

$$E_H \simeq 100 \text{ erg cm}^{-3} \text{ s}^{-1}. \qquad (3\text{-}10)$$

Only a fraction of this energy is deposited in the active region. In fact, mhd waves have been detected by Wentzel (1978) and Hollweg (1981) but the uncertainty of the measurements is still considerable and therefore we prefer here to avoid going into the details but show that the particle energy distribution in the loop can be heated by the waves from the convective region with the result that there are every time more particles injected into the acceleration mechanism.

3.3.2. The role of scattering in the acceleration.

As we mentioned in the last section, once the particles are above the injection energy they can be accelerated diffusively in phase space. In the treatment of the diffusion equation of Kulsrud and Ferrari (1971) by Melrose (1971, 1974) it was required that the turbulence time scale be shorter than the acceleration time for proper coupling between acceleration and scattering to take place. However, it should be remembered that the efficiency of this mechanism requires a large anisotropy of the particle flux. In resonant scattering theory the anisotropy must be defined in terms of the resonant velocity, V_R (the velocity at which the Doppler resonance condition $k_{\parallel} v_{\parallel} = \Omega$, where Ω is the cyclotron frequency eB/mc, is satisfied). (See, for instance, Kennel and Petschek, 1966; and Melrose, 1980). However, according to Kennel and Petschek (1966) for the special case of a velocity distribution that is a product of two Gaussians with different temperatures for perpendicular and parallel velocities, the anisotropy (A) is independent of V_R and can be written as

$$A(T_{\perp}, T_{\parallel}) = \frac{T_{\parallel} - T_{\perp}}{T_{\parallel}} \qquad (3\text{-}11)$$

What we want to show is that the time required for a

particle distribution to acquire a large anisotropy in the presence of acceleration is very short, so that in absence of a proper scattering the energy gained is limited to small values. In fact let us assume that the rate of acceleration can be written as

$$\frac{dE}{dt} = \frac{E}{\tau_a} , \tag{3-12}$$

where τ_a is the characteristic time of the acceleration. If τ_a is constant, we can integrate the equation and obtain

$$\frac{t}{\tau_a} = \ln \frac{E}{E_i} = \ln \frac{p^2}{p_i^2} , \tag{3-13}$$

where p_i is the injection momentum and t is the total time of the acceleration. Now, if we assume that above the injection energy collisions are due to the Cerenkov resonance with longitudinal waves, preserving $V_\perp$ = constant, so that $V^2 = V_\parallel^2 + V_\perp^2$ and $V^2_i = V^2_{\parallel i} + V_\perp^2$. Therefore,

$$\frac{V^2}{V_i^2} = \frac{V_\parallel^2 + V_\perp^2}{V^2_{\parallel i} + V_\perp^2} \tag{3-14}$$

We can use the expression for the anisotropy in (3-11) to express $V_\parallel$ in terms of $V_\perp$, approximately. Then

$$V_\parallel^2 \sim \frac{V_\perp^2}{1 - A} , \tag{3-15}$$

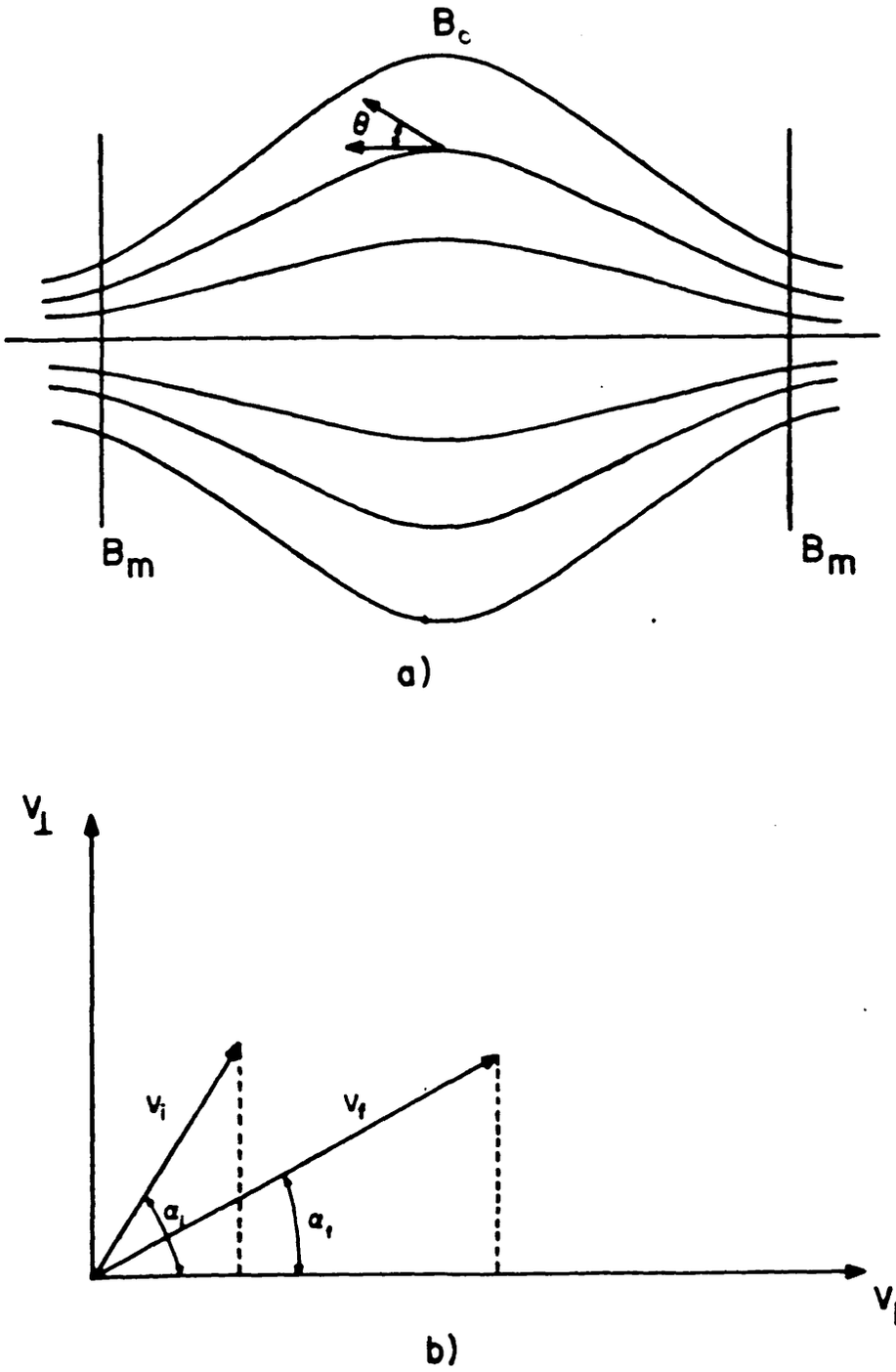


Fig. 3.3. a) Simplified Magnetic Field configuration of Active Region.

b) Velocity change for acceleration process in absence of collisions, such as Fermi I type. α_i and α_f are the initial and final pitch angles.

and substituting in (3-13), we get, after averaging over angles, $A_i \sim 2/3$, and

$$\frac{t}{\tau_a} \sim \ln \frac{1 - A_f}{1 - A_i} = \ln [3(1 - A_f)], \qquad (3\text{-}16)$$

and finally

$$A \sim \frac{1 - e^{\tau^*}}{\frac{1}{2} - e^{\tau^*}} , \qquad (3\text{-}17)$$

Where $\tau^* = t/\tau_a$.

In Figure 3.4, the anisotropy, A, is plotted as a function of the acceleration time, τ^*. We notice that if we ignore collisions, this acceleration process is very inefficient as particles escape very soon from the loop through the loss cone of the magnetic field. Thus collisions of particles with others or with magnetic irregularities (either existing already or developed by the particle flux itself) should not be ignored. Therefore, at least for those energies for which Coulomb collisions and magnetic scattering are more effective than turbulence, these processes are the ones that tend to couple with the acceleration, first to make the acceleration process more efficient and second to indirectly develop turbulence in the plasma. The characteristics of particle trapping in the coronal magnetic field are governed by the scattering process in operation. Except for the self developed turbulence, however, the scattering process becomes less effective as the particle energy increases. So for those particles which are not in the high energy tail of the

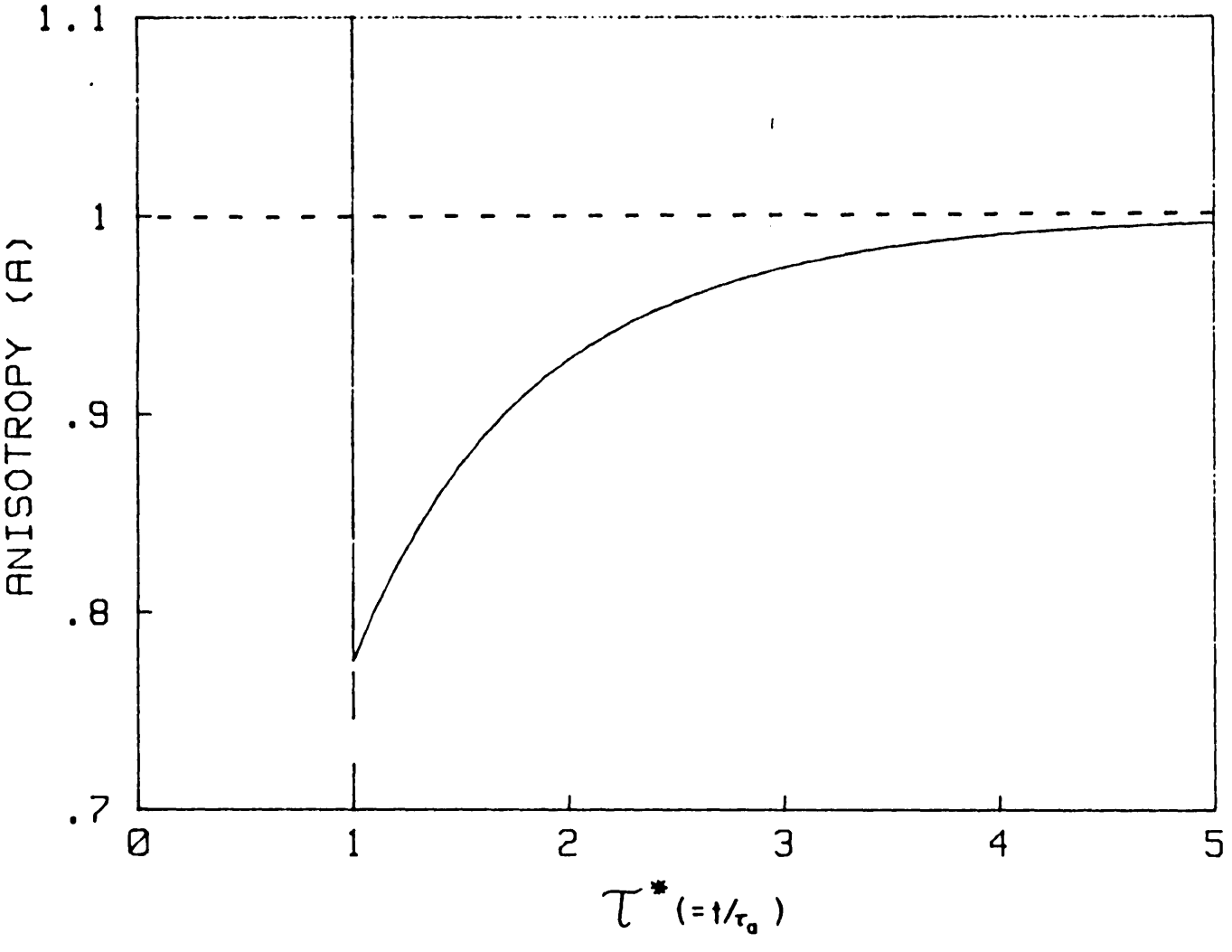


Fig. 3.4. Particle flux anisotropy as a function of the acceleration time τ^*, given in terms of the characteristic acceleration time.

distribution, the probability of trapping would be greater than that of escaping if a heating mechanism were involved. That is, only a fraction of the total number of particles which go into the trap can manage to escape. Thus, the time constant of escape is,

$$\frac{1}{4}\tau_B \, 2\pi / f \qquad (3\text{-}18)$$

where τ_B = bounce period and f = Ω = solid angle of loss cone, providing scattering is strong.

3.3.2.1. Coulomb scattering

The plasma permeating the active region has a temperature of about 10^6 °K. That is, the thermal speed of the particles is $v = \sqrt{\frac{2kT}{m}} = 1.28 \times 10^7$ cm/s. Since the active region has a dimension of order $d = 2 \times 10^9$ cm cm then thermal particles from the plasma take $t = \frac{2 \times 10^9}{1.28 \times 10^7} = 155$s to traverse such region.

The characteristic time for Coulomb collisions, t_c, is given by

$$t_c = \frac{5.6 \times 10^6 \, E^{3/2}}{n\Lambda} \qquad (3\text{-}19)$$

where n is the number density of particles, Λ is the Coulomb logarithm $\sim 9.1 + \ln (T^3/n)^{\frac{1}{2}}$ (Sivukhin, 1966), which for $T \gtrsim 10^6$ °K and $n \gtrsim 3 \times 10^9$ cm^{-3} is about 18.9. Then for the peak of the energy distribution $t_c \gtrsim 0.10$ s. Therefore, most particles at these energies are subject to Coulomb collisions and some may become trapped in the magnetic field of the active region.

In fact, the energy above which Coulomb collions are no longer applicable is approximately 3.8 KeV

obtained from equating t_c to the transit time d/v.

On the other hand, if we consider that the particle population in the coronal loop is built-up from low energy particles in the plasma, we can obtain the rate at which the trapped population increases in the early stages from the factor, f, in equation (3-18) with the substitution

$$f = \Omega = 1 - \cos \alpha_o = B_o/B_m \qquad (3\text{-}20)$$

Now a typical active region has $B_o/B_m \sim 1/5$, and f is then about 0.1. That is most of the particles colliding remain stored in the magnetic loop. Now, as only a fraction of the plasma particles which collide become trapped, the rate at which particles become trapped via Coulomb collisions is

$$dN = N \nu_c \, dt \qquad (3\text{-}22)$$

Where $\nu_c = 1/t_c$ is the collision frequency. If N_o is the total number of particles in the volume of the active region with average speed V then if N is the number of particles in the trap,

$$N_* = N_o \left(1 - e^{- t/t_c} \right) \qquad (3\text{-}23)$$

which is shown in Figure 3.5 for a fixed velocity.

We now compare t_c with $1/4 \, \tau_B \, 2\pi/f$ at 100 KeV and 1 MeV in the following:

Energy	t_c	$1/4 \, \tau_B \, 2\pi/f$
100 KeV	2.9×10^3	36 S
1 MeV	9.3×10^4	11 S

We see that coulomb scattering works slower than particle loss.

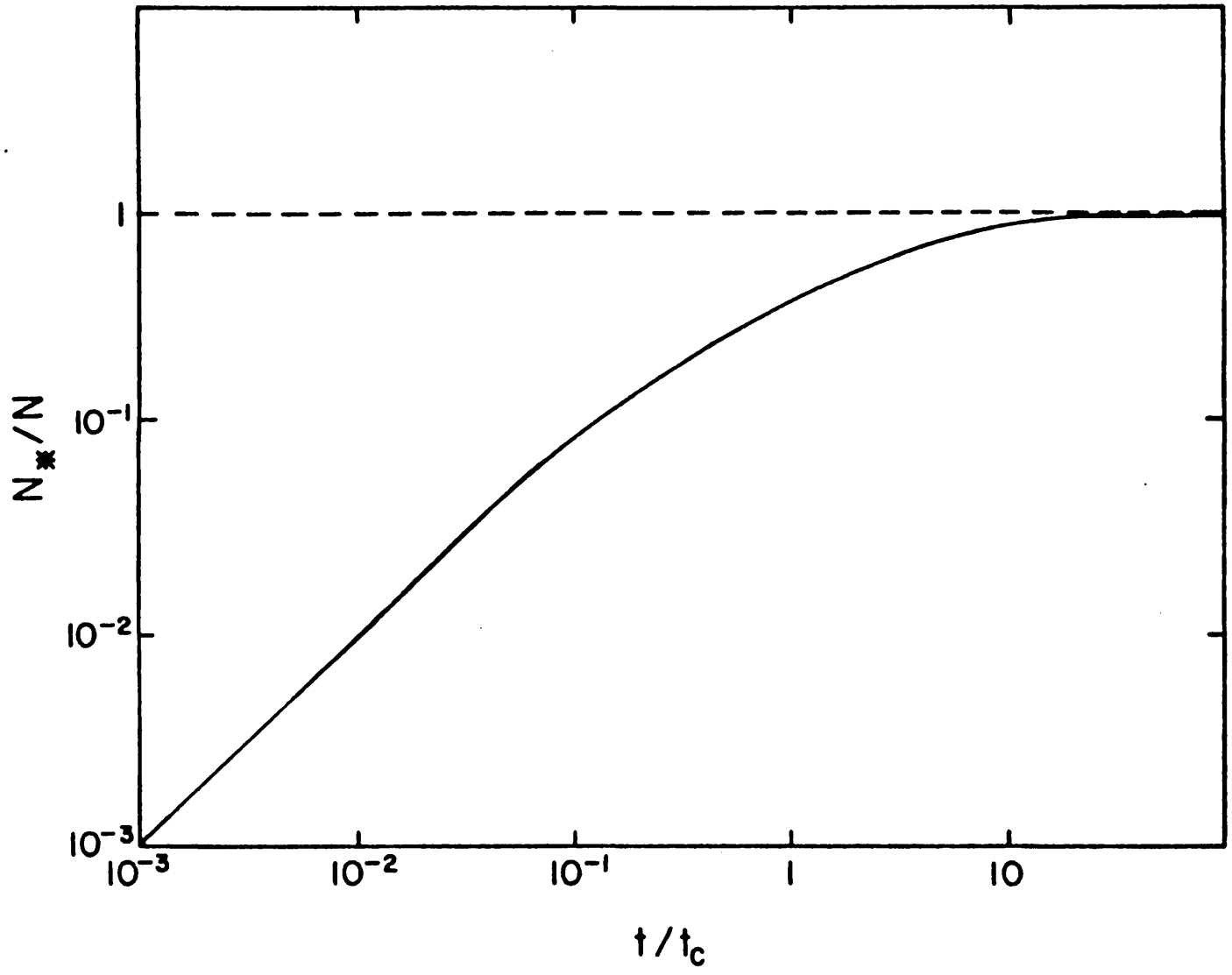


Fig. 3.5. Fraction of particles getting into the trapping region as a function of time for Coulomb scattering.

3.3.2.2. Magnetic Scattering.

The magnetic field above active regions is not a static field. In reality, it presents fluctuations around an average value B_o, say. Therefore, in the presence of hydromagnetic turbulence the magnetic field can be expressed as

$$\underline{B} = \underline{B}_o + \underline{b} \qquad (3\text{-}25)$$

where $\langle \underline{b} \rangle = 0$ and $\underline{b} \ll B_o$. Here angular brackets represent ensemble average.(see for instance Melrose,1980)

In the simple case in which $\underline{b}=\underline{b}_o \exp [i(ks-\omega t)]$, is along $\underline{B}_o$, with ω the wave frequency, the autocorrelation function of the magnetic field is

$$R_{ij}(s') = \langle b_i(s)\, b_j(s+s') \rangle \qquad (3\text{-}26)$$

where s is the distance along the field line. The Fourier transform of R_{ij} is the power spectrum of the magnetic fluctuation (Jokipii 1966; Jokipii, 1971)

$$P_{ij}(k) = \int_{\infty}^{\infty} ds'\, e^{-iks'} R_{ij}(s') \qquad (3\text{-}27)$$

and P_{ij} is proportional to the wave energy. That is, $P_{ij}(k) \propto \langle b^2 \rangle$ where at high frequencies, a power law

$$b(\nu) \propto \nu^{-\gamma} \qquad (3\text{-}28)$$

is obtained.

We shall be using this result when dealing with the interaction of the particles with the fluctuations. The usual way to obtain the time scale for magnetic scattering is usually through the Fokker-Planck equation (Morrison, 1956; Parker, 1956, 1965; Jokipii, 1966, 1971), we try here a simplified approach. Contrary to what happens with Coulomb collisions, scattering by magnetic scattering centres maintains the energy of the particles unchanged, and only introduce changes in direction. In a similar fashion as Rutherford formula is obtained for Coulomb Collisions, we can obtain a cross section for magnetic scattering through the Lorentz force on a particle due to the presence of a magnetic scattering centre. Then for a given number density (n_M) of scattering centres all of the same magnitude (b) we can obtain a characteristic time for magnetic scattering. Suppose first that the Lorentz force changes the trajectory of the particle through 90 degrees. Then we can write

$$\frac{mv^2}{r_c} = \frac{e}{c} vb \sin \Theta \qquad (3\text{-}29)$$

where r_c is the range of the force, v is the speed of the particle and Θ is the angle between the velocity and the direction of the fluctuation (which for simplicity we have put along B_o). If the pitch angle distribution is nearly isotropic $\sin \Theta \approx \sin \alpha \approx 1/3$, and for resonance $r_c \approx r_g$ the gyroradius of the particles. Then

$$r_g = \frac{3mvc}{eb} , \qquad (3\text{-}30)$$

and if we assume a given wave energy as given by (3-28) we can write, for the case of resonance ($S \sim r_g$),

$$r_g^2 \sim \frac{e^2 M}{9 m^2 v^2 c^2} \exp\left(-\frac{r_g^2}{\ell^2}\right) \tag{3-31}$$

where M is the average magnetic field fluctuation intensity. Since we have assumed that $r_g^2 << \ell^2$ we can write,

$$r_g^2 \sim R\left(1 - \frac{r_g^2}{\ell^2}\right) \tag{3-32}$$

where $R = \frac{e M^2}{9 m^2 v^2 c^2}$. We can approximate the cross section for magnetic scattering as $\sigma \sim \pi r_g^2$, and therefore $t_M \sim \frac{1}{n_M v \sigma}$, where n_M is the number density of scattering centres. We express finally the characteristic time t_M between magnetic scattering as

$$t_M \sim 6.21 \times 10^{-10} \frac{v}{\ell^2 n_M M^2} . \tag{3-33}$$

We see then that for a given $L = \ell^2 n_M M^2$, which gives a measure of the size of the fluctuations with respect to the whole region, the life-time for magnetic scattering t_M, is proportional to v, so that it increases more slowly than for Coulomb collisions. This implies that when magnetic scattering is in operation the source energy spectrum should be flatter, because t_M goes as $\sqrt{E}$ instead of as $E^{3/2}$ as in the case of Coulomb collisions. If, for example, L is of the order of 10^{-2}, then for $E = 10^5$ eV, $t_M \sim 27$ sec. On the other hand, the probability of escape, f, for magnetic scattering becomes

$$f = \frac{B_o}{B_m} \tag{3-34}$$

which for the same example we used before gives $f \sim 1/5$.

This means that magnetic scattering is not as efficient as Coulomb collisions in increasing the energy density in the trapping region. Furthermore, the range of energies at which this process work is highly restricted by the value of the parameter, L, in equation (3-33). Therefore, the contribution of magnetic scattering to the overall scattering in the trap depends on the particular physical characteristics of the region in consideration.

3.3.2.3. Scattering by hydromagnetic turbulence.

In the early stages of the particle population build-up in the field, the pitch-angle distribution of the particles is maintained nearly isotropic by coulomb and magnetic scattering. However, as the energy of the particles increases these two mechanism become unable to preserve such isotropy. The anisotropy in particle flux then tends to increase at a rate given by the acceleration rate and the system becomes unstable. The reason is that when a stream of particles move with a speed $v > v_A$, the Alfven speed, hydromagnetic waves are excited in the plasma at a frequency close to the gyrofrequency of the particles. The particles are thus said to be resonant because they interact resonantly with the excited waves. As a result of this interaction the anisotropy should tend to decrease and the process starts all over again as the acceleration process acts to restore the anisotropy.

The result is an equilibrium situation in which the rate of increase of the anisotropy due to direct acceleration $(\frac{dA}{dt})_{acc}$, is balanced by the rate of decrease of the anisotropy by the wave growth $(\frac{dA}{dt})_{sc}$ (from Melrose 1980). Since

$$\left(\frac{dA}{dt}\right)_{acc} = \omega \frac{\delta B}{B} , \qquad (3\text{-}35)$$

where ω is the wave frequency, and

$$\left(\frac{dA}{dt}\right)_{sc} = \frac{A - \frac{v_A}{v}}{t_{\sim A}} \qquad (3\text{-}36)$$

which is obtained from the wave growth, γ,

$$\gamma \sim \frac{n_*}{n} \Omega_i \frac{v}{v_A} \left(A - \frac{v_A}{v}\right) \qquad (3\text{-}37)$$

where t_A is the scattering time, n_* is the number density of resonant particles and $\Omega_{i,e}$ is the ion or electron gyrofrequency. Then (Melrose, 1980)

$$t_A \sim \frac{1}{\omega \frac{v}{v_A} \frac{\delta B}{B}} . \qquad (3\text{-}38)$$

As scattering by hydromagnetic waves has a threshold (the Alfven velocity, v_A, for ions) it is clear that both Coulomb collisions and magnetic scattering could maintain the particle flux isotropic at least for certain range of energy, with self adjusting scattering afterwards. That is to say, for a trapping region such as we have described in which the energy density of the region increases slowly, the contribution of Coulomb collisions and magnetic scattering to shaping the energy spectrum should not be ignored. In Figure 3.6 we have plotted the scattering time for the

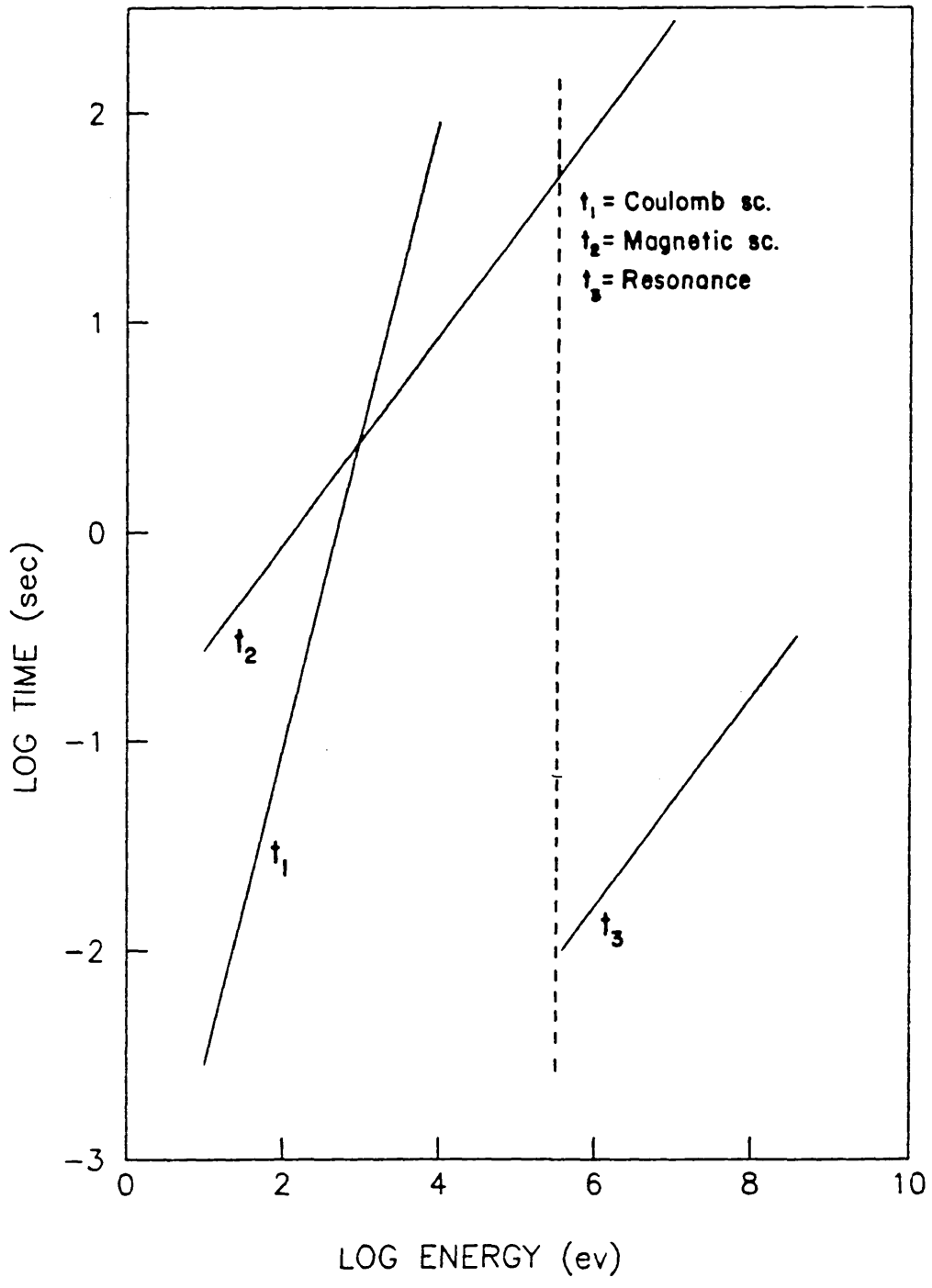


Fig 3.6. Life-time for different scattering mechanisms. The magnetic scattering (t_2) is quite arbitrary because we don't know the actual structure of the irregularities in the Field.

three processes described as a function of energy. Going back to the problem of the acceleration we notice that because of their difference in mass, ions and electrons behave differently in the trapping region and are therefore responsible for different processes. For this reason, the study of protons (or ions) and electrons is better carried out separately although taking into account that they are in a state of continuous interaction. We start with the protons.

3.3.3. The acceleration of the protons.

The theory of energy diffusion developed by Kulsrud and Ferrara (1971) (Section 3.2) in which hydrodynamic turbulence with fluctuations $\delta B_o < B_o$ and frequency ω, is responsible for the acceleration, can be applied only when the scattering rate, ν, is in the range

$$\omega \frac{\nu_A}{\nu} \left(\frac{\delta B}{B}\right)^2 << \nu << \omega \frac{\nu}{\nu_A} \qquad (3\text{-}39)$$

So for the particular case in which the ions are resonant i.e. those which have a velocity greater than the Alfvén velocity $\nu = {}^1/t_A$ where t_A is given by (3-38) lies, in the steady state situation, always in the correct range. The coefficient of systematic acceleration is

$$\left\langle \frac{dE}{dt} \right\rangle = \P\ \omega \frac{\nu_A}{\nu} \left(\frac{\delta B}{B}\right)^2 \left(\frac{\nu}{c}\right) E \qquad (3\text{-}40)$$

An important restriction for explaining the acceleration of energetic as well as relativistic particles becomes now evident. In order for the hydromagnetic turbulence to accelerate the particles (and this is true in general for protons and electrons) there must be enough time for the waves (ion cyclotron and whistlers) to grow. This implies

that the number of resonant particles (see equation (3-37) above) must be large enough at the acceleration time, i.e.,

$$\frac{n_{*i}}{n} \gg \frac{\omega}{\Omega_i} \qquad (3\text{-}41)$$

Otherwise, the total acceleration process must take place in one single acceleration period, $\tau_a = \frac{1}{\pi \omega \frac{v_A}{v} (\frac{\delta B}{B})^2}$. This difficulty is not encountered when the acceleration process extends for long time, that is, when it is assumed that particle acceleration is possible in the magnetic field as soon as there are particles there (i.e. several hours prior to the flare). As a result, when the flare takes place and intense heating at the loop foot points gives rise to a shock wave (this can be so only in large events), there is already a significant number of resonant particles which can be accelerated further by the shock wave to relativistic energies. The shock wave acceleration thus constitutes the second phase of the process.

3.3.4. The acceleration of the electrons.

The main reason why the behavior of the electrons differs so radically from that of the protons stems from the fact that the electrons move much faster. Since the scattering time is inversely proportional to the particle velocity, the electrons are scattered more rapidly than protons of the same energy by a factor $\sqrt{m_p/m_e} = 43$. This implies that while the protons can be injected into an efficient acceleration process, the electrons cannot because they are highly isotropic with a very short time in the trap. Therefore, the number of energetic electrons in the trap should usually be smaller than that of the protons of the same energy. (We discuss this result in the next Chapter). The electrons then gain their energy from their interaction with the protons and from self-generated turbulence, as we shall see in next section. Their pitch angle distribution is then isotropic with an energy source which is thermal in nature.

3.3.4.1. Langmuir turbulence dissipation (Buneman Instability).

The fact that protons are accelerated while electrons are heated implies that soon electrons and protons start streaming with respect to each other. For the case of the electrons this streaming along the magnetic field lines will induce plasma turbulence as follows:

Let an electron beam of number density n_* move with a velocity $\underline{v} = \underline{v_o} + \underline{\delta v_o}$ across the coronal plasma of number density n_e with $\delta v_o << v_o$, where v_o is the average speed.

If $v_o > v_{Te}$, where v_{Te} is the thermal electron plasma velocity, and $v_o - \Delta v_o < v_p < v_o$, where v_p is the phase velocity of waves, then excitation of these waves can take place. The growth rate of waves in a plasma is given in general by

$$\gamma(k) = \frac{1}{(2\pi)^3} \int u_k \left(\underline{k} \cdot \left(\frac{\partial f_p}{\partial p}\right)\right) d^3p \qquad (3\text{-}42)$$

where f_p is the distribution function of the resonant particles and u_k is the probability of emission of the waves. For the case of Langmuir waves,

$$u_k = 2 \frac{e^2 v_p^3}{\omega_{pe}^2 v} \qquad (3\text{-}43)$$

where $\omega_{pe} = \sqrt{\frac{4\pi n_c e^2}{m_e}}$ is the electron plasma frequency and v is the velocity of the particles. Since $(\underline{k} \cdot \frac{\partial f_p}{\partial p}) = \omega_{pe} \frac{\partial f_p}{\partial \varepsilon}$ where ε is the energy of the fluctuations then the rate of wave growth is

$$\gamma(k) = \frac{1}{4\pi} \frac{e^2 v^3 p}{\omega_{pe}} \int \frac{1}{v} \frac{\partial f_p}{\partial \varepsilon} d^3p \qquad (3\text{-}44)$$

which can be calculated approximately since

$$\int \frac{1}{v} \frac{\partial f_p}{\partial \varepsilon} d^3p \sim \frac{(2\pi)^3 n_*}{\ln_e (\Delta v)^2 v_o} \quad . \quad \text{So}$$

$$\gamma \sim \frac{\pi}{2} \omega_{pe} \left(\frac{v_o}{\Delta v_o}\right)^2 \frac{n_*}{ne} \qquad (3\text{-}45)$$

where $me\ (\Delta v_o)^2$ is the "temperature" of the beam. For a beam of only one particle and $v_o \sim v_{Te}$ with $\Delta v_o \sim 0.1\ v_o$ then the rate of growth is

$$\frac{\gamma}{\omega_{pe}} = 50\pi\ v_{te}^2 \frac{1}{ne} = 7.92 \times 10^8\ \text{sec}^{-1} \qquad (3\text{-}46)$$

where we have taken $ne \sim 3 \times 10^9\ \text{cm}^{-3}$ and a temperature of 10^5k.

Langmuir plasmons are easily generated for example by "run away" electrons, i.e., electrons whose electric field is greater than the Dreicer field, $E_D = 4\pi\ e\ \omega_{pe}^2 / v_{Te}$. One expects Langmuir turbulence at $T_e \sim T_i$ to be well damped, but the Buneman instability at higher electron

streaming velocities is likely (Buneman, 1959). This is produced when the turbulent pulsations are excited with frequencies of the same order as the growth rate.

$$\gamma_B = \sqrt{\frac{3}{2}} \left(\frac{me}{2m_i}\right)^{1/3} \omega_{pe} , \qquad (3\text{-}47)$$

which is equal to 3.09×10^9 sec^{-1} for $ne = 3 \times 10^9$ cm^{-3}

Therefore, we can find, from equation (3-47), the number density at which the Buneman instability allows tubulent growth at the rate (3-46) as a function of temperature. The result is

$$n_e \sim 1.4 \times 10^5 \, T^{2/3} \qquad (3\text{-}48)$$

So for $T = 10^6$ K the critical number density is 1.4×10^9 cm^{-3}, while for 10^5 K it is 3×10^8 cm^{-3}. Thus since these conditions are fullfilled in the corona we can conclude that the Buneman instability can occur. As a result of Landau damping of this instability the electron temperature increases so that soon $T_e >> T_i$.

In fact, as early as 1966 Zirin reported observations of active regions with temperatures of 3 to 4 $\times 10^6$ K, and James (1966), using Radar data, show that there are relatively narrow zones (tenths of $R_\odot$) of rapid heating and acceleration. However, probably the first calculations concerning the par -

ticle heating of coronal loops are those of Jeffries and Orrall (1965) in connection with optical emission from loop prominences containing energetic protons. The heating of the coronal plasma has been extensively studied (most recent works are Ionson 1982; Hollweg, 1984; Sakurai and Granik, 1984).

According to Bisnovatyi-Kogan and Gordon (1969) and Gordon (1969), it is possible to heat the corona by electron stream excitation of turbulent dissipation only when $6 \times 10^{-5} < n_s/n < 10^{-3}$, where n_s and n are the densities of beam and plasma. But like Cheng (1972), the estimates are made under the assumption of no losses. Instead, Levin (1979) suggests that the heating predominates in those regions where there are more streams (i.e. above active regions). The rate of thermal energy $Q/_{vol}$ release by the passage of such a single beam is

$$\frac{dQ}{dt} = \frac{\nu_{eff}^{ei}}{2} W^* (t) \qquad (3\text{-}49)$$

where ν_{eff}^{ei} is the effective frequency of electron-ion collision and W* is the energy density of non-resonance plasma waves:

$$W^*(t) = \begin{cases} W^* & \text{for } 0 \lesssim t \leq \tau \quad (3\text{-}50a) \\ W^* e^{\nu_{eff}^{ei}(t-t)/2} & \text{for } t > \tau \quad (3\text{-}50b) \end{cases}$$

τ being the duration of the burst at a given frequency.

For decametric wave length range, $\tau\nu_{eff}^{ei} \sim 1$ so the power released in the plasma is

$$Qst \underset{\sim}{\sim} 2\ W^*N \qquad (3\text{-}51)$$

where N(sec^{-1}) is the average number of electron streams passing through the plasma layer in ΔT ($\Delta T \sim$ 1-2 hours). Holman et al (1979) have shown that nonthermal protons in a hot plasma due to resonant damping of waves can stream at a speed equal or larger than the ion sound speed so that the number of electrons N is nonneglegible. The implications of this is that after some time ion acoustic waves in the plasma become possible and Te >> Ti. After the event of 21 May 1980 a hot loop with Te $\sim$ Ti was maintained by about 10 min, implying that at least during that stage Te $\sim$ Ti (Duijvman, 1983). This is not the case, however, as soon as turbulence and dynamics have to be considered.

In these conditions then at the time of the flare the electrons travelling downwards through the chromosphere produce the hard X-rays. Hence, as it has been pointed out by Bai et al (1983) and by Smith and Brecht (1984) if the heating of the chromosphere is strong enough material "evaporates" a a shock wave travelling upwards towards the active region can be produced. The interaction of a hitherto trapped

proton population in the loop with the shock then accelerates further the protons to relativistic energies and their subsequent interaction with the ambient medium gives rise to the gamma-rays.

Now, for the particle model of solar flares the acceleration of the particles is not an instantaneous process. As we have mentioned before, the particles are continuously escaping from the region due to changes of the geometric configuration of the magnetic trap or due to emergence of new magnetic flux to the region. In this sense, we expect particle precipitation down the legs of the loop sometimes during the life-time of the active region whether there is a flare or not. In fact, some authors have observed preflare increases in particles and X-rays, and based on various observations of the X-ray flare by Pallavicini et al (1975) Petrasso et al (1975) as well as statistical studies of many events by Thomas and Teske (1971) and Spangler and Shawhan (1974). It was thought that the X-ray emission started minutes or tens of minutes previous to the flash phase of the flare (Svestka, 1976). In this sense, the modelling of the flare ought to take this into account just as Heyvaerts et al (1977) and Spicer (1977) have done. However, preflare studies of X-ray emission by Wolfson et al (1978), Kahler (1979) and Wolfson (1982) arrive to the conclusion that these preincreases are not

typical of the flare. So for example, only one third of the events analysed by Spangler and Shawhan (1974) presented a preincrease, and Petrasso et al (1975) pointed out that there are occasions in which the active region brightens gradually only to fade away in a similar manner afterward without an event being present. This is confirmed by Svestka et al (1982 a, b), de Jager et al (1983) and Schadee et al (1983). The interpretation of these results comes from the fact that in the stable situation the energy equation in the loop is balanced by the heat input and the radiation outwards. Only when a turbulent mechanism, such as has been explained, leads to a plasma instability can there be energetic particle flux excape through the loss cone with the consequent heating of the material at the feet of the loop and the production of bursting X-rays.

3.4. The Flare.

As we saw in section 3.1., the coronal heating seems to be most important in coronal loops above active regions where the magnetic field is more intense and presents a closed geometric configuration. This is to be expected since in those regions the plasma is confined by the magnetic field and so the energy that is deposited there cannot escape freely. In fact we have argued in last section on the possibility that the energy density in the magnetic field can increase thanks to heating and acceleration. In other words, we propose that the flare energy can be stored in the form of particles. Concerning the release of this energy into the chromosphere and outer space an instability in the system must be produced. This could be either due to the chromospheric heating. generated by the surplus energy from the trap or it could come from the emergence of new magnetic flux. Let us start with the preflare situation.

3.4.1. The preflare situation.

That energetic particles are often present at the time of the flare is well established. What remains still to be properly explained is if the particles acquire their energy in the extremely short time between the flare and the hard X-ray emission, presumably produced by the nonthermal bremss strahlung of the energetic electrons, or whether they have started acquiring energy before the onset of the flare. Although the observational evidence is not very clear in this respect, there are other physical environments such as the Earth's magnetosphere where particles trapped in the bipolar magnetic field are known to be accelerated with a long time constant . We have shown how something similar happen to the particles trapped in the magnetic loop. In such case the energy density in the form of particles can increase substantially depending on the time that there is available for the process before the magnetic geometry changes or the stability of the region is disrupted in some other way. There is a limit, however, to the energy density that may build up inside the region. That limit is imposed by the magnetic field itself (Kennel and Petschek, 1966); $nE < B^2/8\P$. We saw in last section how the trapping can be maintained even for particles which are above the critical energy

for stable trapping Ec = $B^2/8\P n$. These particles produce the waves which will isotropically scatter them and keep them in the container. When the energy density of the region becomes comparable to the magnetic pressure the stable situation can be maintained only because the wave energy adjusts itself in such a way that the energy obtained by the particles from the acceleration mechanism is balanced by the energy loss through scattering out of the trap. The time it takes to the system to arrive in the equilibrium situation can be roughly calculated in the following way. The rate of acceleration is of the order of E/τ_A, where, τ_A, the acceleration time must be smaller than the scattering time τ_{sc} if acceleration is to take place at all. As we have seen in section 3.3.2.1 the scattering time for a 10^6 °K $n_p \sim 3\times10^9 cm^{-3}$ plasma is extremely short (0.1$) so that only particles in the high energy tail of the distribution (10^3-10^4 eV, say) could be accelerated if $\tau_A \sim 5.\bar{5}$. For such case

$$\frac{d\ (nE)}{dt} = \frac{B^2/8\P}{t_{eq}} \qquad (3\text{-}52)$$

if for simplicity we assume n = const then

$$t_{eq} \sim \frac{B^2}{\frac{8}{5}\P nE} \simeq 4 \times 10^4 \quad \text{sec} \qquad (3\text{-}53)$$

thus a steady state situation can be reached in a typical trapping region in around 11 hrs.

Martens and Kuperus (1983) have examined the problem of the stability of a heating coronal loop based on the electrodynamic coupling theory of Ionson (1982) and the evaporation/condensation scenario of Krall and Antiochos (1980). They found that X-ray brightenings of purely thermal origin can be produced in the loop due to gradual changes of the length of the loop or in its magnetic field intensity. In such cases the stability of the system is maintained throughout.

3.4.2. Instability by chromospheric heating.

If we take into account the heating produced by the resonant interaction of particles and waves at the loss cone and this results in being nonneglegible, the situation may become unstable. The reason is that an increasing number of particles can go beyond the 300 eV energy which is required for a proton to escape the solar gravitational field This means that eventually there will be jet of plasma invading the trapping field. As a result of this, the critical energy diminishes by the increase in number density and particles which were trapped stably in the field find themselves suddenly beyond the limit of stability. Therefore, temperature increase makes the precipitation process repeat itself and further heating of the chromosphere takes place, so that once Ec begins to diminish, the precipitation of particles out of the trapping field grows catastrophically with time until practically all particles are released from the trap in all directions very rapidly. The time scale for the process is of the order of the time required for the plasma particles to travel to the top of the magnetic configuration where the trapping region lies.

If the energy of the plasma particle is $\sim$ 300 eV then the time it takes for it to reach the

trapping region at region at 2×10^9 cm is

$$v = \sqrt{\frac{2E}{m}} = 1.28 \times 10^7 \text{ cm/s} \qquad (3\text{-}54)$$

or

$$t = \frac{d}{v} = 155 \text{ s}. \qquad (3\text{-}55)$$

So the time for the process is of the order of three minutes. Now the energy required for the particles to reach this energy, 300 eV, was calculated by Elliot (1978), as

$$W \sim 600 \text{ NcR eV/cm}^2 \qquad (3\text{-}56)$$

Where Nc is the number density of protons in the chromosphere and R is the range, distance that particles travel before colliding. The resulting energy is

$$W = 6 \times 10^{11} E^2 \text{ eV/cm}^2 \qquad (3\text{-}57)$$

For protons of energy 10^4eV stored in a tube of $\sim 10^{10}$ cm^3 of volume, having a density of 3×10^9 cm^3, the total energy of the tube is 3×10^{23}eV. Meanwhile, $W = 6 \times 10^{10}$, which is only 10^{-4} times the total energy available, and therefore the energy requirements can be very easily satisfied by the

trapped particle population.

On the other hand, after the 22 hrs have elapsed in which the energy density of the trapped population increases to just below the magnetic pressure, a small flux of particles escapes at the feet of the magnetic field. If $\frac{B^2}{8\pi n}$ is the energy limit for stable trapping but acceleration continues at a rate $\frac{Ec}{t_a}$ then the energy flux into the chromosphere is

$$J = \frac{B^2}{8\pi n t_a} \sim 2.6 \times 10^{-8} \text{ erg/cm}^2 \text{ sec} \quad (3\text{-}58)$$

and the power dissipated is

$$W = J \times \text{Area} \sim 10^{8} \text{ erg/sec} \quad (3\text{-}59)$$

so that in 10 to 100 secs the temperature of the chromosphere could reach the 10^6K necessary to rise toward the active region.

3.4.3. Instability by emergence of new flux.

The dynamical behavior of the atmosphere specially above active regions is such that situations in which the loop remains static for long periods of time will not be most expected. On the contrary, although loop structures have been observed to be quite stable, there is a continuous evolution of the coronal loop regions. In general, therefore, changes in the geometry and or magnetic field intensity are expected to take place and disrupt the building-up of the flare, particularly in complex magnetic field configurations. In those occasions, the flare instability can be triggered by the emergence of new magnetic flux just as it has been observed for many flares now with the aid of the SMM satellite (see for instance Hoyng et al,1981; Woodgate et al,1981).

Concerning the way in which this kind of instability is produced, we would like to stress that we believe that the emergence of new magnetic flux does not constitute a sufficient condition, on its own, to produce a flare. In order for a flare to be generated in this way, the energy density in the trap must be large enough. That is to say, the coronal arcade of loops must be already populated by hot, dense material.

Otherwise, the emergence of new magnetic flux can only increase the magnetic tension in the region with no catastrophic consequences.

When a dense, hot plasma populates the trapping region, the increase in the tension along the field lines would inhibit any motion in the transverse direction and this would lead to increased particle precipitation along the legs of the magnetic loop down its footpoints. The catastrophic release of the particles into the chromosphere could trigger the flare in this case.

The situation can be explained very much in the way that Martens and Kuperus (1983) have done to explain the X-ray brightenings sometimes observed from coronal loops. The emergence of new magnetic flux from the photosphere up into the loop structure is equivalent to an increase in magnetic tension. A sudden increase in field strength may provoke a shrinkage of the trapping region and a release of particles down the legs to the footpoints of the region. The difference, in this case, compared to the picture presented by Martens and Kuperus, is that although the loop stability could on occasions be preserved, in others the trapping region can be totally disrupted to produce the solar flare.

3.5. The Overabundance Problem.

As we have seen in chapter 2, on of the most puzzling problems associated with solar flares is the overabundance of some isotopes, mainly helium-3 and iron, observed in some small flares. Since the time of the first observations concerning this problem, there have been mainly three ideas to explain such events. In what follows, we shall examine first these propositions and then shall study the problem in the context of the particle model.

3.5.1. The Nuclear Reactions Model.

Based on the early treatment of the production of H and ^{4}He isotopes in the solar atmosphere by Ramaty and Lingenfelter (1969), Meyer (1971), and Meyer (1972), Ramaty and Kozlovsky (1974) and Rothwell (1974) studied the problem in more detail and found that the isotropic picture of the reaction production is quite insufficient for explaining the composition of these products in solar flares.

In the Ramaty-Kozlovsky model, it is assumed that energetic particles (principally protons) travel downward from the flare region and interact nuclearly with the chromospheric plasma to produce a secondary flux containing deuterium, tritium and helium-3 with the pecularity that the angular distribution of these isotopes does not coincide. The nuclear reactions responsible for the production of these three isotopes in the solar atmosphere are shown in Table 3-1. The reactions without a threshold E_s(min), which is around 10 MeV/nucl for the p reactions, are really the only ones to consider if our interest is to be centred in energies below 10 MeV/nucl where most of the flare particle energy lies. Therefore, the rate of production of the three different isotopes is nearly the same,

TABLE 3-1. ISOTOPE PRODUCTION IN pp. pα and αp REACTIONS

(Ramaty and Koslovsky, 1974)

REACTION		E_{th} (MeV/nucleon)	E_s (min) (MeV/nucleon)
Deuterium production			
1. p + α	$^2H + {}^3He$	23	...
2. α + p	$^2H + {}^3He$	23	9.1
3. p + α	^2H + n+p	31.7	...
4. α + p	^2H + n+p	31.7	12.5
5. p + α	$2\,^2H$ + p	29.9	...
6. α + p	$2\,^2H$ + p	29.9	11.8
7. p + p	$^2H + \pi^+$	286.5	13.1
Tritium production			
8. p + α	$^3H + {}^2p$	24.8	...
9. α + p	$^3H + {}^2p$	24.8	13.1
Helium-3 production			
10. p + α	$^3He + {}^2H$	23	...
11. α + p	$^3He + {}^2H$	23	12.1
12. p + α	^3He + n+p	24.8	...
13. α + p	^3He + n+p	24.8	13.1

but due to the different angular distributions of the three isotopes and the fact that deuterium is produced mainly in the same direction of the incident beam,that is, towards the Sun, while ^{3}He has an appreciable component in the backward direction, that is, away from the Sun, the secondary flux in the flare region can therefore become overabundant in ^{3}He as compared to ^{2}H. Concerning ^{3}H, even though its kinematics are not well known, it can be rapidly destroyed by spallation reaction in the chromosphere.

Two models were considered for the reactions: a thick target model which takes into account the energy loss of the primary beam as it crosses the chromosphere, and a thin target model which assumes that the energy loss is balanced by the gain of energy due to acceleration. Both these models give anisotropic angular distribution for the reaction products and both coincide in that ^{3}He is produced preferentially in the backward direction. The thick target model gives, nevertheless, better agreement with the observations.

A close examination of the p reactions for the primary spectra of the type observed from flares indicates that there should be a production of about one neutron per ^{3}He nucleus. In other words, the model predicts the production of a small photon flux in the

2.2 MeV γ-line. Evidence of this has been reported from some flares, for instance that of 4 August 1972 where a photon flux of about 3 photons/cm^2 was detected (Chupp et al,1973).

The Ramaty-Kozlovsky model is nevertheless quite incapable of explaining the big ratios observed in the relative composition of flare particle fluxes. The fact that the values obtained are small compared to the observations has apparently ruled out the plausibility of this model. However, the very presence of the H and He isotopes in the flare plasma implies that nuclear reactions do take place in the flare environment although perhaps they are only a part of a much more complicated picture.

3.5.2. The Plasma Models.

The plasma models are mainly two: the preferential turbulent injection of ^{3}He into the acceleration mechanism which has been proposed by Ibragimov and Kocharov (1978), and the heating of ^{3}He due to resonance with ion cyclotron waves proposed by Fisk (1978a). The latter shall be described first.

Fisk's model is based on the assumption that a plasma in which the temperatures of electrons and ions are different in such a way that electrons drift relative to the ions, thus establishing an unstable current in the plasma. The instability, product of the electric field induced in the plasma, develops electrostatic waves which are related to a disturbance in the particle distribution function and also to the resulting disturbance on the electric field E. According to Fisk, if the magnetic field pressure of the plasma is much bigger than the thermal pressure the waves most likely induced are electrostatic ion cyclotron waves rather than ion acoustic waves. Furthermore, were the ^{4}He/H ratio larger than normal (as has certainly been observed in some small flares) the excited waves would lie in a narrow frequency just above ^{4}He cyclotron frequency. Since only ^{3}He has a cyclotron

frequency between those of ^{4}He and H, it is precisely this isotope which interacts resonantly with the excited waves and may therefore be preferentially heated with respect to other species. As a result of this heating, the distribution function of the ^{3}He will grow a high energy tail so that if the acceleration process has an energy threshold, which must be assumed in general, the ^{3}He will be preferentially injected into it and will be overabundant when the release of the particles from the flare region takes place.

One particularity of this model over others is that it can explain, in a natural way, the enhancements of heavier particles. In fact, the ion cyclotron waves can interact not only with those particles whose gyrofrequency lies close to their own frequency but also with those whose second harmonic of their gyrofrequency lies close to it. Thus, if the state of ionization of certain species is such that the second harmonic of their gyrofrequency has the correct value, these species can also be heated by resonance. Fe^{+17}, for instance, according to Fisk's model, has the correct value to be heated and thus be preferentially injected into the acceleration mechanism in flares. Nevertheless, for the event of 14 May 1974, rich in iron, the state of ionization of iron could be measured and was 11.6 rather than 17 (Gloeckler et al,1976), although it was recognized later (Ma Sung et al,1981; Klecker et al,1984)

that $Fe^{+16,17}$ was also present. On the other hand, there have been ^{3}He-rich events for which the $^{4}He/H$ ratio was smaller than 10^{-2} (see figure 2.14 of last Chapter).

A further problem, which should be mentioned, is that the current instability seems to occur, according to Fisk, just prior to or during the flare process. It is difficult to think of any mechanism, other than a happy accident, that would make these two things to happen simultaneously. Certainly if the instability occurs much before the flare there is no way in which the plasma can keep memory of it and the relative composition of the particles in the plasma could not be preserved for much time. This implies that the plasma mechanism of ^{3}He-rich flares cannot be independent of the flare model itself. Furthermore, only a model, for which there is the possibility of particle confinment, would be able to preserve the relative composition imposed by the resonance of ^{3}He with ion cyclotron waves until acceleration takes place.

Ibragimov and Kocharov (1978), on the other hand, propose that the highly ionized and rarefied plasma in the upper atmosphere is an ideal reservoir for the development of various instabilities and hence turbulence. Similarly to Fisk's model, if the electron temperature exceeds the temperature of the ions, dif-

ferent plasma oscillations occur resulting in ion acoustic waves, whistlers and Langmuir waves. Due to the high velocity of this waves, only particles from the high energy tail of the Maxwellian distribution can interact with them giving rise to a slow heating of the distribution. This process strongly depends on charge ($\sim Z^4$) and thus the change of the original Maxwellian distribution is different for different isotopes as shown in Fig. 3.7, where initial and final distribution of protons, alpha particles and ^{3}He are plotted before and after dissipation by nonlinear scattering, respectively.

According to this model then there is an enrichment of multicharge particles and ^{3}He. Kocharov (1979) calculated the ratios of ^{3}He/^{4}He for different conditions of plasma and found values of 1.3 and 9 which resemble closely the observations.

Finally, the conditions which must be fullfilled in order for this mechanism to operate in the Solar Corona are that the level of turbulent energy and the plasma density are not high so that it is more efficient for small flares. The ^{3}He, Fe and other enhancements depend on three things: a) the threshold energy (given by T_e/T_i); b) the level of turbulence in the acceleration region; and c) the degree of ionization of the elements in the region.

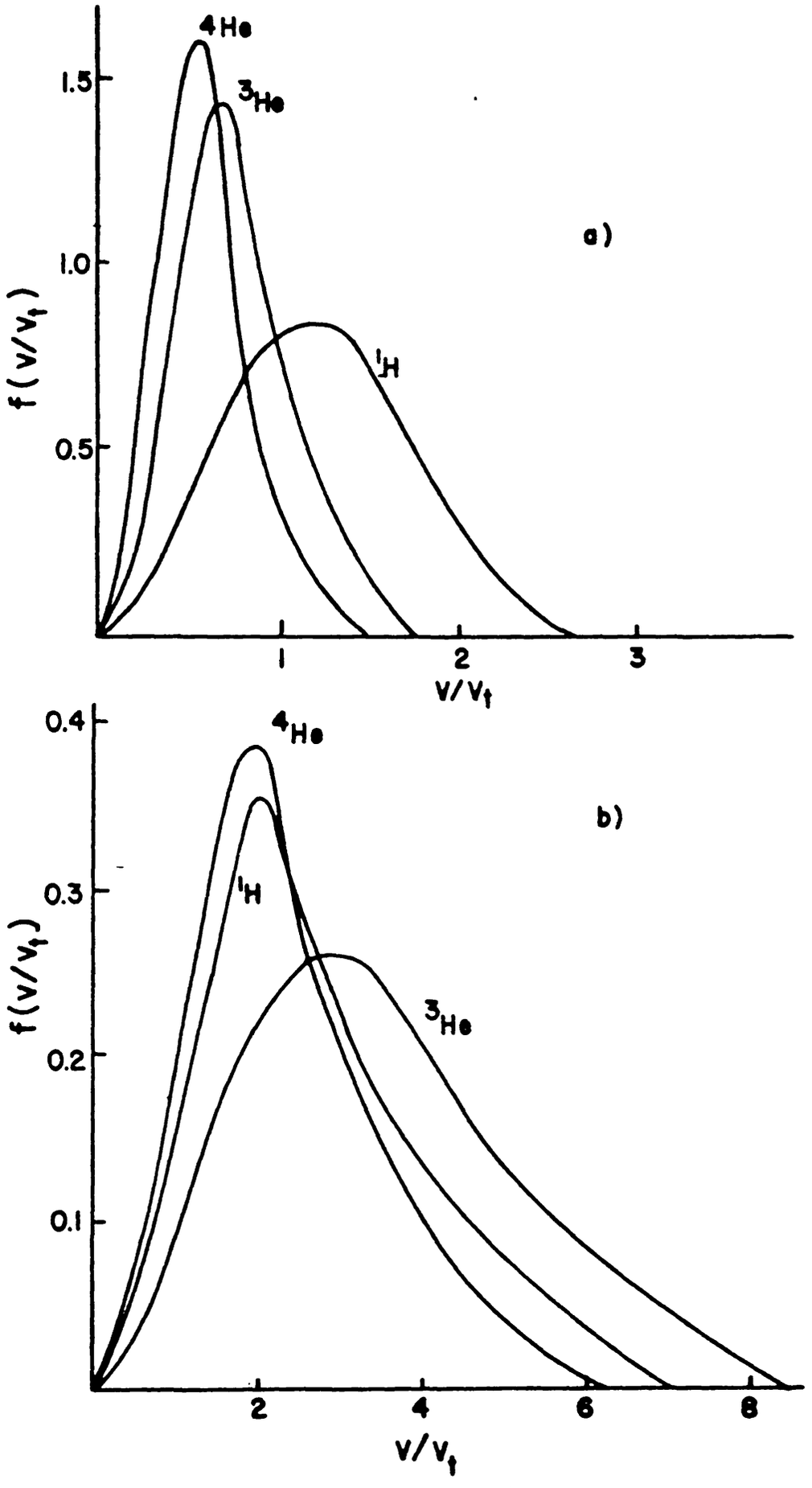


Fig. 3.7. Velocity distribution of particles: a) initial, b) final (shifted to the right along the velocity axis due to nonlinear scattering). (from Kocharov, 1979)

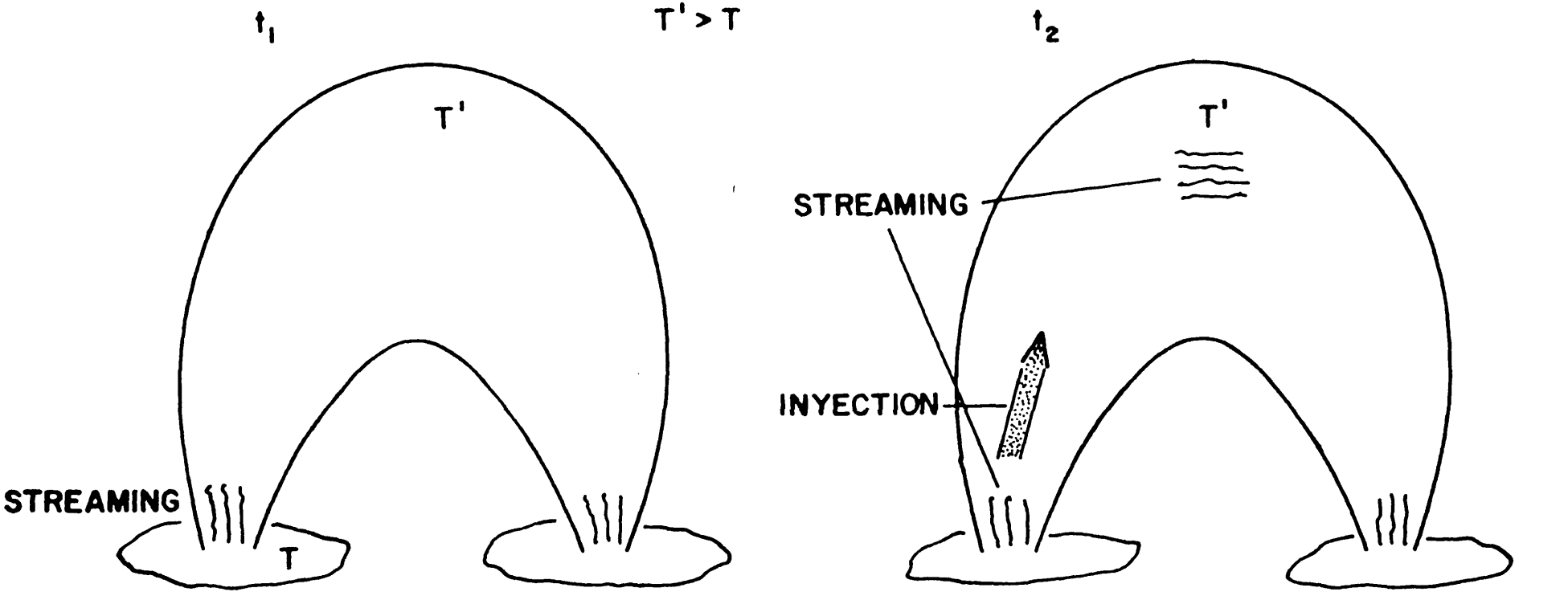
3.5.3. The Overabundance Problem and the Particle Model.

The difference between the two plasma models lies in the assumption concerning the temperature of the electrons with respect to that of the protons. If the electrons stream relative to the ions, the system is unstable and waves are excited to counteract the instability. If T_e is around an order of magnitude larger than T_i, ion cyclotron waves are most likely excited in the plasma and if the composition is right ^{3}He and Fe isotopes will be heated by the first and second harmonics of the ion cyclotron waves. But if, on the other hand, $T_e >> T_i$, ion sound turbulence is most likely excited thus heating ^{3}He only. The controversy still persist today concerning which of the two models is correct. Although Fisk's model seems to be more favoured because it can explain the heating of the iron, it presents one problem. According to the theory, the charge state of the iron should be Fe+17. Observations of Gloekler et al (1976) and Ma Sung et al (1981) show, however, that the charge state of iron for the iron-rich event of 14 May 1974 was both +11,6 and +16,17. Furthermore, Hovestadt et al (1982) observed an evolution of the charge state for September 1978

event. It started with 13.5±0.5, and was later 15.6±1.7. A further problem, also extensible to the ion sound turbulence model, consists of the rather difficult timing involved in the heating. That is to say, it looks like only a chance coincidence will make the preferential heating coincide with the acceleration at the time of the flare. These two problems are overcome when the question is examined on the light of the energetic particle model of solar flares. In such case, the heating of the plasma is of primary importance all through the building-up of the flare. That means that preferential heating of ^{3}He and Fe isotopes is not restricted to the time of the flare but extends throughout the active region lifetime as it evolves dynamically during the building-up stage. First the preferential heating is restricted to the loss cone where the ion streaming takes place and only later can the heating extend through other parts of the region (when the chromospheric instability progresses). In other words, low ionized particles should be heated first during the building-up, and highly ionized particles should be preferentially heated close to the time of the flare. Also, depending on the level of the turbulence, either Fisk's or Ibragimov and Kocharov's theory applies. Therefore, like Ma Sung et al (1981),

we conclude that the preferential heating takes place in two different temperature regions, but we also conclude that the process works prior to the flare. This is better illustrated by the schematic diagram of Fig. 3.8, where two different times during the flare building-up are shown. At t_1, the streaming is restricted to the loss cone, where the temperature is T, whereas later, at t_2, thanks to the chromospheric heating instability, the streaming extends also to hotter T' regions. As we saw in last Chapter, the emergence of new magnetic flux, which we expect to give rise to the Impulsive Flares (as classified with X-ray information), would prevent the region from reaching step t_2 and, therefore, should produce only low ionized iron ($Fe^{+11,12}$, say) and ^4He. The Gradual Flares, on the contrary, would also show overabundances in Fe^{+16-20} and ^3He, principally.

In order to show that this is actually the case, it is necessary to analyse overabundant events in relation to X-ray events. As we have seen, the X-ray information provides a way to distinguish those events which have been produced by the chromospheric heating instability from those in which the emergence of new magnetic flux was involved.



STREAMING → TURBULENT INSTABILITY → PREFERENTIAL HEATING

Fig. 3.8. Particle streaming in the Active Region for times t_1 and t_2, both at the feet and at the top of the Loop.

CHAPTER 4

DISCUSSION AND CONCLUSIONS

In dealing with high-energy Astrophysical problems one finds that the contribution of particles to the development of the different phenomena is sometimes considered of minor importance. Such is also the case of the solar flare problem for which all models proposed so far impose on the solar atmospheric environment conditions so severe that, in our opinion, they have prevented a better understanding of the problem. We have therefore proposed to reexamine the problem from a radically different point of view; that proposed 20 years ago by Elliot, Schatzman and others in the sense that energetic particles accelerated in the coronal loops above active regions may be the cause rather than the effect of the flare. We have shown here that according to Elliot's model most features of the flare process are explained.

For the energetic particle model of solar flares everything happens in a consistent way. The magnetic field relevant to the problem is always assumed to have a configuration capable of storing particles for some time, in actual accordance with observations (c.f. Spicer, 1976, 1977). The corona is heated from below to produce the solar wind and,

in a similar manner, a trapped particle population can be accelerated. The time constants for the acceleration of the proton flux and the subsequent isotropization of the particles by scattering are of the right values to permit the protons in the tail of the energy distribution to be above the Korchak and Syrovatskii's energy threshold for acceleration, with adequate time for the flux to induce turbulence and subsequently be accelerated more efficiently to high energies.

In this way, several particle populations can originate in the solar atmosphere. While sometimes protons can be accelerated, in most cases the electrons are the ones which accelerate. Fig. 4.1 shows schematically the most important steps undergone by the solar atmosphere to produce the transient phenomena frequently observed. From the release into the atmosphere of low energy particles with the consequent soft X-ray emission before a flare or in absence of it,through magnetic field prominences in which the field first increases in size due to the pressure of the hot plasma, only to fall back again to the chromosphere (in this case some heating is produced and consequently there is a weak electromagnetic emission);to the high energy release of a flare in which low as well as high

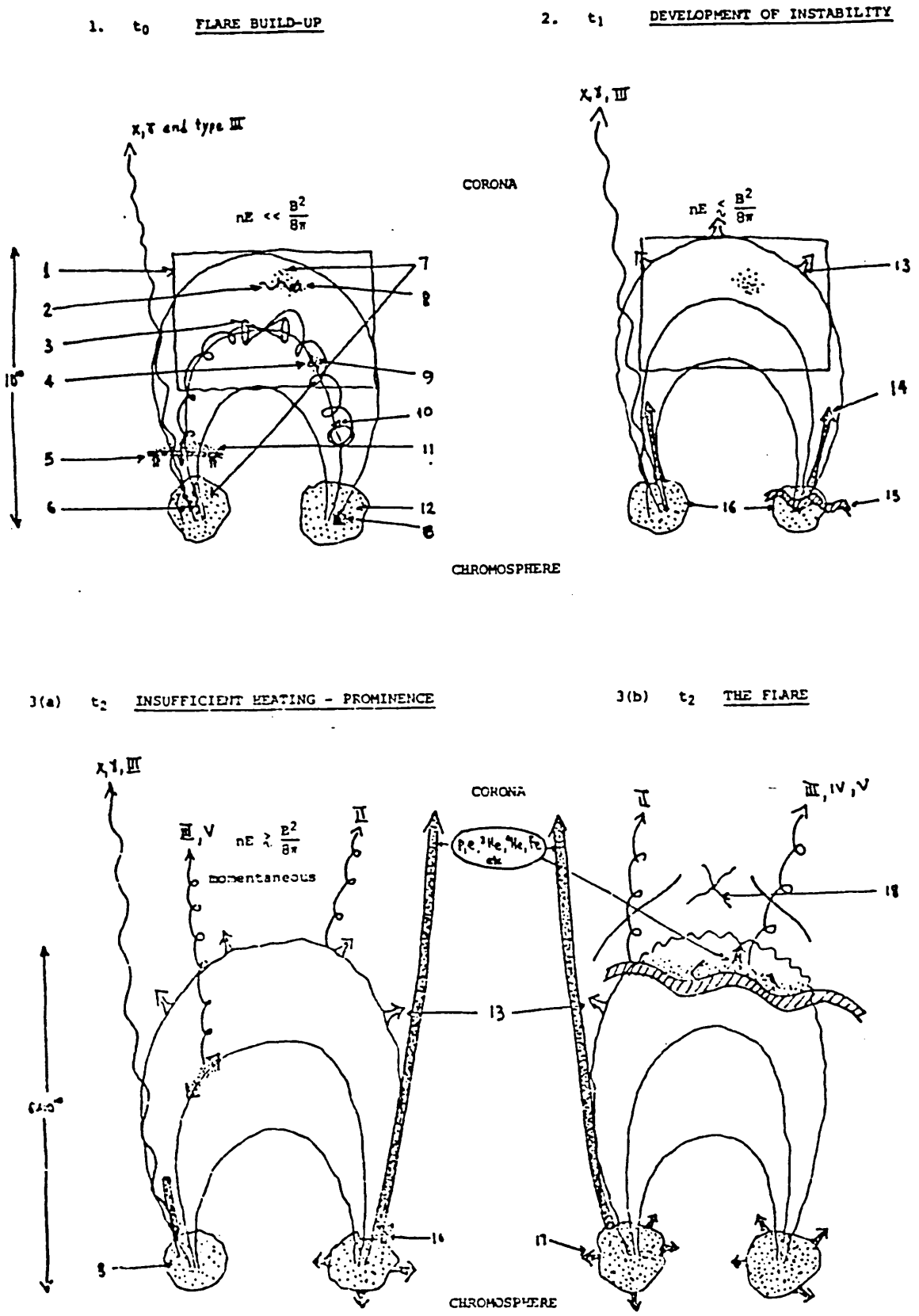


Fig. 4.1 - Schematic representation of Flare energy build-up and release according to energetic particle model.

energy particles are dumped into the atmosphere but with an important component going outwards. In this case all kinds of emission are produced; from X-rays due to electrons impinging into the atmosphere below, to white-light produced by the interaction of the ions with the chromospheric material; radio bursts by interaction of ions and electrons with shocks and the magnetic field loop; and on occasions mass ejecta produced by the expansion of the field, and γ-ray emission as a result of nuclear interactions of the accelerated ions in the solar atmosphere.

Then, assuming that the magnetic field can store a sufficient population of particles for the time required for the flare to build-up, it is possible that the particle energy density of the trapped population can be smaller than the magnetic energy density. If in the early stages the energy contained in the particles is usually very small, it tends to increase rapidly as a consequence of heating and acceleration. This has the result that, if the stable situation is maintained in the system, the energy density may soon be comparable to the magnetic pressure. Further heating and acceleration leads eventually to the dumping of some particles (those from the high energy tail of the particle distribution) into the loss cone where they

excite resonant waves which scatter them or they produce nuclear reactions.

Further heating of the region may eventually lead to the expansion of the region if it not were for the fact that the continuous dumping of the particles into the chromosphere with the consequent energy dissipation by the wave-particle interaction may be sufficiently unstable to introduce radical changes in the conditions of the region.

4.1 Predictions of the model

Up to the present time no direct observational evidence for the presence of energetic particles and their acceleration in the magnetic loop above active regions has been found. This is perhaps the main argument against solar flare models which rely on energetic particles playing a most important role. However, as we shall see in section 4.2 when we deal with the observational testing of the model, hard X-ray imaging for the last Solar Maximum with HXIS on board the SMM satellite have provided indirect evidence for particle acceleration in active regions. First, we follow step by step the development of the flare and related phenomena in accordance to the model proposed here indicating what we should expect to observe in each case.

4.1.1 The building-up stage.

Very early in the life of a bipolar region a trapped population of ions and electrons begins to become established in the loop. Part of the wave energy travelling up continually from the convective zone is absorbed by the particles and a slow heating process starts in the region. The building-up stage is thus concerned with the evolution of the active region, from a void situation just after the formation of the coronal loop to a state in which there is a population of hot particles trapped in the magnetic field with an energy density comparable, in the most favourable cases, to that of the magnetic field itself. On many occasions, during the building-up process, the stability of the region can be threatened by the presence of small changes either in the geometry of the trapping field or by the emergence of new magnetic flux. According to Martens and Kuperus (1983), if the field intensity increases or the loop contracts, particle precipitation should be enhanced, and if the reverse (decrease of magnetic field intensity or loop expansion) thermal soft X-ray emission should take place.

If the equilibrium is maintained then, because

of their difference in mass, the behavior of protons and electrons is different, with the result that electrons and protons start streaming with respect to each other. The electrons escape more readily from the trapping field than the ions so that while mirroring in the loop by the ions is possible, so that they can absorb wave energy more efficiently, the electrons only absorb energy by their collisions with the ions and therefore their energy is thermal in nature. As the electron streaming continues they try to generate Langmuir waves which are damped by Buneman instability thus increasing the electron temperature very substantially. Eventually the ratio T_e/T_i becomes very large and so does the level of turbulence. While this happens, the protons keep absorbing wave energy. Only those above the Kennel and Petschek's critical energy are sufficiently anisotropic to escape through the loss cone. As the suprathermal tail of the particle energy distribution continues to increase, more particles become anisotropic and the flux in the loss cone becomes unstable. Resonant waves are thus excited to counteract the instability. It is therefore during this stage that the composition of the particles in the trap is formed. In the early stages the ratio T_e/T_i is not extremely large and

ion cyclotron waves are most likely to be produced at the footpoints of the loop. Hence, preferential heating of ^{3}He and Fe according to Fisk's (1978) model takes place. However, as the trapping region envolves, the ratio T_e/T_i increases in such a way that the level of turbulence also increases. In this situation ion-sound turbulence becomes the most likely instability and preferential heating of ^{3}He takes place in accordance to Ibraginov and Kocharov's (1978) theory. At the time of the flare when particles from the trap are released into the atmosphere and interplanetary space these isotopes are expected to be overabundant.

Although the electron precipitation is rather weak during this stage and would not lead to any appreciable emission, thermal emission (soft X-rays) from the top of the loop is a possibility. However, the wave generation at the footpoints of the loop by the protons may have important consequences later because of the energy which is dissipated there and its consequent heating of those parts of the chromosphere. But whatever the results of that heating are, some of the waves which are involved in the heating may escape and if they get into an adjacent open magnetic field tube they will travel with the solar wind where they could remain undamped for a very long time and making it possible to observe them at 1 AU.

4.1.2. Development of the instability and the Flare.

When the particle energy density in the trapping region becomes closer to the magnetic pressure, the processes described above become more intense. But as we mentioned in the last section, for certain geometric configurations or for changes in the geometry, the stability of the trapped particle flux can weaken or even break down. Therefore even when the conditions for the flare are far from being satisfied, important particle fluxes can escape through the loss cone. This imply that burst-like emission of particles, soft X-ray emission from Martens and Kuperus' theory of thermal readjustment, hard X-ray emission from bremsstrahlung of the precipitating electrons, and even small type III radio burst emission if beaming of electrons spiraling along the field lines take place should be sometimes observed before flares or even without any.

Two types of instability in the region can lead to the solar flare and related phenomena. If the equilibrium situation can be maintained in the region throughout the building-up, the most likely instability will be due to the enhanced chromospheric heating. However, the emergence of new magnetic flux to the region is not an unusual phenomenon in the solar

atmosphere so that on many occasions it can constitute the instability. Although we expect the latter possibility to be more common, we shall see in next section that the first possibility cannot be completely ruled out.

Because of the different ways in which the flare instability can be produced in the trapping region, some characteristics should become evident. For instance, unless the second instability (emergence of new magnetic flux) leads to the first (chromospheric heating) the release of the particles into the chromosphere to produce the flare should take place as one sudden burst. Furthermore, since the emergence of new magnetic flux can take place at almost any time, only in some cases will the particle energy density be near the magnetic pressure. In consequence, flares produced in this way are expected to be impulsive in nature (in Ohki et al's classification 1983)very rarely accompanied by a huge prominence. In other words, in most cases flares produced in such a way are expected as small flares. Concerning the isotopic abundances, while the ^{3}He is a very volatile species and its normal abundance in the atmosphere is very low ($\sim 10^{-4}$ w.r.t. ^{4}He) the first harmonic of the ion cyclotron waves is not very efficient in the heating of the isotope. Therefore, flares which take place when only this process is in operation

(i.e. small flares for which the level of turbulence is low) should not present very dramatic ^{3}He increases. Iron, on the contrary, because of its greater mass, remains in the chromospheric part (at the feet of the active region) and can be efficiently heated by the second harmonic of the ion cyclotron waves. Whether the level of the turbulence increases or not is of no importance whatever to the iron. Therefore as long as the trapping region passes through a building up stage the relative overabundance of iron is expected to remain basically the same whether or not the flare is small.

In the case that the system manages to preserve its stability for a time long enough for the instability be due to chromospheric heating, the flare process is a step by step catastrophic spiral which is expected to take longer and to produce more than one burst. It starts with the heating of chromospheric material which rises towards the trap. This triggers more fast particles towards the chromosphere with even more heating and so on. This kind of flares are expected to be more of the two-ribbon large flares kind (depending of course on the magnetic energy available) involving hard X-rays from the bremsstrahlung of the precipitating electrons, microwave emission from the beaming of the electrons along the magnetic field lines (type III from open field lines and type V from

the loop), shock wave generation in the chromospheric heated area accompanied by type II and IV radio emission and the relativistic electrons and protons produced by the shock. Finally gamma-ray emission is expected on occasions due to nuclear reactions of the high energy protons in the atmosphere, and mass ejecta behind the shock. Flares produced in this way are therefore expected to be of the gradual, more intense type accompanied by suprathermal emission and particles.

Anomalous particle composition is not expected from the largest flares. The reason is that by the time the anisotropic flux at the loss cone is sufficiently unstable (the critical energy is too high) the level of the turbulence is already too high to produce the enhancements. Instead, smaller flares in which the magnetic field involved is not very strong and the system passes through all levels of low and high turbulence are expected to be better candidates for the "dramatic" isotopic overabundances.

There is one further feature of large two-ribbon flares produced by the chromospheric heating instability. Because of the trapping characteristics of the region (Kennel and Petshek's limit for stable trapping) the precipitation into the chromosphere starts first with the highest energy particles in the distribution, followed by more particles but of lower energy.

Thus the hardest X-rays are expected to produce the first burst followed by less energetic ones in the following bursts. Also the energy flux density from each burst is not expected to be substantially different.

4.1.3. Magnetic expansion without a Flare.

Inside the trap, the equilibrium situation is maintained by the fact that the surplus energy (i.e. that which will lead to an energy density in the trap larger than the magnetic energy density) escapes through the loss cone to preserve the balance. Then in the event that the heating in the chromosphere by wave dissipation and particle precipitation is much too low to provoke the invasion of the trap with "cool" material, and no emergence of new magnetic flux is intense enough to disrupt the stability of the trap, there is no instability in the region and the system comes to a steady state situation. Eventually, however, as most particles become unstable the turbulence blocks the loss cone thus permitting the energy density of the particles to increase beyond the limit imposed by the field. As a result the region expands. How far the expansion can go depends on the possibility that the balance between magnetic and kinetic pressure can be restored somewhere in the corona. In general, if the magnetic field is not disrupted, it could keep the balance as the gas cools as it expands. Therefore, for these cases of "failed" flares, mass ejecta accompanied by wave emission would in some circumstances be expected.

4.2. Observational evidence available for testing the Model.

As we have already mentioned, our chances of understanding the flare phenomenon have increased substantially now that the results observed during the last Solar Maximum by a number of instruments on board the SMM and Hinotori satellites have become available to the scientific community. Their analysis alone and in comparison to Hα movies and VLA radio observations on Earth, as well as to particles and electromagnetic emission observation made by other satellites have perhaps offered a new insight in the study of the active region. In what follows we shall describe how do our model stand against this information.

4.2.1. Thermal Energy vs Magnetic Flux.

The first requirement of the particle model is that the magnetic field be closed in order for a population of particles to arise in the active region, where they can be subsequently heated and accelerated. That this is in fact what happens comes from the results of Rosner et al (1978) who after analysing the Skylab data considered the closed loop as the basis for the construction of the corona. Furthermore, we have assumed the coronal loop to be in a dynamic state of evolution with the particle energy density in the trap increasing due to heating and acceleration. The maximum value that the particle energy density can acquire is, in the best cases, comparable to the magnetic field pressure. Golub et al, (1980) have studied the heating of the corona in relation to the magnetic field in the active region. They have found that there is a good correlations between the magnetic flux and the thermal energy in the region (Fig. 4.2). Moreover, the kinetic pressure, p, was also found well correlated to the average longitudinal magnetic field, $\langle B \rangle$, (Fig. 4.3). Although the relation between p and $\langle B \rangle$ was found by Golub et al to be roughly $p \sim \langle B \rangle^{1.6}$ instead of $p \sim \langle B \rangle^{2}$ as the particle model predicts, this

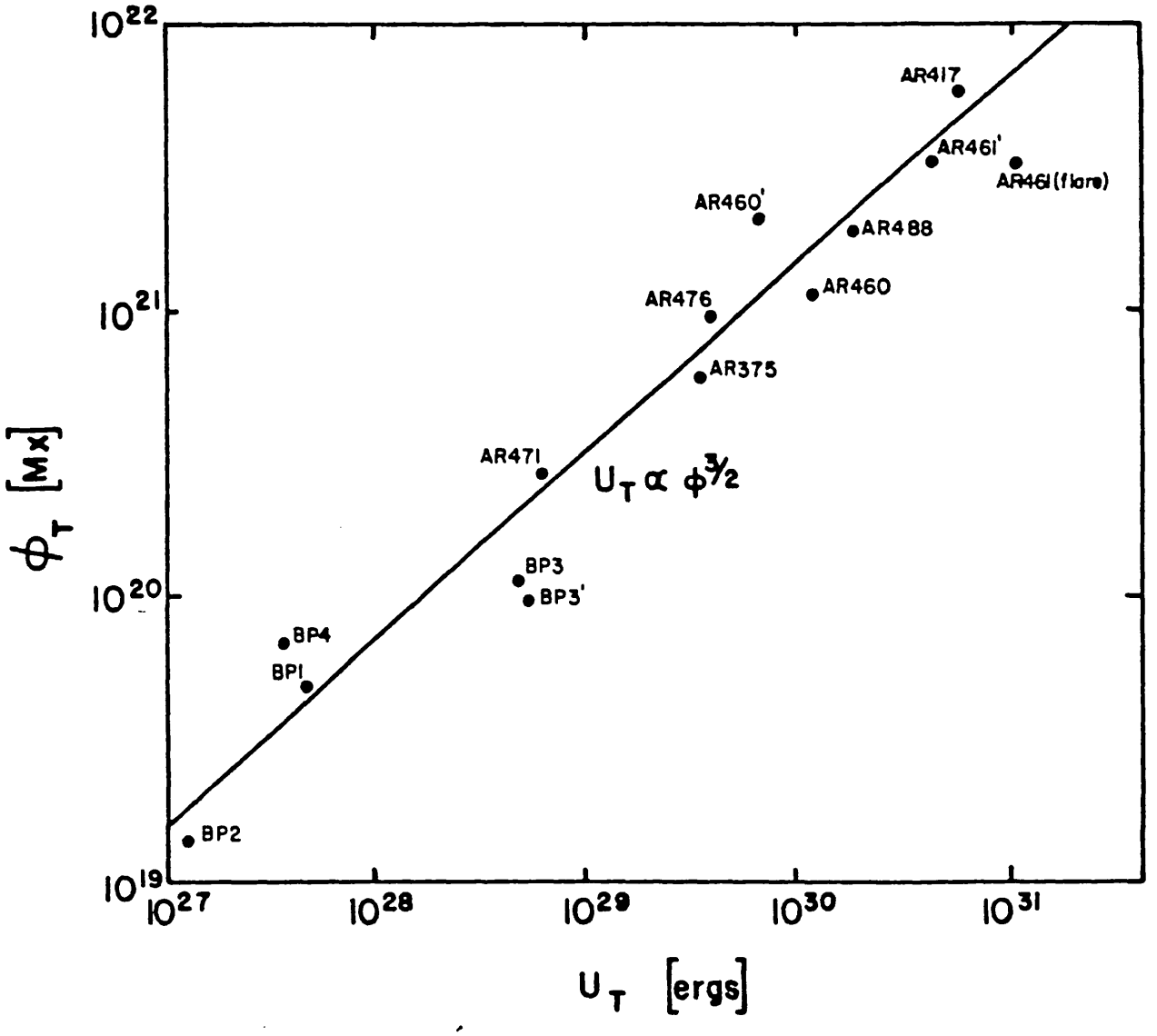


Fig. 4.2. Total magnetic flux versus total thermal energy content in active regions and bright points (from Golub et al,1980).

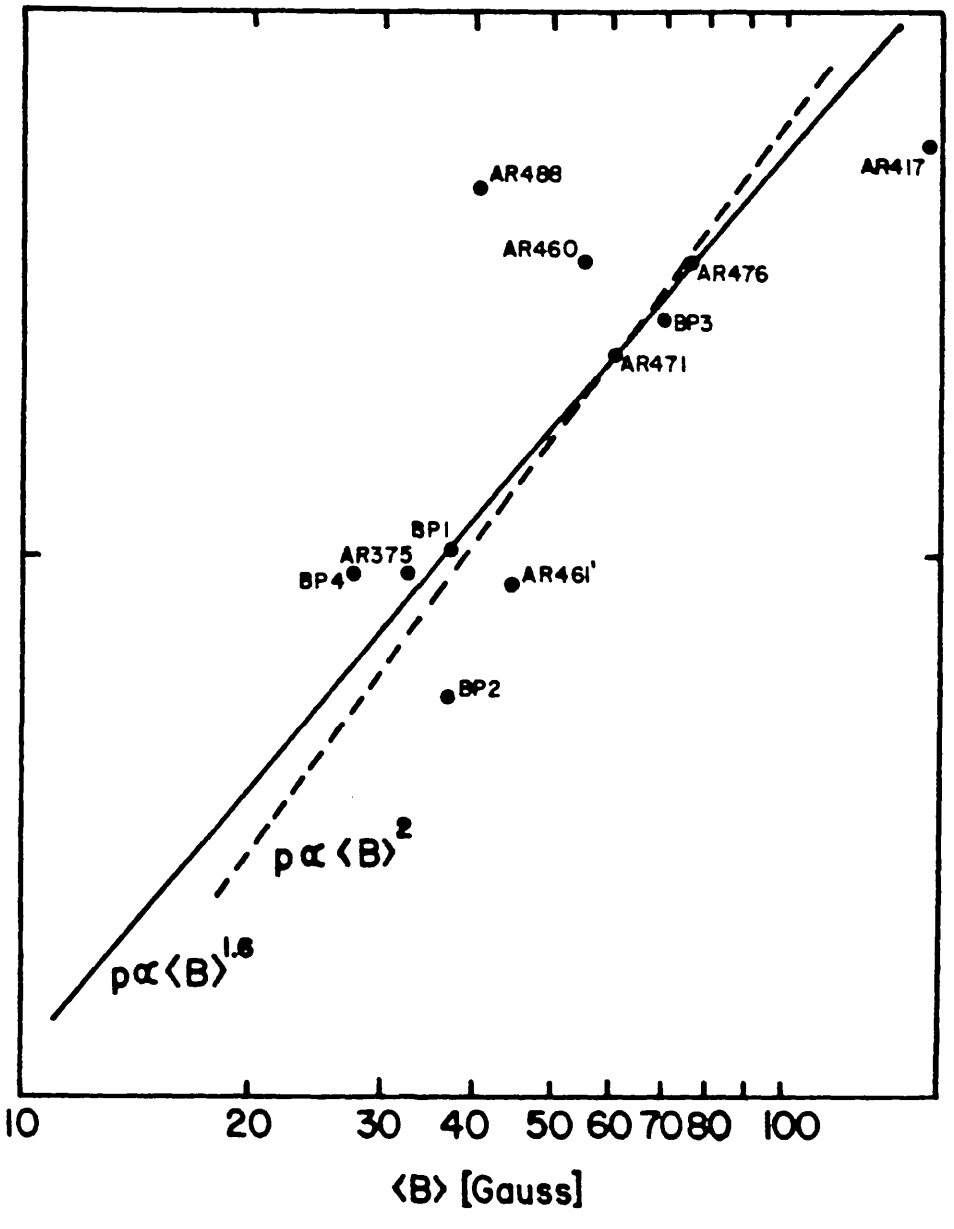


Fig. 4.3. Average coronal pressure versus longitudinal magnetic field. The solid line represents the best fit while the dashed line represents the limit imposed by the field (from Golub et al,1980).

result is sufficiently important to conclude that there is a real dynamic evolution of trapped plasma in coronal loops above active regions.

4.2.2. Energetic particles and soft- and hard-X-ray emissions from non-flaring regions.

As we have mentioned before, there are many occasions during the building-up stage, in which the stability of the region is threatened by the presence of small changes either in the geometry of the trapping field or by the emergence of new magnetic flux. According to Martens and Kuperus's theory, during their evolution, magnetic loops run through different equilibrium states. An increase in the size of a loop implies thermal emission from the region in the form of X-ray brightenings such as it has been reported by Howard and Svestka (1977). A decrease in the size of the loop is accompanied by particle precipitation down the legs of the loop such as it has been reported by Levine and Withbroe (1977). Actually, the energetic particle model predicts that particles as well as accompanying non thermal emission should be sometimes present before the flare or even without a flare. Events of this sort have been observed in the past. Block and Kushevsky (1979) and Block et al (1981) have reported particle pre-increases (Fig. 4.4) and Svestka et al (1982 a, b); de Jager et al (1983); Shadee et al (1983) have reported hard X-ray preincreases (Fig. 4.5). Although hard X-rays are usually observed as flare precursors de Jager et al (1983), Svestka and

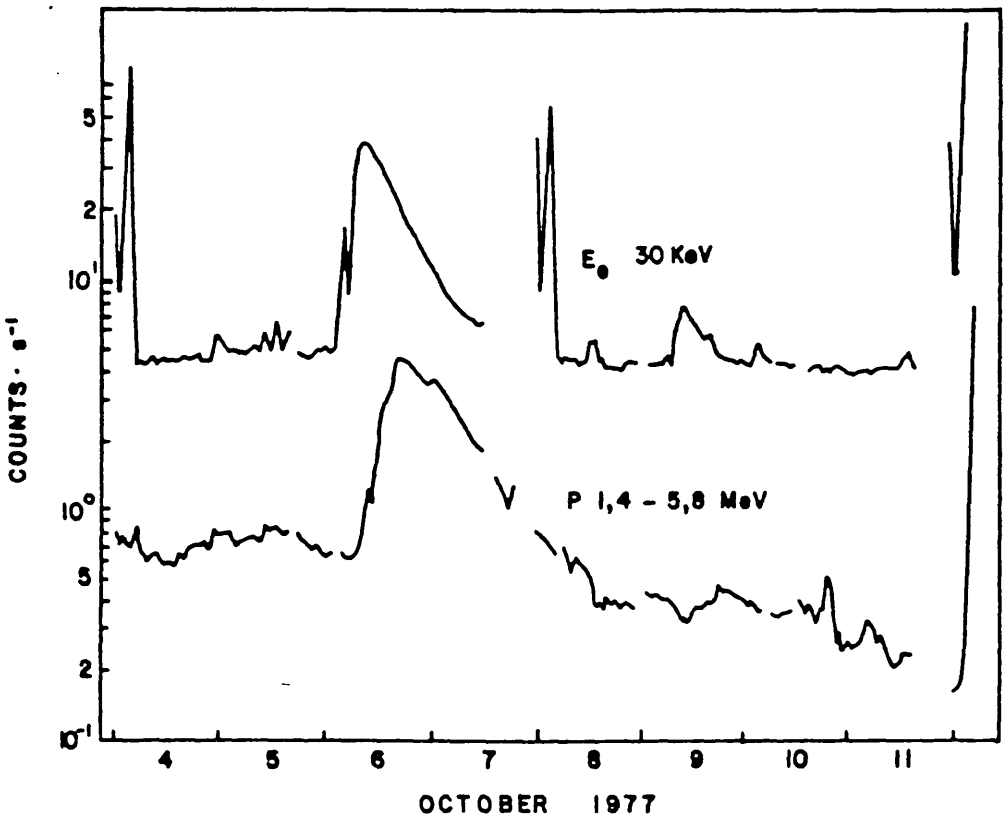


Fig. 4.4 - Preflare increase in the cosmic ray intensity for the October 1977 event (Block et al 1981)

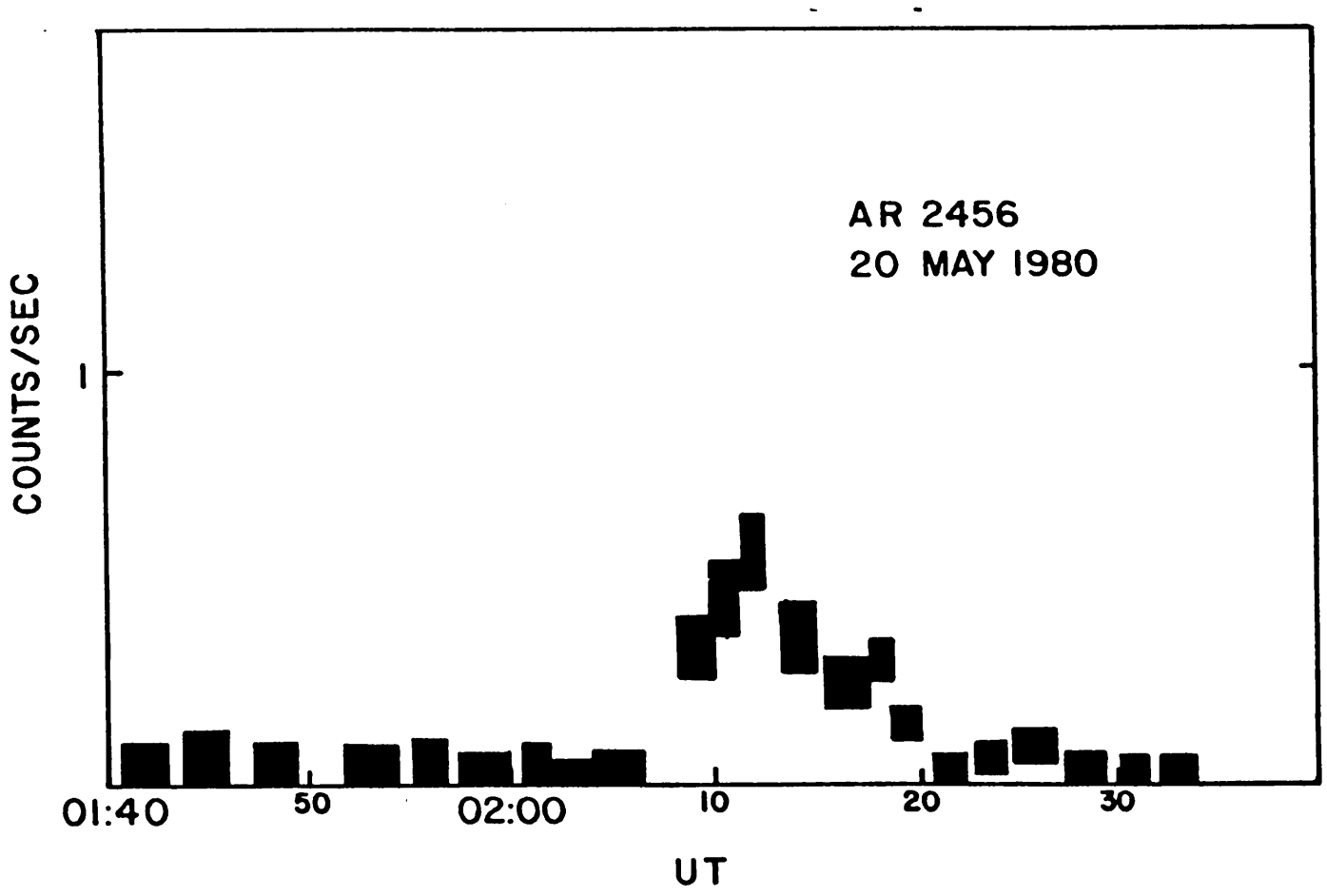


Fig. 4.5. Time development record of two typical X-ray brightenings on 20 May 1980 in AR 2456. (After Svestka and Shadee,1083).

Schadee (1983) and Schadee et al (1983) have found that there are cases in which hard X-ray emission was unaccompanied by a flare. Table 4-1 shows solar events of importance 1F upwards for the period June-Dec 1978 in which the number of those with a) simultaneous optical and X-ray emission, b) absence of X-ray emission, and c) pre-flare X-rays is obtained with their respective percentage.

TABLE 4-1. Events of importance 1F upward for the period June-Dic 1978 in relation to the soft X-ray emission.

Month	Total N° of events	Events with simultaneous optical and X-ray emission		Events with pre X-ray emission		Events with no apparent X-ray emission	
		N°	%	N°	%	N°	%
June	28	10	35.7	6	21.4	12	42.9
July	47	19	40.4	11	23.4	17	36.2
August	9	0	0	6	66.7	3	33.3
September	48	27	56.3	6	12.5	15	31.3
October	33	21	63.6	6	18.2	6	18.2
November	17	9	52.9	3	17.6	5	29.4
December	63	38	60.3	12	19.0	13	20.6
T o t a l	245	124	50.6	50	20.4	71	29.0

4.2.3. Flare instability and related phenomena.

As the system runs throughout the building-up stage, there are two possible instabilities leading to the flare or to other related phenomena. When the instability is due to the emergence of new magnetic flux (observed for instance by Hoyng et al.,1981; Woodgate et al., 1981; de Jager et al., 1983) we mentioned earlier that the release of the particles into the chromosphere to produce the event is expected to take place as one sudden burst (see Ohki et al., 1983 and Chapter 2). This is not expected to be the case when chromospheric heating instability is involved. Then the process takes longer and more than one burst should be the result in most cases. The proof that flares can be produced by processes other than the emergence of new magnetic flux comes, for instance, from the 1 November 1980 two-ribbon flare studied by Tandberg-Hansen et al (1984). Likewise, that more than one burst is involved comes from the complex two-ribbon flare of 5 July 1980 observed by HXIS on the SMM spacecraft (Harrison et al., 1983), and from the 25 June 1980 flare studied by Holman et al., (1984). Two intense bursts in the 5 July 1980 flare and more than two in the 25 June 1980 flare were observed and after each burst hot plasma invaded the loop.

The flare classification of Ohki et al (1983) has been enhanced by the work of Dwivedi et al (1984). They studied more than 20 events comparing ISEE-3 X-ray emission with high-resolution Big Bear Hα movies. They found that small compact flares are more impulsive with a single X-ray spike, while the more gradual flares were more intense, lasted longer and presented a complex X-ray emission. The latter were almost invariably associated with two-ribbon type flares and also they found three flares for which the X-ray spikes coincide with Hα brightenings covering the sunspot umbra. That not only flares can be classified in this way can be seen from the work of Schadee et al (1983). They compared the rise time and duration of X-ray brightenings from two different regions during 1980. Their results are shown in table 4-2. From it is clear that the events in region AR2466/69/70 were generally more intense than those in region AR2456. Furthermore, table 4-3 in which the basic characteristics of the two regions are quoted seem to imply that indeed regions in which the development is slow and the magnetic flux is high present better conditions for more intense and complex events. In the younger region AR2466/69/70 the flaring sites were preserved for several days.

According to our model the particle population forms in the magnetic field long before the flare.

TABLE 4-2. Mean rise time and duration of short-lived X-ray brightenings (Schadee et al, 1983).

	Region AR 2456			Region AR 2466/69/70		
	Number of events	Mean (min)	Median (min)	Number of events	Mean (min)	Median (min)
Biased duration	13	9.6	7.0	44	13.3	11.0
Minimum Duration	21	$\geq$10.6	$\geq$8.	75	$\geq$15.4	$\geq$15.0
Rise time	17	5.0	4.0	79	5.4	4.0
Rise/min Time		$\leq$0.47	0.5		$\leq$0.35	$\leq$0.27

TABLE 4 - 3. Characteristics of active regions AR 2456 and AR 2466/69/70

	Number of X-ray brightemings	Rise/min duration (min)	Amount of Magnetic flux	Proportion of Hα flares in X-ray brightemings	Development
Region AR 2456	51	0.47	less	5	Fast
Region AR 2466/69/70	98	0.35	more	26 of 111 23.4%	Slow

Since the way in which the build-up occurs in terms of the scattering in and out of the trapping field, the fact that the electrons move faster than the protons imply that they are scattered more readily by a factor $\sqrt{\frac{me}{mi}} \approx 43$. The ratio of electrons-to-protons at the time of the flare is therefore expected to reflect approximately this factor. In fact, the curve of regression (Fig. 4.5) shows a constant ratio of electrons-to-protons, whereas the particle energy spectra (Fig. 4.6) show that for particles of the same energy the ratio of electrons to protons is about 10^{-2} or smaller. Here the proton spectrum was constructed from the gamma-ray line emission and the electron spectrum from X-ray and gamma-ray continum emissions (Ramaty et al, 1980).

The mass ejecta from the largest flares or from so-called "failed" flares (eruptive or non eruptive prominences) have been analysed by Rust and Webb (1977). Their results are Summarised in Table 4 - 4. As the table shows, only 3.8 percent of the total number of events are not correlated with Hα emission.

On board the SMM satellite there was a Gamma-Ray Spectrometer (GRS) which permits the analysis of this emission in comparison to X-ray imaging, for example.

The analyses which have been carried out by Chupp (1983) and Bai et al (1983), are still highly controversial, specially in relation to the possibility

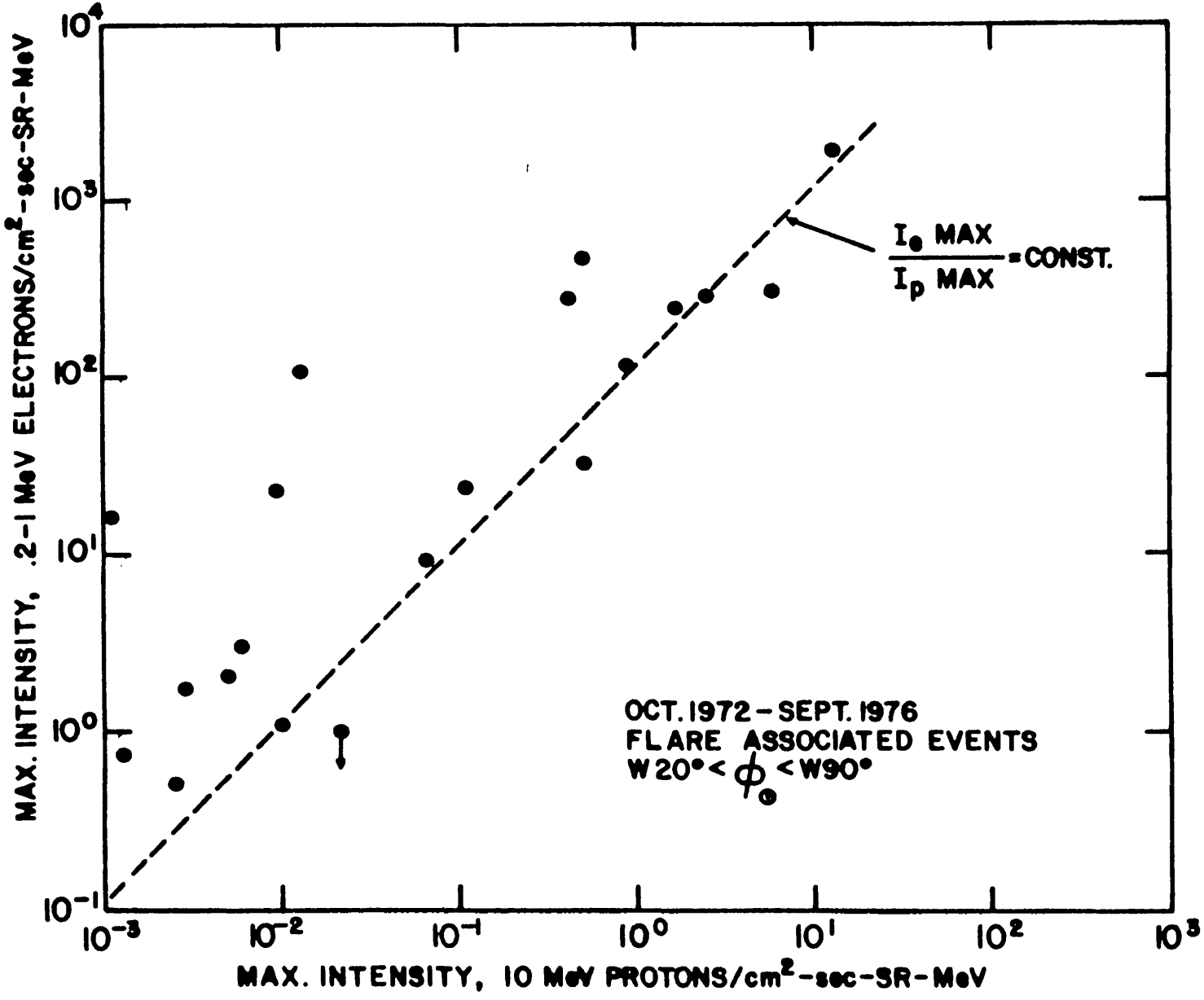


Fig. 4.5. Maximum electron to proton intensities from flares (from Ramaty et al, 1980).

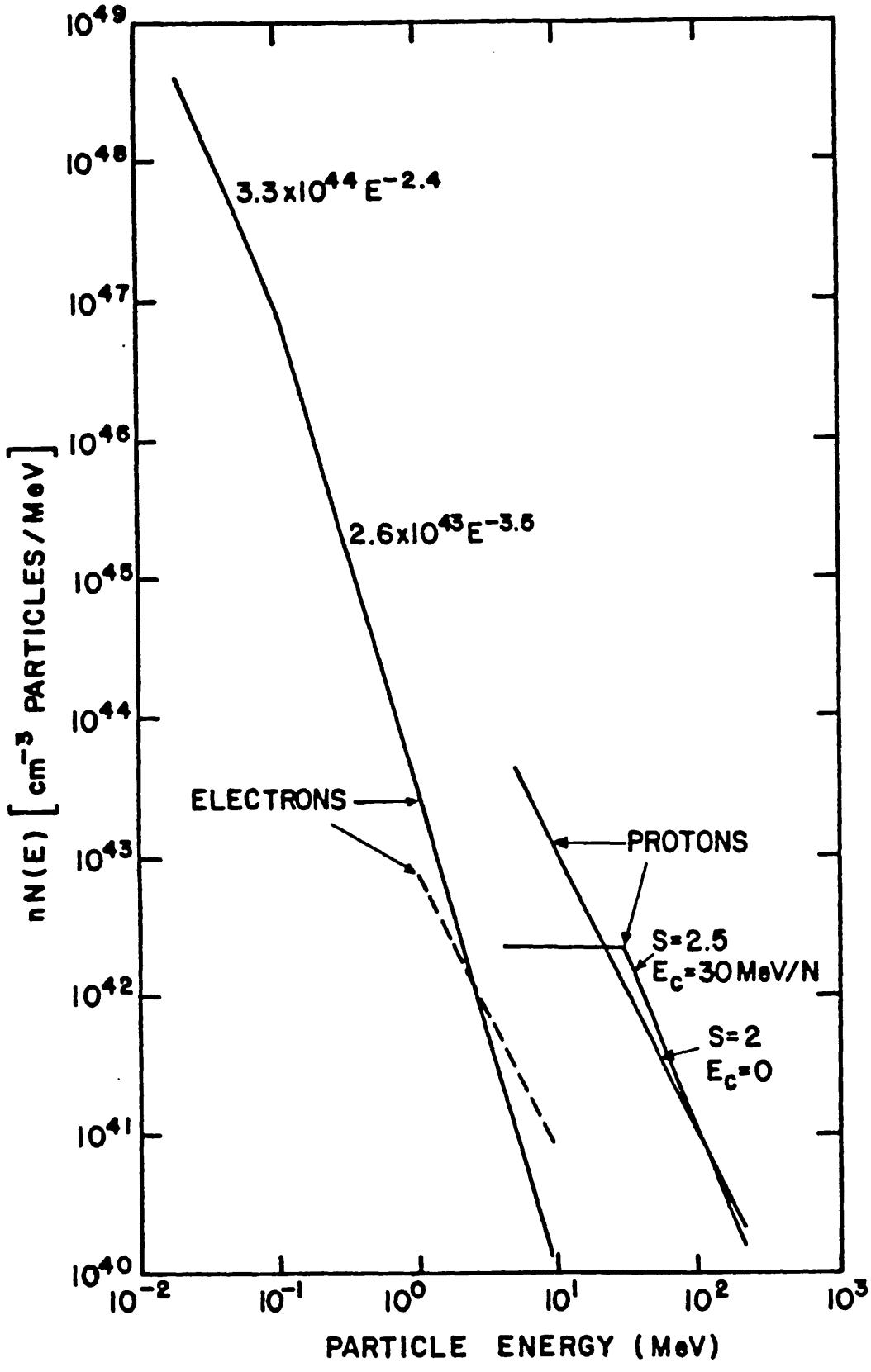


Fig. 4.6. Particle energy spectra for the August 1972 event. The proton numbers are deduced from gamma ray line observations (from Ramaty et al,1980).

TABLE 4 - 4. Large Scale (> 60,000 Km) soft X-ray enchancements in active regions and their association with mass ejections.

Type of event	No. of events		Hα filament activity		Eruptive nature		No Hα activity	
	N°	%	N°	%	N°	%	N°	%
Mass ejection	156	100	126	80.8	94	20.6	6	3.8
Flare events	69	44.2	63	91.3	69	100	6	8.7

of a delay between the emission of the low energy particles and the production of the higher ones. Bai et al (1983) and Smith and Brecht (1984) have interpreted the delay of the gamma-ray emission in terms of shock wave acceleration of protons in the magnetic field loop. Whether this is so or not, the fact is that only the energetic particle model has tried to explained the presence of the protons in the magnetic loop before, during and after the flare.

We end this section by summarising the interpretation for our model of the isotopic composition.

1) The enhancement of certain isotopes by resonant heating and by nuclear reactions takes place during the building-up.

2) When ^{3}He and Fe isotopes start being preferentially heated by first and second harmonics of ion-cyclotron waves, respectively, the temperature of the coronal plasma is still relatively low.

3) As Te>>Ti later, ion-sound turbulence becomes the predominant "mode" and only ^{3}He is in resonance.

4) When the flare takes place the temperature is high. The iron previously heated which lies trapped in the magnetic field is then more ionized and its charge state, as observed in interplanetary space does not correspond with

the conditions of cooler temperature when it was enhanced in the trapped particle population.

The discrepancy between theory (Fisk's model) and experiment (Gloeckler et al, 1976; Sciambi et al 1977; Ma Sung et al, 1981) is then solved by the energetic particle model. While Fisk's calculations show that Fe + 17 is the isotope which should be preferentiably heated in the flare, observations show that the most common overabundant isotope of iron is Fe + 11, instead, with Fe + 16, 17 being present only in some cases. This result strongly supports the idea that particles are trapped in the field long time before the flare occurrance.

4.2.4. Evolution of Solar Flare Electrons.

A further test of the model can be performed by looking at the energy released into the solar atmosphere at the time of the flare. The particle model predicts that if the instability which produces the flare is of the chromospheric heating type then the suprathermal particles in the tail of the distribution are dumped first to be followed later by more particles but of lower energy.

The 25 June 1980 flare was analysed by Holman et al (1984) in impulsive microwave with VLA and X-ray emission from the HXRBS on SMM satellite. Since no indication of any change in the magnetic field structure was apparent for this flare it makes an excellent candidate for probing the particle model. In fact, before the flare the electrons don't beam. They do so only after they are stimulated by the flare instability. When this occurs the highest energy electrons are dumped into the loss cone producing hard X-ray emission and spiral along open field lines to produce the microwaves. The X-ray producing electrons heat the chromosphere below and new chromospheric material rises enhancing a second precipitation of electrons this time more in number but lower in energy. The results of Holman et al's analysis (Fig. 4.7 and 4.8)

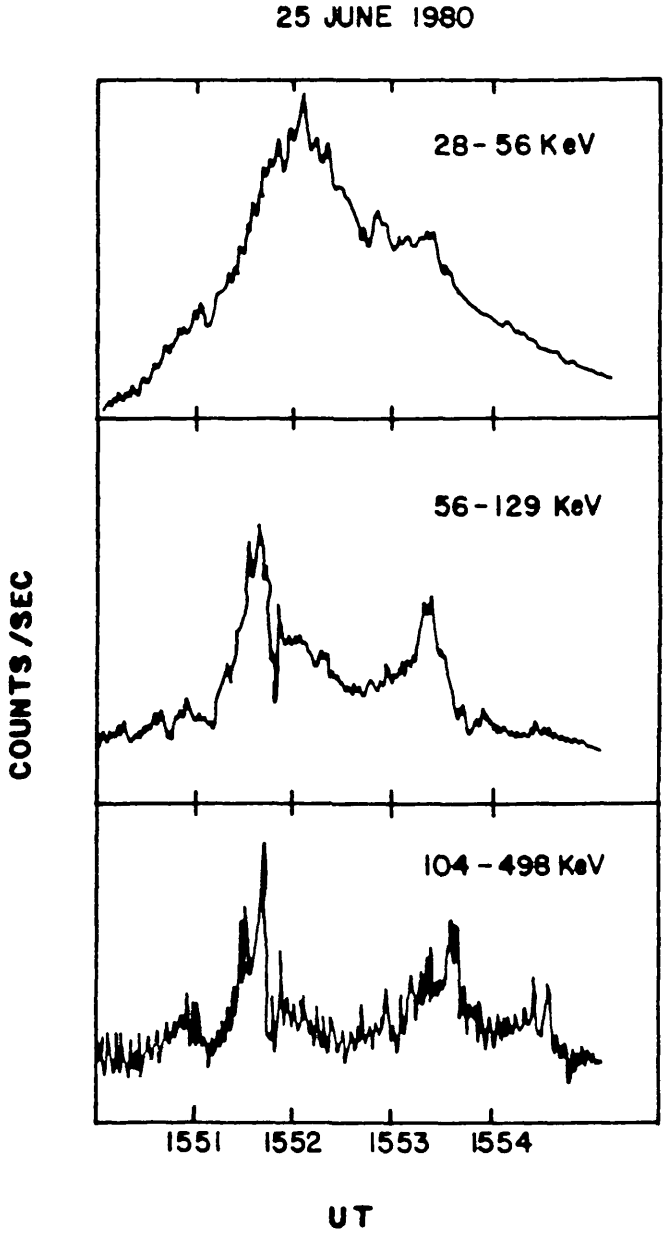


FIG. 4.7. Hard X-ray emission for 25 June 1980 event with HXRBS on SMM Satellite (After Holmes et al, 1984)

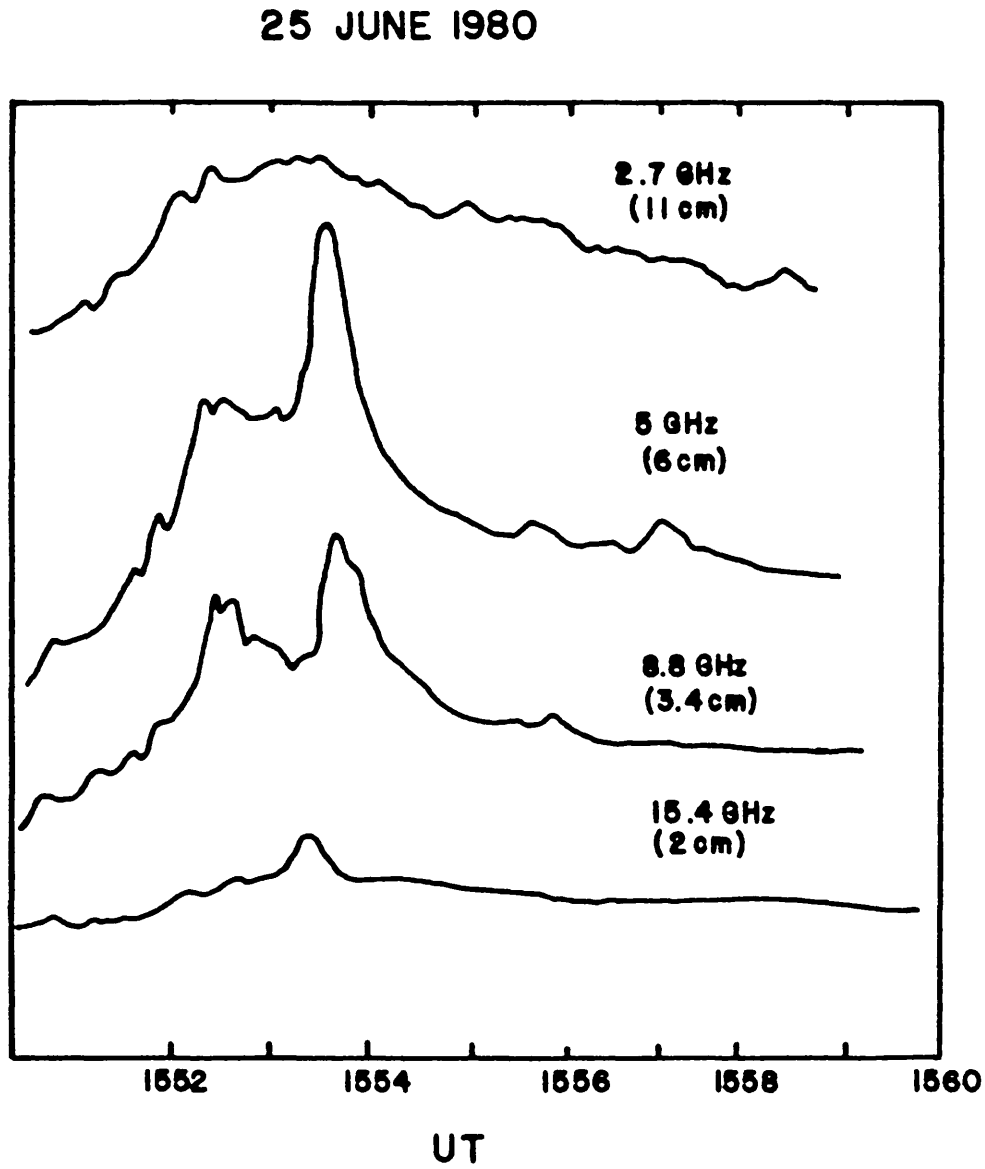


Fig. 4.8. Microwave emission for the 25 June 1980 event with VLA (after Holmes et al,1984).

show very clearly that the hardest X-rays represent the first burst (also evident in the microwaves) and the second burst is produced by lower energies. Furthermore the total energy content in the different bursts is of the same order of magnitude. This is in essential agreement with the model because of the limitations on the energy flux imposed by the magnetic field.

4.3. Future Measurements for testing the Model.

For the near future neither the direct observation of particles trapped in the magnetic field and their acceleration, nor the observation of the microscale of the magnetic field in the loops seems plausible. However, new evidence, although indirect, of the presence of these particles and their acceleration is, we believe, in view. They are the observation in space of ion cyclotron waves and the introduction, in the X-ray classification of flares, of those which present anomalous composition.

4.3.1. Ion cyclotron waves in space.

We cannot observe directly the particles in the trap nor can we ascertain that the flare particle composition arises prior to the flare. Nevertheless, we have discussed the possibility that if acceleration of a trapped population of particles takes place during the building-up stage, ion-cyclotron waves are excited by anisotropic ions at the loss cone when the ratio Te/Ti is of the order of ten. Resonant interactions between particles and waves then take place which work against the anisotropic instability. Although most of the waves deposit their energy in this way in the chromosphere, there are a few which escape; if some could get into an open magnetic field tube they would propagate out into the solar wind. Since once in the tube damping is small because of the high frequency of the waves (see below), it should be possible to observe them in the interplanetary medium. According to theory the waves which are excited have a frequency near the ion cyclotron frequency. If for simplicity we assume that most particles are protons, the frequency of the waves excited is $\omega = eB/m\,c$. At the loss cone, the magnetic field of a large active region is of the order of 10^2 to 10^3 gauss. So

$$\omega \sim 9.6 \times 10^5 - 9.6 \times 10^6 \text{ Hz} \qquad (4\text{-}1)$$

If preferential heating of ^3He takes place $\omega = 6.4 \times 10^5 - 6.4 \times 10^6$ Hz. To try to detect these waves in solar wind tubes whose origin lies near active regions is therefore of great importance for the indirect detection of particle acceleration in magnetic loops.

So far only the ISEE satellites have engaged in the observation of plasma waves directly in space. Unfortunately, their detection frequency range is below the required by our theory. On the other hand, the observation of type III waves from the footpoints of active regions is restricted by the low intensity that is expected when no flare is yet present and by the high level of the noise from such regions.

4.3.2. X-ray and isotope-rich flares.

Thanks to the comparative analysis of X-ray ISEE-3 records and high-resolutions Hα movies made from Big Bear Observatory by Dwividi et al (1984), it has proved possible to find some important features of two-ribbon flares. A similar analysis is suggested in which flares with an abnormal composition become integrated to an extended analysis of X-ray flares. This would then constitute a further test for the particle model since it clearly suggests that flares which are produced by emergence of new magnetic flux only (one spike in X-rays) or those which come from a region which is too large for anisotropic flux simultaneous to low levels of turbulence shoud not present dramatic isotopic overabundances.

The theory presented here satisfactorily explains the general behavior of the solar atmosphere above active regions in its contribution to the particle acceleration, in general, and to the solar flare in particular. We can thus conclude by summarising the relevant points of the model and which we believe would no longer be underestimated if we are to understand the numerous processes taking place continuously in the active solar atmosphere.

1) Charged particles are efficiently trapped in the magnetic field loop above active regions. Particles around the thermal velocity are scattered in and out of trapped orbits and, in the low energy range, heat and acceleration enhance the trapped population as the efficiency of the scattering is inversely proportional to the energy. In fact, $\tau \alpha E^{3/2}$, for Coulomb collisions, and $\tau \alpha E^{\frac{1}{2}}$ for magnetic scattering, τ being the scattering time.

2) The same scattering processes but accompanied by self developed turbulence when the particle flux becomes sufficiently anisotropic ($\langle v \rangle > v_A$) effectively scatters the trapped particles. This produces a diffusion in energy which leads to an energy increase in the trapping region as a Fermi process of acceleration by

hydromagnetic waves becomes important.

3) Particles in the tail of the energy distribution which are above the Kennel and Petschek's limit for stable trapping (fig. 3.5) try to diffuse out of the magnetic field through the loss cone, producing resonant waves. The chromospheric material absorbs the energy dissipated and is slowly heated. As the acceleration process and the building-up of the particle population are in operation, the Maxwellian distribution widens and builds a suprathermal tail. Meanwhile, Ec tends to decrease. Therefore, as the suprathermal tail is formed there are every time more particles which contribute to the heating of the chromosphere. If this limit is not reached, the region expands as the energy contained in the region overcomes the magnetic energy. If it reaches the required limit before the expansion, Ec decreases suddenly and most particles in the magnetic loop are dumped into the chromosphere to produce the flare.

4) While the acceleration process is in operation, energetic protons interact with the chromospheric material to produce deuterium, tritium and helim-3. Simultaneously, resonant waves (ion-cyclotron waves when Te is mildly greater

than Ti and ion-sound turbulence when Te >> Ti) are produced by the anisotropic flux in the loss cone. These then preferentially heat ^{3}He by resonant interaction and its energy distribution grows a high energy tail (see fig. 3-5). The second harmonic of the ion-cyclotron waves heat the iron which at the early stages of the build-up has a charge state of + 11 or + 12. When the flare takes place later, the iron is more ionized (to a value of + 16 or + 17 for instance) which is then preferentially heated according to Fisk's model and as such is observed in space. Thus while Fe + 11, 12 are expected to be more common, Fe + 16, 17, will be present only in those cases in which the system envolves to meet Fisk's assumptions. This is in substantial agreement with observations (Gloekler et al 1976, Ma Sung et al, 1981).

5) The X-ray observations which take place previous to the optical flare are well explained by the particle model because according to it the acceleration takes place at all times through the building-up of the flare, ie., the acceleration is not restricted to a time shortly after the optical flare.

6) The recent observations by the SMM satellite concerning the delay of the γ-rays constitute

strong support to the energetic particle model because they provide evidence that there are particles in the magnetic loops even when the flare has already occurred. These particles can then be accelerated by the shock generated by the intense heat due to the electrons impinging into the chromosphere. The nuclear interactions of the shock accelerated particles finally produce the γ-ray emission.

REFERENCES

Alexeyev,I.I. and Kropotkin,A.P.1970,Geom.Aeron.,10,755.

Anglin,J.D.1975, Astrophys.J., 198, 733.

Anglin,J.D.,Ditriech,W.F. and Simpson,J.A.1973,in R.Ramaty and R.G. Stone eds.,"High Energy Phenomena on the Sun", (NASA SP-342),p. 315.

Anglin, J.D., Dietriech, W.F. and Simpson, J.A. 1977, 15th ICRC (Plovdiv), 5, 43.

Antonucci, E., Dennis, B.R., Gabriel, A.J. and Simnett, G.M. 1985 Solar Phys., 96, 129-142.

Athai,R.G. 1981, in S. Jourdan,ed.,"The Sun as a Star", (NASA SP-450),p.85.

Athai,R.G. and White,O.R. 1979, Astrophys. J.,229,1142.

Axford,W.I. 1981, Proc. 17th ICRC (Paris),12,155.

Bai,T., Hudson,H.S., Pelling,R.M., Lin,R.P., Schwartz, R.A. and van Rosenvinge,T.T. 1983, Astrophys. J.,267,433.

Berger,J.M., Newcombe,W.A., Dawson,J.M., Friedman,E.A., Kulsrud,R.M. and Lennard,A. 1958,Phys. Fluids,1,301.

Berman,N.M. 1982, IAU-Symp., Book of Abstracts (Zürich)p.II14.

Bertsch,D.L., Biswas,S., Fichter,C.E., Pellerin,C.J. and Reames,D.V. 1973, Solar Phys.,31,247.

Billings,D.E. and Saito,K. 1964, Astrophys. J.,140,760.

Bisnovatyi-Kogan,G.S. and Gordon,I.M. 1969, Astrophys. Letters,4,149.

Biswas,S., Fichtel,C.E. and Guss,D.E. 1962, Phys. Rev.,128,2756.

Biswas,S. and Radhakrishnan,B. 1973, Solar Phys.,28,211.

Brown,J.C. and Smith,D.F. 1980, Rep. Prog. Phys.,43,9.

Brown, J.C. and Smith, D. F. 1980, Rep. Prog. Phys. 43, 125

Buneman, O. 1959, Phys. Rev., 115, 503.

Cameron, A. G. W. 1973, in "Explosive Nucleosynthesis", D. N. Schramm and W. D. Arnet, eds, (Austin: Univ. of Texas).

Cheng, C. C. 1972, Solar Phys., 22, 178.

Chirkov, A. G., Khodgaev, K. Sr., Shatolov, S. D. and Vasiliev, V. N. 1981, Proc. 17th ICRC (Parfs), 3, 500.

Chiuderi, C. 1981, in "Solar Phenomena in Stars and Stellar Systems", R. M. Bonnet and A. K. Dupree, eds., (Reidel: Dordrecht) p. 269.

Chiuderi, C. 1983, in "Solar and Stellar Magnetic Fields: Origins and Coronal effects", J. O. Stenflo, ed., 1 AU Symp. No. 102, p. 375.

Chupp,E. L. 1983, Solar Phys., 86, 383.

Chupp, E. L., Forrest, D. J., Hibbie, P. R., Suri, A.N., Tsai, C. and Cumphy, P. P. 1973, Nature, 241, 5388.

Chupp, E. L., Forrest, D. L., Ryan, J. M., Cherry, M. L., Reppin, C., Kambach, G., Rieger, E., Pinkan, K., Share, G. H., Kinzer, R. L., Strickman, M. S., et al'75 Johnson, W. N. and Kurfuss, J. D. 1981, Astrophys. J., 244, L171.

Colgate, S. A., Audouze, J. and Fowler, W. A. 1977, Astrophys. J., 213, 849.

Crawford, H. J., Price, P. B., Cartrwight, B. J. and Sullivan, J. D. 1975, Astrophys. J. 195, 213.

Davis, L. K. 1956, Phys. Rev., 101, 351.

de Jager, C. 1968, in K. O. Kiepenheuer, ed., "Structure and Development of Solar Active Regions", 1 AU Symp. 35, 480.

de Jager, C., Machado, M. E., Schadee, A., Strong, K.T., Svestka, Z., Woodgate, B. E. and van Tend, W. 1983, Solar Phys., 84, 205.

Dietrich, W. F., 1973, Astrophys. J., 180, 955.

Dietrich, W. F. and Simpson, H. A. 1978, Astrophys. J. (Lett), 225, L41.

Dorman, L. I. and Freidman, G. I. 1959, "Problems of MHD and Plasma Physics", (Riga), 77.

Dryer, M., Wu, S. T., Steinolfson, R. S. and Wilson, R.M. 1978, Astrophys. J. 227, 1059.

Duijrman, A. 1983, Solar Phys., 84, 189.

Dwivedi, B. N., Hudson, H. S., Kane, S. R. and Svestka, Z. 1984, Solar Phys., 90, 331.

Elliot, H. 1964, Planet. Space Sci., 12, 657.

Elliot, H. 1969, "Solar Flares and Space Research" (N. Holland), 356.

Elliot, H., 1973, in "High-Energy Phenomena on the Sun, ed. R. Ramaty and R. G. Stone (NASA SP-342), p. 12.

Elliot, H. 1979,(Preprint)

Ellison, M. A., Mckenna, S. M. P. and Reid, J. H. 1961, Mon. Not. R. astr. Soc. 122, 491.

Farnik, F., Kaastra, J., Kalman, B., Karlicky, M., Slottje, C. and Valnicek, B. 1983, Solar Phys. 89, 355.

Fermi, E. 1949, Phys. Rev., 75, 1169.

Fermi, E. 1954, Astrophys. J., 119, 1.

Fisk, L. A. 1978a, Astrophys. J., 224, 1048.

Fisk, L. A. 1978b, Proc. 10th Leningrad Seminar on Space Phys., p. 1.

Fisk, L. A. and Axford, W. I. 1969, Solar Phys., 7, 486.

Fleisher, R. L. and Hart, H. R. 1973, Phys. Rev. Letters, 30, 31.

Forrest, D. J., hupp, E. L., Ryan J. M., Heslin, J., Reppin, C., Rieger, E., Kanbach, G., Pinkau, K., Share, G. and Kinzer, G. 1981, 17th ICRC 10, 5 (Paris).

Freir, P. S. and Webber, W. R. 1963, J. Geophys. Res., 68, 1605.

Foukal, P. 1975, Solar Phys., 43, 327.

Gabriel, A. H., Actron, L. W., Culhane, J. L. and 12-coauthors 1983, Astrophys. J. (Lett.), 244, L147

García-Muñoz, M., Mason, G. M. and Simpson, J. A. 1975a, Astrophys. J. (Lett). 201, L145.

García-Muñoz, M., Mason, G. M. and Simpson, J. A. 1975b, Astrophys. J., 202, 265.

Garrard, T. L., Stone, E. C. and Vogt, R. E. 1973, in "High Energy Phenomena on the Sun", Symp. Proc., R. Ramaty and R. G. Stone, eds., (NASA SP-342) p.341.

Gergely, E. T., Kundy, M. R., Erskine III, F. T. Sawyer, C., Wagner, W. J., Illing, R., House, L. L., McCabe, M. K., Stewart, R. T., Nelson, G. J., Koomen, M. J., Michels, D., Howard, R. and Sheeley, N. 1984, Solar Phys., 90, 161.

Ginzburg, V. L. and Syrovatskii, S. I. 1957, "The Origin of Cosmic Rays", (Oxford, Pergamon).

Giovanelly, R. G. 1939, Astrophys. J. 89, 555.

Gloeckler, G., Hovestadt, D., Vollmer, O. and Fan, C. Y. 1975, Astrophys. J. (Lett.), 200, L45.

Hovestadt, D., Klecker, B., Höfner, H., Scholer, M., Gloeckler, G. and Ipavich, F. M. 1982, Astrophys. J. (Lett.), 258, L57.

Gloeckler, G., Sciambi, R. K., Fan, C. Y. and Hovestadt, D. 1976, Astrophys. J. (Lett.), 209, L93.

Goldman, M. V. 1983, Solar Phys., 89, 403.

Golub, L. 1983, in "Solar and Stellar Magnetic Fields: Origins and Coronal Effects", J. O. Stenflo, ed., 1 AU Symp. 102, p. 345.

Golub, L., Maxon, C., Rosner, R., Serio, S. and Vaiana, G. S. 1980, Astrophys. J., 238, 343.

Gordon, I. M. 1969, Soviet Astron., 12, 796.

Hartquist, T. W. and Morfill, G. E. 1983, Astrophys. J., 266, 271.

Hempe, H., Mueller-Mellin, R., Kunow, H. and Wibberenz, G. 1979, 16th ICRC, 5, 95 (Kyoto).

Heyvaerts, J. and Schatzman, E. 1980, in Procedings of ghe Japan-France Seminar on Solar Physics, F. Moriyama and J. C. Henoux, eds., p. 77.

Heyvaerts, J., Priest, E. R. and Rust, D. M. 1977, Astrophys. J., 216, 123.

Hollweg, J. W. 1981, in S. Jourdan, ed., "The Sun as a Star" (NASA SP-450), p. 355.

Hollweg, J. V. 1984, Astrophys. J., 277, 392.

Holman, G. D., Ionson, J. A. and Scott, J. S. 1979, Astrophys. J., 228, 576.

Hood, A. W. 1983, Solar Phys., 87, 279.

Hovestadt, D., Klecker, B., Vollmer, O., Gloeckler, G. and Fan, C. Y. 1975, 14th ICRC, 5, 1613 (Munich).

Hoyng, P., Duijvman, A., Machado, M. e., Rust, D. M., Svestka, Z. and 7-coauthors, 1981, Astrophys. J. (Lett), 246, L155.

Howard, R. and Svestka, Z. 1977, Solar Phys. 54, 65.

Hsieh, K. C. and Simpson, J. A. 1970, Astrophys. J. (Lett.), 162, L191.

Hudson, H. S., Bai, T., Gruber, D. E., Matteson, J. L. Nolan, P. L. and Paterson, L. E. 1980, Astrophys. J. (Lett.), 236, L91.

Hudson, P. D. 1965, Monthly Notices Roy. Astron. Soc., 131, 23.

Hurford, G. J., Mewalt, R. A., Stone, E. C. and Vogt, R. E. 1975, Astrophys. J. (Lett.), 201, L95.

Ibraginov, J. A., Kocharov, G. E. and Kocharov, L. G. 1978, Dokl, Akad, Nauk SSSR, Jofee Phys. Tech. Inst. Nr. 588.

Ionson, J. A. 1982, Astrophys. J., 254, 318.

James, J. C. 1966, Astrophys. J., 146, 356.

Jeffries, J. T. and Orvall, F. Q. 1965, Astrophys. J., 141, 519.

Jokipii, J.R. 1966, Astrophys. J., 146, 480-487.

Jokipii, J.R. 1971, Rev. Geophys. Space Sci., 9, 27-87.

Jordan, C. 1981, ed. of Proc. 3rd European Solar Meeting, Oxford.

Kadomtzev, V. V. 1966, Rev. Plasma Phys., 2, 153.

Kahler, S. W. 1979, Solar Phys., 62, 347.

Kane, S. R. 1971, Astrophys. J., 170, 587.

Kapan, S. A. 1956, Soviet Phys. JETP, 2, 203.

Kennel, C. F. and Petschek, H. E. 1966, J. Geophys. Res. 71, 1.

Klecker, B., Hovestadt, D., Gloeckler, G., Ipavich, F.M., Scholer, M., Fan, C. Y. and Fisk, L. A. 1984, Astrophys. J. 281, 458.

Kocharov, L. G. 1979, Proc. 11th Leningrad Seminar on Space Phys., p. 43.

Kocharov, G. E. and Kocharov, L. G. 1978, Proc. 10th Leningrad Seminar on Space Phys., p. 98.

Kolchin, A. A., Lebedev, V. V., Levchenka, V. F., Repin, A. I., Shubin, V. L. and Skrebtsov, G. P. 1979, Proc. 16th ICRC, 5, 122 (Kyoto).

Korchak, A.A. and Syrovatskii, S.I.1958,Soviet Phys. Dokl.,3, 983

Krall, N. A. and Antiochos, S. K. 1980, Astrophys. J., 242, 374.

Kulsrud, R. M. and Ferrara, A. 1971, Astrophys. Space Sci. 12, 302.

Kuperus, M., Ionson, J. A. and Spicer, D. S. 1981, Ann. Rev. Astron. Astropys., 19, 7.

Lanzarotti, J. J., McLenna, C. G. and Graedal, T. E. 1972, Astrophys. J. (Lett.). 187, L105.

Levin, B. N. 1979, Soviet Astron. 23, 728.

Levine, R. H. and Withbroe, G. L. 1977, Solar Phys. 51, 83.

Lin, R. P. 1974a, Space Sci. Rev., 16, 189.

Lin, R. P. 1974b, "Coronal Disturbances" G. A. Newkirk, (ed) 1AU Symp. No. 57, (Dordrecht: Reidel), p. 201.

Martens, P.C.H. and Kuperus, M. 1983, in J. O. Stenflo ed. "Solar and Stellar Magnetic Fields: Origins and Coronal Effects" 1AU p. 397.

Mason, G. M. Hovestadt, D. and Gloeckler, G. 1979, Proc. 16th ICRC, 5, 110 (Kyoto).

MaSung, L. S., Gloeckler, G., Fan, C. Y. and Hovestadt, D. 1981, Astrophys, J. 245, L45.

Mauger, B. 1981, PHD. Thesis, New Mexico State University.

McCracken, G. G. and Rao, U.R. 1970, Space Sci. Rev., 4, 155.

Mc Donald, F. B., Fichtel, C. E. and Fisk, L. A. 1974, in "High Energy Particles and Quanta in Astrophysics", F.B. Mc Donald and C.E. Fichtel, eds., (MIT Press), p. 212.

Mc Donald, F. B., Teegarden, B. J., Trainor, J. H. and Webber, W. R. 1975, Astrophys. J. (Lett.), 187, L105.

McGuire, J. P., Tandberg-Hansen, E., Krall, K. R., Wu, S. T., Smith, J. B. and Speich, D. M. 1977, Solar Phys., 52, 91.

McGuire, R. E., von Rosenfinge, T. T. and McDonald, F. B. 1976, 16th ICRC, 5, 90 (Kyoto).

McIntosh, P. S., Krieger, A. S., Nolte, J. T. and Vaiana, G. S. 1976, Solar Phys., 49, 57.

Meerson, B. I. and Rogachevskii, I. V. 1983, Solar Phys., 87, 337.

Melrose, D. B. 1971, in R. D. Davies and F. E. Smith, eds., "The Crab Nebula", (Reidel, Dorcrecht), p. 96.

Melrose, D. B. 1974, Solar Phys., 37, 353.

Melrose, D. B. 1980, "Plasma Astrophysics: Nomthermal Processes in Diffuse Magnetazed Plasmas" Vol. 2 (Gordon and Breach, London) p.187.

Mewe, R. and Zwaan, C. 1980, in "Cool Stars, Stellar Systems and the Sun", vol.1, M. S. Gianpapa and L. Golub, eds., (SAO SR-389), p. 123.

Meyer, F. 1971, in C. Macris, ed., "Physics of Solar Corona" (Dordrecht: Reidel), p. 29.

Meyer, J. P. 1972, Astr. and Ap. Suppl., 7, 417.

Meyer, J. P. 1978, Proc. 22 Liége International Astrophys. Symp.

Meyer, J. P. and Reeves, H. 1977, 15th ICRC (Provdiv), 2, 137.

Mogilevsky, E. I. and Shelting, B. D. 1966, Proc. of the Meeting on Solar Magnetic Fields and High Resolution Spectroscopy, G. Barbera, ed., p. 222.

Mogilevsky, E. I., Demkina, L. B., Ioshpa, B. A. and Obridko, V. N. 1968, in IAU Symp. Num. 35, K.O. Kiepenhewer, ed. (Dordrecht: Reidel), p. 202.

Mogro Campero, A. and Simpson, J.A. 1972, Astrophys. J. (Lett.), 177, L37.

Morrison, P. 1956.,Physical Review, 103, 1397.

Neidig, D. F. 1978, AFGC report TR-78 0194.

Newton, H. W. 1948, Observatory, 68, 29.

Nishimura, J., Fuji, M., Aizu, E., Hiraiwa, H., Kobayashi, T., Niu, K., Ohta, I., Golden, R. L., Koss, T. A., Lord, J. J. and Wilkes, R. J. 1980, Astrophys. J., 238, 394.

Ohki, K., Takakura, T., Tsuneta, S. and Nitta, N. 1983, Solar Phys. 86, 301.

Ormes, J. F. and Protheroe, R. J. 1983, Astrophys. J., 272, 756.

Pallavicini, R., Golub, L., Rosner, R. and Vaiana, G. S. 1982, in "Cool Stars, Stellar Systems, and the Sun", Vol. 1, M.S. Giampapa and L. Golub, eds., (SAO SR-389), p. 79.

Pallavicini, R., Vaiana, G. S., Khler, S. W. and Krieger, A.S. 1975, Solar Phys., 45, 411.

Parker, E. N. 1958, Phys. Rev., 109, 1328.

Parker, E. N. 1963, Astrophys. J. Suppl., 8, 177.

Parker, E. N. and Tidman, D. A. 1958, Phys. Rev. 111, 1206.

Parker, E.N. 1956, Physical Review, 103- 1518

Parker, E.N., 1965, Planetary Space Sci., 13, 9

Paterson, L. E. and Winckler, J. R. 1959, J. Geophys. Res., 64, 697.

Pesses, M. 1981, 17th ICRC (Paris), 3, 171.

Petrasso, R. D., Kahler, S. W., Krieger, A. S. and Silk, J. K. 1975, Astrophys. J., 199, L127.

Petrosian, V. and Leach, J. 1983, Solar Phys. 87, 165.

Poland, A. and Tandberg-Hansen, E. 1983, Solar Phys., 84, 63.

Price, P. B., Hutcheon, I., Cowsik, R. and Barber, D. J. 1971, Phys. Rev. Letters, 26, 916.

Priest, E. R. 1982, "Solar MHD", (Reidel: Dordrecht) Ch. 8.

Prince, T. A. 1979, Astrophys. J. 227, 676.

Prince, T. A. Luig, J. C., Mahoni, W. A., Riegler, G. R. and Jacopson, A. S. 1982. Astrophys. J. (Lett.) 255, L81.

Ramaty, R. and Kozlovsky, B. 1974, Astrophys. J., 193, 729.

Ramaty, R. and Lingenfelter, R. E. 1969, Astrophys. J., 193, 729.

Ramaty et al 1980, in P. A. Sturrock, ed. "Solar Flares" (Boulder: Colo. Ass. Univ. Press).

Ramaty, R., Koslovsky, B. and Lingenfelter, R. E. 1975, Space Sci. Rev., 18, 341.

Ramaty, R., Koslovsky, B. and Lingenfelter, R. E. 1979, Astrophys. J. Suppl., 40, 487.

Ramaty, R., Murphy, R. J., Koslovsky, B. and Lingenfelte, R. E. 1983, Solar Phys. 86, 395.

Rieger, E. 1982, in "Honotory Symp. on Solar Flares", (Tolio: Inst. Spac. Astronautical Sci.), p. 246.

Rosenberg, H. 1976, Phil. Trans. R. Soc. A281, 461.

Rosenberg, H. 1976, Phil. Trans. R. Soc., A281, 461.

Rosner, R. and Vaiana, G. S. 1980, in "X-ray Astronomy", R. Giaconi and R. Setti, eds., (Dordrecht: Reidel), p. 129.

Rothwell, P. L. 1974, Bull. Am. Phys. Soc., 19, 458.

Rothwell, P. L., Katz, L., Sellers, B. and Hanser, F. A. 1973, Phys. Rev. Letters, 31, 407.

Rust, D. M. 1976, Phil. Trans. R. Soc. A 281, 427.

Rust, D. M. et al. 1980, in "Solar Flares", P. A. Sturrock, ed., Ch. 6 (Colo. ASS. Univ. Press).

Sakurai, T. and Granik, A. 1984, Astrophys. J., 277, 404.

Sarris, E. and Van Allen, J. 1974, J. Geophys. Res., 79, 4157.

Serlemitsos, A. T. and Balasnbrahmanyan, V. K. 1975, Astrophys. J., 198, 195.

Schadee, A., de Jager, C. and Svestka, Z. 1983, Solar Phys. 89, 287.

Scheffer, O. A. and Zähringer, J. 1962, Phys. Rev. Lett. 8, 389.

Schatzman, E. 1967, Solar Phys., 1, 411.

Schlüter, A. 1950, Z. Naturforsch. 5a, 72.

Schlüter, A. 1957, Z. Naturforsch. 12a, 822.

Sciambi, R. K., Gloeckler, G., Fan, C. Y. and Hovestadt, D. 1977, Astrophys. J. 214, 316.

Severny, A. B. 1964, Space Sci. Rev., 3, 2.

Shabansky, V. P. 1961, Soviet Astron.- A. J., 5, 647.

Simnet, G. M. 1974, Space Sci. Rev. 16, 257.

Simnett, G.M. 1985, Proc. 19th ICRC, 4, 70-73.

Simnett, G.M. and Ryan, J.M. 1985, Proc. 19th ICRC. 4, 82-85.

Simnett, G.M. and Strong, K.T. 1984, Astrophys. J., 284, 839-847.

Sivukhin, P.V., 1966, Rev. of Plasma Phys., 4, 93.

Smith, D.F. and Brecht, S.H. 1984, in "AGU Chapman Conference on Collisionless shock waves in the Heliosphere" (Book of Abstracts).

Smith, J.B., jr., Speich, D.M., Wilson, R.M., Tandberg-Hansen, E. and Wu, S.T. 1977, Solar Physics 52, 379.

Spangler, S.R. and Shawan, S.D. 1974, Solar Phys., 37, 189.

Spicer, D.S. 1977, Solar Phys., 53, 305.

Stein, R.F. and Leibacher, J.W. 1980, in D.F. Gray and J.L. Linsky, eds., "Mechanical Energy Transpot", Proc. IAU Colloquium on Stellar Turbulence, 51, (Berlin: Springer-Verlag), p. 225.

Sturrock, P. A. 1980, "Solar Flares" Colo. Ass. Univ. Press

Sullivan, J. D. and Price, P. B., Proc. 13th ICRC (Denver) 2, 1470.

Svestka, Z. 1966, Space Sci. Rev., 5, 388.

Svestka, Z. (ed) 1977, Solar Phys., 53, 217.

Svestka, Z. Dennis, B. R., Pick, M., Raoult, A., Rapley, C. G., Setwart, R. T. and Woodgate, B. E. 1982b, Solar Phys. 80, 143.

Svestka, Z., Krieger, A. S., Chase, R. C. and Howard, R. 1977, Solar Phys., 52, 69.

Svestka, Z., Stewqrt, R. T., Hoyng, P., van Tend, W., Acton, L. W., Gabriel, A. H., Raply, C. J. and 8 co-authors 1982a, Solar Phys., 75, 305.

Swann, W. F. G. 1933, Phys. Rev., 43,217.

Syrovatsky, S. I. 1982, Solar Phys., 76, 3.

Tanaka, K. and Nakagawa, Y. 1973, Solar Phys., 33, 187.

Tandberg-Hansen, E., Kaufman, P., Reichman, E. J., Teuber, D. L., Moore, R. L., Orwig, L. E. and Zirin, H. 1984, Solar Phys., 90, 41

Teegarden, B. J., van Rosenvinge, T. T. and McDonald, F. B. 1973, Astrophys. J., 180, 571.

Thompson, W. B. 1955, Proc. Roy. Soc., A233, 402.

Toptygin, I. N. 1980, Space Sci. Rev., 26, 157.

Thomas, R. J. and Teske, R. G. 1971, Solar Phys., 16, 431.

Trubnikov, B. A. 1965, Rev. Plasma Phys., 1, 105.

Tverskoi, B. A. 1967, Soviet Phys. JETP, 25, 317.

Vaiana, G. S. 1981, in "X-ray Astronomy with the Einstein Stellite", R. Giaconi, ed., (Dordrecht: Reidel), p. 1.

Vaiana, G. S. 1983, in "Solar and Stellar Magnetic Fields: Orignis and Coronal Effects", J. O. Stenflo, ed., IAU Symp. 102, p. 165.

Vaiana, G. S. and Rosner, R. 1978, Ann. Rev. Astr. Ap., 16, 393.

Vaiana, G. S., Krieger, A. S. and van Speybroeck, L. P. 1970, in "Solar Magnetic Fields", R. Howard, ed, IAU Symp. 43, p. 397.

Vaiana, G. S., Krieger, A. S. and Timothy, A. F. 1973, Solar Phys., 32, 81.

van Speybroedk, L. P., Krieger, A. S. and Vaiana, G. S. 1970, Nature, 227, 818.

Veck, N.J., Strong, K.T., Jordan, C., Simnett, G.M., Cargill, P.J. and Priest, E.R. 1984, Mon. Not. R. astr. Soc., 210, 443-462.

Vorpahl, J.A. 1976, Astrophys. J., 205, 868.

Vorpahl, J.A., Gibson, E.G., Landecker, P.B., Mckenzie, D.L. and Underwood, J.H. 1975, Solar Phys., 45, 199.

Waddington, C.J. and Fréier, P.S. 1964, Phys. Rev., 136, B1535.

Webber, W.R., Roelof, E.C., McDonald, F.B., Teegarden, B.J. and Trainor, J. 1975, Astrophys. J., 199, 482.

Wentzel, D. G. 1962, Astrophys. J., 137, 135.

Wentzel, D. G. 1964, Astrophys. J., 140, 1563.

Wentzel, D. G. 1978, Solar Phys., 58, 307.

Wentzel, D. G. 1981, in "The Sun as a Star", S. Jordan, ed., (NASA SP-450) Ch. 14.

Widing, K.G. and Cheng, Ch. Ch. 1974, Astrophys. J. Lett, 194, L 111.

Wild, J. P. 1950, Australian J. Sci. Re., A3, 399.

Wild, J. P., Smerd, S. F. and Weiss, A. A. 1963, Ann, Rev. Astron. Astrophys. 1, 291.

Withbroe, G. L. 1981, in S. Jourdan, ed., "The Sun as a Star" (NASA SP-450), p. 321.

Withbroe, G. L. and Noyes, R. W. 1977, Ann. Rev. Astr. Ap., 15, 363.

Wolfon, C. J. 1982, Solar Phys., 76. 377.

Wolfon, C. J., Acton, L. W. and Leibacher, J. W. 1978, Bull, Am. Astron. Soc., 10, 456.

Woodgate, B. E., Shine, R. A., Brandt, J. C. Chapman, R. D. and 12-coauthors. 1981, Atrophys. J. (Lett.), 244, L133.

Yoshimori, M, Okudaira, K., Hirasima, Y. and Kondo, I. 1983, Solar Phys., 86, 375.

Zirìn, H. 1966, "The Solar Atmosphere" (Bleisdel: Waltham, Mass).

Zirin, H. 1974, in "Chromospheric Fine Structure", R. G. Athay, ed., IAU Symp. No. 56 (Dordrecht: Reidel).

Zurin, H. Proc. NSO/SMM Summer meeting, Sac Peak Workshop on Solar Flares, Aug. 1985.